JOURNAL OF MATERIALS SCIENCE 28 (1993)2841–2886

Review

Preparation, properties and chemistry of glass- and glass-ceramic-to-metal seals and coatings

I. W. DONALD
Atomic Weapons Establishment, Aldermaston, Berkshire, UK

An overview is given outlining the materials and technologies that have been employed in the preparation of glass- and glass-ceramic-to-metal seals and coatings. Metal/non-metal bonding theories are summarized, and the conditions required for the formation of strong chemical bonding are described and discussed. Particular reference is given to the interfacial chemistry involved for individual glass/metal and glass-ceramic/metal combinations. The major factors responsible for the preparation of high-quality seals and coatings, free from porosity and other undesirable defects, are also outlined and discussed. In addition, a number of applications for seals and coatings are briefly described.

1. Introduction

It has long been recognized that many glasses will, under suitable conditions, bond well to a number of metals and alloys, including copper, silver and gold, and iron-based materials. This property of forming a strong, well-adherent bond to metals has led to the extensive use of glasses for the coating (vitreous or porcelain enamelling) of metals and alloys. For example, in ancient Egyptian times glasses were applied to metal surfaces in the production of decorative enamelled jewellery, whilst the enamelling of iron cooking utensils and baths to give a hard, protective and aesthetically acceptable coating was started in the nineteenth century. More recently, glassy coatings have been applied to metal substrates for the production of a wide range of components, from printed circuit boards to acid-, abrasion- or oxidation-resistant protective coatings for metals subjected to hostile environments, e.g. low-pressure turbine blades in jet engines. In addition to coatings, glasses have also found wide-scale use for applications involving the production of electrically insulating hermetic seals; for example, glass-to-metal feed-through seals in vacuum tubes and related devices. More recently it has been discovered [1] that superior seals and coatings exhibiting more refractory properties together with a greater ability to tailor the properties to meet the requirements of specific applications can be formed using the newer glass-ceramic materials.

In order to form a mechanically strong, adherent and, if necessary, hermetic seal or coating to a metal, certain specific requirements are necessary; for example, the formation of a chemical bond at the interface between the glass (or glass-ceramic) and the metal. In addition, the thermal expansion characteristics of the glass must ideally be matched as closely as possible to those of the metal in order to prevent the formation of undesirable tensile stresses in the coating or seal after cooling from the fabrication temperature (or, indeed, in the case of a heat-resistant coating, during subsequent thermal cycling of the component).

Following the pioneering work of King *et al.* [2], and later work by Pask and co-workers [3–5], which was aimed at establishing the factors responsible for the formation of strong bonding between metals and glasses, it is now recognised that strong *chemical* bonding can be obtained between a metal and a glass only if the conditions are such that the glass at the interface can become saturated with an appropriate substrate metal oxide. This can occur by dissolution into the glass of an oxide layer already present on the metal or, alternatively, by suitable redox (reduction–oxidation) reactions directly between the glass and the substrate. Under ideal conditions a well-defined transitional region may be absent and bonding occurs via a "mono-oxide layer" where there is a very rapid switch in atomic bonding between the metallic substrate and the covalent-ionic glass. Under less favourable conditions, when excess metal oxide is present at the interface, a microstructurally defined oxide-rich transitional layer may be formed. Bonding is then directed via this oxide layer, and the resulting seal or coating will only be strong if the oxide layer is well bonded to the metal substrate.

In the present paper, a brief overview is given of the types of material employed and the factors involved in the preparation of high-quality seals and coatings. Early bonding theories, leading up to the current chemical theory of bonding between a glass and a

metal, are also reviewed. The bonding behaviour of glass and glass-ceramic materials to a number of specific metals and alloys is then reviewed in some detail, with particular reference being made to the interfacial chemistry involved for each system. Finally, a number of applications for coatings and seals are briefly summarized.

2. Materials employed in the preparation of glass- and glass-ceramic-to-metal seals and coatings

2.1. Glasses

Glasses used for sealing and coating applications are sometimes classified according to their thermal expansion and temperature characteristics into "hard" and "soft" glasses. Hard glasses have low thermal expansion coefficients, i.e. $\alpha < 5 \times 10^{-6}\,°C^{-1}$, whilst soft glasses possess higher thermal expansions, i.e. $\alpha > 8 \times 10^{-6}\,°C^{-1}$. In general, glasses of high expansion possess relatively low softening and working temperatures, whilst low-expansion glasses have higher softening points. Glasses with low softening temperatures are often referred to as "solder" glasses. This is because they are used for sealing or joining glasses to each other or to other inorganic materials including crystalline ceramics and metals in much the same way as a metallic solder is used to join metallic materials [6–8]. Glasses can also be broadly classified according to their composition, as summarized below. Thermal expansion data for a number of glasses are given in Tables I and II. Compositional data for the glasses listed in Table I are given in Table III. Typical thermal expansions curves for a number of glasses are shown in Fig. 1.

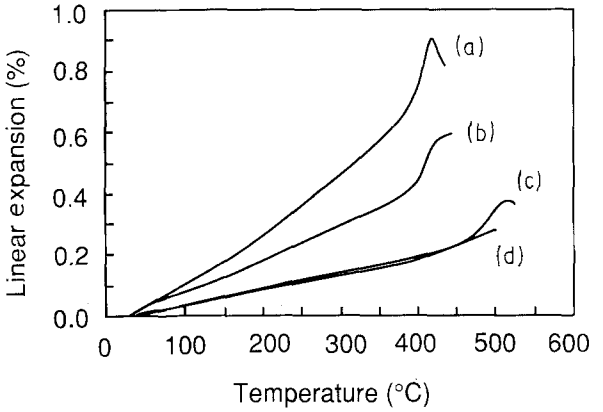

Figure 1 Typical thermal expansion curves for a number of glasses. Glass details are as follows: (a) phosphate glass (Composition not specified), after Chambers *et al.* [34]; (b) lithium zinc silicate glass (composition AZS6), after Donald *et al.* [98]; (c) lead alumino-borosilicate solder glass (composition BS8), after Kataoka and Manabe [14]; (d) borosilicate glass (composition BS7), after Dalton [9].

TABLE I Sealing and solder glass systems

Glass code	Softening or sealing temperature (°C)	Thermal expansion, (α, $10^{-6}\,°C^{-1}$)	Temperature range (°C)	Reference
Silicate glasses				
S1	480	14.1	20–400	[12]
S2	500	11.9	20–400	[12]
S3	500	10.9	20–400	[12]
S4	–	7.4	Not specified	[14]
S5	840	2.3	0–300	[13]
Borosilicate glasses				
BS1	435	14.4	20–400	[12]
BS2	515	8.3	20–400	[12]
BS3	–	8.0	Not specified	[14]
BS4	525	7.7	20–400	[12]
BS5	500	7.6	20–400	[12]
BS6	465	6.1	20–200	[12]
BS7	460 (set point)	5.4	25–460	[9]
Alumino-borate glasses				
AB1	650	3.8	0–300	[20]
AB2	570	3.5	0–300	[20]
Lead borate glasses				
LB1	370	11.0	Not specified	[23]
LB2	380	10.4	Not specified	[23]
LB3	–	9.3	Not specified	[14]
Zinc borate glasses				
ZB1	300	12.0	30–250	[20]
ZB2	300	11.5	30–300	[21]
ZB3	336	10.3	30–300	[21]
ZB4	400	7.7	30–300	[12]
ZB5	280	6.6	20–200	[12]
ZB6	535	5.4	20–400	[12]
ZB7	400	5.0	20–400	[12]
ZB8	571	5.0	0–425	[17, 18]
ZB9	Not specified	4.5	50–350	[19]
ZB10	700	4.2	30–300	[22]

TABLE I (Continued)

Glass code	Softening or sealing temperature (°C)	Thermal expansion, (α, 10^{-6} °C^{-1})	Temperature range (°C)	Reference
Lead zinc borate glasses				
LZB1	–	12.1	Not specified	[43]
LZB2	334	11.7	50–250	[24]
LZB3	410	10.7	20–400	[12]
LZB4	–	8.6	Not specified	[43]
LZB5	435	8.4	20–400	[12]
LZB6	450	7.6	20–400	[12]
LZB7	490	5.9	20–400	[12]
Lead or zinc borate glasses containing a metal halide				
BH1	290	15.2	20–200	[26]
BH2	295	14.2	20–200	[26]
BH3	200	13.7	20–100	[26]
BH4	230	11.5	20–100	[26]
BH5	295	10.1	20–200	[26]
BH6	440	7.5	Not specified	[25]
BH7	490	6.3	Not specified	[25]
BH8	510	5.8	Not specified	[25]
Phosphate glasses				
P1	212	34.7	100–250	[37]
P2	221	30.0	100–250	[37]
P3	266	26.8	100–250	[37]
P4	317	26.0	100–250	[36]
P5	303	25.6	100–250	[36]
P6	313	24.0	100–250	[36]
P7	350	22.0	100–250	[36]
P8	374	20.0	100–250	[36]
P9	310	17.1	100–200	[30]
P10	255	15.3	100–200	[30]
P11	345	13.2	100–200	[30]
P12	325	12.1	100–200	[30]
P13	450	11.6	20–400	[12]
P14	330	11.6	100–200	[30]
P15	305	11.0	20–200	[12]
P16	460	9.6	20–400	[12]
P17	540	7.1	20–400	[12]
P18	475	7.0	20–400	[12]
P19	500	6.4	20–400	[12]
Antimonate glasses				
A1	252	21.2	Not specified	[38]
A2	250	19.2	Not specified	[38]
A3	292	18.2	Not specified	[38]
A4	290	15.0	Not specified	[38]
A5	312	13.3	Not specified	[38]
A6	342	12.2	Not specified	[38]
Vanadate glasses				
V1	328	11.8	25–150	[41]
V2	308	10.1	25–150	[41]
V3	335	7.3	25–150	[41]
Devitrifiable solder glasses				
DS1	330	11.3	20–300	[43]
DS2	374	10.7	20–300	[43]
DS3	356	10.0	20–300	[43]
DS4	380	9.6	Not specified	[46]
DS5	503	9.3	100–300	[44]
DS6	390	8.0	20–300	[43]
DS7	600	7.9	100–300	[44]
DS8	424	7.4	20–300	[43]
DS9	406	6.6	20–300	[43]
DS10	550	6.6	Not specified	[45]
DS11	600	5.4	Not specified	[45]
DS12	440	5.2	20–300	[43]
DS13	620	4.8	Not specified	[45]
DS14	595	4.8	100–300	[44]
DS15	620	4.4	20–500	[17, 18]

TABLE II Commercially available sealing glasses

Manufacturer and code	Type of glass	Application	Softening temperature (°C)	Working temperature (°C)	Thermal expansion (10^{-6} °C^{-1})	Temperature range (°C)
Schott 8474	Alkali phosphate glass	Solder sealing	420	512	19.0	20–300
Corning 1990	Potash soda lead glass	Fe sealing	500	756	12.4	0–300
Schott 8472	Lead borate glass	Solder sealing	360	426	12.0	20–300
Schott 8471	Lead borate glass	Solder sealing	389	456	10.6	20–300
Schott 8470	Lead-free glass	Solder sealing	570	748	10.0	20–300
Corning 7595	Crystallizable solder glass	Solder sealing	415 (solder temperature)		9.7	25–set point
Schott 8468	Lead borate glass	Solder sealing	405	460	9.6	20–300
Corning 7572	Crystallizable solder glass	Solder sealing	450 (solder temperature		9.5	25–set point
Schott 8597	Crystallizable solder glass	Solder sealing	435 (solder temperature)		9.2	20–300
Schott 8467	Lead borate glass	Solder sealing	418	518	9.1	20–300
Schott 8095	Alkali lead silicate glass	Cu sealing	630	982	9.1	20–300
Schott 8512	FeO-containing glass	52Ni/Fe alloy sealing	660	975	9.1	20–300
Schott 8418	Alkali alkaline earth silicate glass	51 Ni/1Cr/Fe alloy sealing	708	1035	9.0	20–300
Schott 8531	Lead silicate glass	Cu sealing/encapsulation of semi-conductors	585	822	9.0	20–300
Corning 7575	Crystallizable solder glass	Solder sealing	450 (solder temperature)		8.9	25–set point
Corning 9010	Potash soda barium glass	–	650	1010	8.9	0–300
GB Glass X88	Lead zinc borate glass	Solder sealing	550 (solder temperature)		8.8	50–200
Schott 8596	Crystallizable solder glass	Solder sealing	450 (solder temperature)		8.7	20–300
Corning 7570	High lead glass	Solder sealing	440	558	8.4	0–300
GB Glass GS85	Alkali alkaline earth borosilicate glass	For graded seals	710	–	8.3	50–400
Corning 7583	Crystallizable solder glass	Solder sealing	480 (solder temperature)		8.3	25–set point
Schott 8465	Lead borate glass	Solder sealing	461	566	8.2	20–300
Schott 8593	Crystallizable solder glass	Solder sealing	520 (solder temperature)		7.7	20–300
GB Glass X76	Lead zinc borate glass	Solder sealing	550 (solder temperature)		7.6	50–200
GB Glass GS77	Alkali alkaline earth borosilicate glass	For graded seals	720	–	7.5	50–400
Corning 7578	Crystallizable solder glass	Solder sealing	530 (solder temperature)	–	6.8	25–set point
Corning 7556	High lead glass	Solder sealing	330	–	6.7	25–set point
Schott 8436	Alkali alkaline earth silicate glass	28Ni/23Co/Fe alloy and sapphire sealing	810	1095	6.6	20–300
Schott 8595	Crystallizable solder glass	Solder sealing	500 (solder temperature)		6.5	20–300
Schott 8454	Alkali alkaline earth silicate glass	28Ni/23Co/Fe alloy and alumina ceramics sealing	745	1050	6.4	20–300
GB Glass GS65	Alkali alkaline earth borosilicate glass	For graded seals	745	–	6.2	50–400
Corning 7056	Borosilicate glass	Kovar sealing	718	1058	5.2	0–300
Schott 8245	High boron glass	Mo and 28Ni/18Co/Fe alloy sealing	710	1040	5.2	20–300
Schott 8250	High boron glass	Mo and 28Ni/18Co/Fe alloy sealing	715	1060	5.0	20–300
GB glass GS50	Alkali alkaline earth borosilicate glass	For graded seals	770	–	4.9	0–400
GB glass X49BK	Zinc vanadium borate glass	Solder sealing	610 (solder temperature)		4.8	–
Schott 2877	Alkaline earth borosilicate glass	Mo sealing	790	1170	4.9	20–300
Corning 7040	Borosilicate glass	Kovar sealing	702	1080	4.8	0–300
Corning 7052	Borosilicate glass	Kovar, Mo or W sealing	712	1128	4.6	0–300
Corning 7574	Crystallizable solder glass	Solder sealing	750 (solder temperature)		4.5	25–set point
GB glass GS44	Alkali alkaline earth borosilicate glass	For graded seals	790	–	4.3	50–400

TABLE II (Continued)

Manufacturer and code	Type of glass	Application	Softening temperature (°C)	Working temperature (°C)	Thermal expansion (10^{-6} °C^{-1})	Temperature range (°C)
Corning 1720	Aluminosilicate glass	–	915	1190	4.2	0–300
Corning 7593	Crystallizable solder glass	Solder sealing	650 (solder temperature)		4.2	25–set point
Schott 8486	Alkaline earth borosilicate glass	W sealing	805	1230	4.1	20–300
Corning 3320	Borosilicate glass	W sealing	780	1171	4.0	0–300
Schott 8487	High boron glass	W sealing	770	1135	3.9	20–300
Corning 9700	Borosilicate glass	–	805	1200	3.7	0–300
Corning 7720	Borosilicate glass	W sealing	755	1146	3.6	0–300
Corning 7740	Borosilicate glass	–	820	1145	3.3	0–300
GB Glass GS30	Alkali alkaline earth borosilicate glass	For graded seals	1075	–	3.0	50–400

TABLE III Glass and glass-ceramic compositional data

Glass code	Composition (mol %)															
	Li_2O	Na_2O	K_2O	MgO	CaO	BaO	TiO_2	ZrO_2	ZnO	B_2O_3	Al_2O_3	SiO_2	P_2O_5	Sb_2O_3	PbO	Others
S1	12.90	–	19.50	4.94	3.55	–	–	–	–	–	6.11	53.00	–	–	–	–
S2	40.05	–	–	–	–	–	–	–	–	–	7.52	52.43	–	–	–	–
S3	35.20	–	–	–	–	–	–	–	–	–	7.48	57.32	–	–	–	–
S4	–	–	–	–	–	–	–	–	–	–	–	59.92	–	–	40.08	–
S5	21.12	–	–	–	–	–	–	–	–	–	8.93	56.02	–	–	–	11.45 Cu_2O + 2.48 Fe_2O_3
BS1	–	15.14	5.02	–	–	10.09	–	–	4.98	12.19	–	44.87	–	–	–	7.21 CaF_2 + 0.25 NiO + 0.25 CoO
BS2	25.27	–	–	5.76	–	–	–	–	–	63.39	1.71	3.87	–	–	–	–
BS3	–	–	–	–	–	–	–	–	–	26.58	–	30.79	–	–	42.63	–
BS4	4.43	5.34	1.41	3.28	–	–	–	–	–	73.21	1.30	11.03	–	–	–	–
BS5	14.42	–	–	4.58	–	–	–	–	–	70.75	–	10.25	–	–	–	–
BS6	4.44	5.35	1.41	1.63	–	–	–	–	–	63.79	1.30	22.08	–	–	–	–
BS7	1.73	2.82	1.58	–	–	1.27	–	–	–	14.14	4.70	72.89	–	–	–	0.87 KCl
BS8	7.60	–	–	–	–	–	–	–	–	13.44	10.88	52.70	–	–	15.38	–
AB1	–	–	–	–	–	–	–	–	–	51.48	6.70	–	–	–	–	41.82 CuO
AB2	–	–	–	–	–	–	–	–	–	43.43	13.83	–	–	–	–	42.74 CuO
AB3	–	–	–	–	–	–	–	–	–	33.26	14.83	–	–	–	–	51.91 CuO
LB1	–	–	–	–	–	–	–	–	4.64	21.27	3.31	4.21	–	–	61.02	4.62 CuO + 0.93 Bi_2O_3
LB2	–	–	–	–	–	–	–	–	4.99	21.11	3.40	4.33	–	–	60.60	4.58 CuO + 0.99 Bi_2O_3
LB3	–	–	–	–	–	–	–	–	–	33.77	3.78	–	–	–	49.74	12.71 Tl_2O
ZB1	–	–	–	–	–	–	–	–	8.11	28.44	–	2.75	–	–	53.97	6.73 PbF_2
ZB2	–	–	–	–	–	–	–	–	–	30.09	1.67	2.83	–	–	65.41	–
ZB3	–	–	–	–	–	–	–	–	4.02	31.01	1.60	2.71	–	–	60.66	–
ZB4	–	–	–	–	–	–	–	–	61.37	38.63	–	–	–	–	–	–
ZB5	–	–	–	–	–	–	–	–	43.78	17.05	–	–	–	–	–	39.17 V_2O_5
ZB6	4.94	–	–	–	–	–	–	–	46.62	33.50	4.99	9.95	–	–	–	–
ZB7	–	–	–	–	–	–	–	–	66.63	33.37	–	–	–	–	–	–
ZB8	–	–	–	–	–	–	–	–	41.06	24.01	–	18.07	–	–	6.36	10.50 CuO
ZB9	–	–	–	–	–	–	–	–	60.13	25.78	–	12.28	–	0.11	0.70	1.0 SnO_2
ZB10	–	–	–	–	–	–	–	–	56.34	23.12	–	17.40	1.13	–	–	0.91 Ta_2O_5 + 0.93 CeO_2 + 0.17 Bi_2O_3
LZB1	–	–	–	–	–	–	–	–	10.85	20.30	–	–	–	–	68.85	–
LZB2	–	–	–	–	–	–	–	–	14.54	21.85	–	–	–	–	63.61	–
LZB3	–	–	–	–	–	–	–	–	9.50	22.21	–	12.89	–	–	55.40	–
LZB4	–	–	–	–	–	–	–	–	16.66	41.67	–	–	–	–	41.67	
LZB5	–	–	–	–	–	–	–	–	16.72	29.31	–	11.32	–	–	42.65	–
LZB6	–	–	–	–	–	–	–	–	37.67	44.02	–	–	–	–	18.31	–
LZB7	–	–	–	–	–	–	–	–	46.02	33.61	–	7.79	–	–	12.58	–
BH1	–	–	–	–	–	–	–	–	–	19.26	–	8.99	–	–	66.73	5.02 $PbBr_2$
BH2	–	–	–	–	–	–	–	–	–	19.34	–	8.78	–	–	66.84	5.04 $PbCl_2$
BH3	–	–	–	–	–	–	–	–	–	21.16	–	–	–	–	52.80	26.04 PbF_2
BH4	–	–	–	–	–	–	–	–	–	19.32	–	8.89	–	–	48.12	23.67 PbF_2

TABLE III (Continued)

Glass code	Composition (mol %)														
	Li_2O	Na_2O	K_2O	MgO	CaO	BaO	TiO_2	ZrO_2	ZnO	B_2O_3	Al_2O_3	SiO_2	P_2O_5	Sb_2O_3	PbO	Others
BH5	–	–	–	–	–	–	–	–	18.16	21.22	–	–	–	–	46.33	14.29 ZnF_2
BH6	–	–	–	–	–	–	–	–	35.00	35.00	–	–	–	–	–	30.00 PbF_2
BH8	–	–	–	–	–	–	–	–	40.00	42.50	–	–	–	–	–	17.50 PbF_2
P1	–	25.00	25.00	–	–	–	–	–	–	–	–	–	50.00	–	–	–
P2	–	35.00	15.00	–	–	–	–	–	–	–	–	–	50.00	–	–	–
P3	–	15.00	–	–	–	–	–	–	–	–	–	–	50.00	–	–	35.00 Ag_2O
P4	–	–	38.00	–	–	–	–	–	–	–	3.00	–	56.00	–	–	3.00 Fe_2O_3
P5	–	–	38.00	–	–	–	–	–	–	–	–	–	56.00	–	–	6.00 Fe_2O_3
P6	–	–	34.00	–	–	–	–	–	–	–	8.00	–	58.00	–	–	–
P7	–	–	34.00	–	–	–	–	–	–	–	4.00	–	58.00	–	–	4.00 Fe_2O_3
P8	–	–	30.00	–	–	–	–	–	–	–	10.00	–	60.00	–	–	–
P9	–	–	–	–	–	–	–	–	–	–	–	–	50.00	–	50.00	–
P10	–	–	–	–	–	–	–	–	–	–	–	–	58.80	–	41.20	–
P11	–	–	–	–	–	–	–	–	20.00	–	–	–	40.00	–	40.00	–
P12	–	–	–	–	–	–	–	–	20.00	–	–	–	50.00	–	30.00	–
P13	–	–	–	–	–	26.47	–	–	–	9.72	6.63	–	57.18	–	–	–
P14	–	–	–	–	–	8.11	–	–	30.57	–	–	–	61.32	–	–	–
P15	–	–	–	–	–	–	–	–	30.00	–	–	–	50.00	–	20.00	–
P16	–	–	–	–	–	15.78	–	–	29.74	–	11.87	–	42.61	–	–	–
P17	–	–	–	–	–	–	–	–	–	–	26.84	–	32.88	–	–	40.28 CuO
P18	–	–	–	–	–	–	–	–	40.42	7.87	5.38	–	46.33	–	–	–
P19	–	–	–	–	–	2.82	–	–	42.48	–	4.77	8.08	41.85	–	–	–
A1	–	–	24.31	–	–	–	–	–	–	–	–	–	–	30.19	–	45.50 As_2O_3
A2	–	–	19.99	–	–	–	–	–	–	–	–	–	–	60.03	19.98	–
A3	–	–	22.76	–	–	–	–	–	–	–	–	11.04	–	66.20	–	–
A4	4.88	4.03	4.86	–	–	–	–	–	7.16	14.35	–	–	–	57.54	7.18	–
A5	6.23	3.00	9.88	–	–	–	–	–	–	13.37	–	9.30	–	41.51	16.69	–
A6	–	–	–	–	–	–	–	–	–	42.15	–	–	–	42.95	14.90	–
V1	–	–	–	–	–	–	–	–	–	–	–	–	–	–	47.50	5.00 As_2O_3 + 47.5 V_2O_5
V2	–	–	–	–	–	–	–	–	–	–	–	–	–	–	30.00	10.00 As_2O_3 + 60.00 V_2O_5
V3	–	–	–	–	–	–	–	–	–	–	–	–	–	25.00	–	50.00 V_2O_5 + 25.00 As_2O_3
DS1	–	–	–	–	–	–	–	–	18.75	21. 91	–	6.36	–	–	52.98	–
DS2	–	–	–	–	–	–	–	–	18.65	19. 61	1.49	6.31	–	–	50.99	2.95 CdO
DS3	–	–	–	–	–	–	–	–	18.75	19.73	1.50	6.35	–	–	51.28	2.39 Fe_2O_3
DS4	–	–	–	–	–	–	–	–	–	26.99	–	–	–	–	60.24	9.49 TeO_2 + 3.28 Tl_2O
DS5	–	–	–	–	–	–	9.83	–	–	33.85	–	–	–	–	56.32	–
DS6	–	–	–	–	–	1.99	–	–	20.67	19.77	0.75	5.09	–	–	51.73	–
DS7	–	–	–	–	–	–	9.12	–	–	41.89	–	–	–	–	48.99	–
DS8	–	–	–	–	–	–	–	–	18.29	21.37	2.92	7.43	–	–	49.99	–
DS9	–	–	–	–	–	–	–	–	18.55	17.34	1.48	2.51	–	0.26	50.37	9.49 CuO
DS10	–	–	–	–	–	–	8.12	–	23.92	13.98	–	16.20	–	–	37.78	–
DS11	–	–	–	–	–	4.30	19.79	–	8.10	14.19	–	16.44	–	–	37.18	–
DS12	–	–	–	–	–	–	–	–	19.63	14.91	1.57	6.65	–	–	57.24	–
DS13	–	–	–	–	–	–	19.34	–	15.83	12.02	2.53	13.93	–	–	36.35	–
DS14	–	–	–	–	–	–	17.24	–	–	39.56	–	–	–	–	43.20	–
DS15	–	–	–	–	–	–	–	–	50.86	16.65	–	26.18	–	–	6.31	–
AS1	–	9.68	–	–	–	–	–	–	–		1.07	78.93	–	–	–	10.32 F
AS2	–	9.19	–	–	–	–	–	–	–	–	–	80.82	–	–	–	9.99 F
AS3	24.40	–	–	–	–	–	–	–	–	2.68	2.88	69.02	1.02	–	–	–
AS4	–	14.12	–	–	–	–	–	–	–	–	–	85.88	–	–	–	–
AS5	20.29	–	2.50	–	–	–	–	–	–	2.22	2.40	71.75	0.84	–	–	–
AS6	23.70	–	2.80	–	–	–	–	–	–	2.60	2.80	67.10	1.00	–	–	–
AS7	23.46	–	2.90	–	–	–	–	–	–	2.57	2.77	66.35	1.95	–	–	–
AS8	23.09	–	2.85	–	–	–	–	–	–	5.06	2.73	65.31	0.96	–	–	–
AS9	22.30	–	1.50	–	–	–	–	–	3.00	–	–	72.50	0.70	–	–	–
AS10	22.86	–	–	19.31	–	–	–	–	–	–	–	56.77	1.06	–	–	–
AS11	23.04	–	2.85	–	–	–	–	–	–	2.52	5.44	65.19	0.96	–	–	–
AS12	22.53	–	1.48	–	–	–	–	–	–	–	2.13	72.68	1.18	–	–	–
AS13	28.45	–	3.51	–	–	–	–	–	–	3.12	3.36	60.37	1.19	–	–	–
AS14	24.06	–	2.97	–	–	–	–	–	–	2.05	2.84	68.08	–	–	–	–
AAS1	–	–	–	22.50	–	–	4.90	2.10	–	–	19.10	46.50	4.90	–	–	–
AAS2	–	–	–	–	–	16.51	12.70	–	–	–	10.68	60.12	–	–	–	–
AAS3	–	–	–	–	10.97	–	9.60	–	–	–	18.10	61.33	–	–	–	–
AAS4	–	–	–	21.13	–	–	7.08	–	–	–	11.65	60.14	–	–	–	–

TABLE III (Continued)

Glass code	Composition (mol %)															
	Li_2O	Na_2O	K_2O	MgO	CaO	BaO	TiO_2	ZrO_2	ZnO	B_2O_3	Al_2O_3	SiO_2	P_2O_5	Sb_2O_3	PbO	Others
AAS5	15.90	3.80	–	18.90	–	–	3.80	1.20	–	3.40	10.40	41.60	1.00	–	–	–
AAS6	–	–	–	23.07	–	–	6.98	–	–	–	12.16	57.79	–	–	–	–
AAS7	–	–	–	14.34	–	–	9.02	–	–	–	14.14	62.50	–	–	–	–
AAS8	–	–	–	6.07	6.42	–	9.44	–	–	–	17.79	60.28	–	–	–	–
ZAS1	–	–	–	–	–	–	2.58	–	29.75	–	10.20	57.47	–	–	–	–
ZAS2	–	–	–	–	–	–	1.80	–	25.92	–	13.79	58.49	–	–	–	–
ZAS3	–	–	–	7.45	–	–	7.61	–	22.42	–	11.93	50.59	–	–	–	–
ZAS4	–	–	–	–	–	–	6.68	–	24.65	–	13.09	55.58	–	–	–	–
ZAS5	–	–	–	3.50	–	–	–	–	32.04	2.02	9.67	52.77	–	–	–	
ZAS6	22.09	–	–	–	–	–	5.35	–	12.62	–	9.47	50.47	–	–	–	–
ZAS7	–	4.31	–	–	–	2.24	–	–	28.84	–	6.90	56.60	1.11	–	–	–
ZAS8	23.18	–	–	–	–	–	–	0.74	13.23	–	9.93	52.92	–	–	–	–
TAS1	–	–	–	–	–	–	8.30	–	–	–	18.16	49.61	–	–	–	23.93 CoO
TAS2	–	–	–	–	–	–	8.15	–	–	–	15.94	54.22	–	–	–	21.69 CoO
TAS3	–	–	–	–	–	–	9.61	–	–	–	18.23	52.33	–	–	–	19.83 MnO
TAS4	–	–	–	–	–	–	19.90	–	–	–	19.90	60.20	–	–	–	–
AZS1	18.10	–	1.30	–	–	–	–	–	20.10	–	–	59.40	1.10	–	–	–
AZS2	18.11	4.85	–	–	–	–	–	–	18.91	3.54	–	53.33	1.27	–	–	–
AZS3	18.16	–	1.28	–	–	–	–	–	20.23	–	–	59.20	–	–	–	1.13 MoO_3
AZS4	18.74	4.81	–	–	–	–	–	–	18.67	3.51	–	53.35	0.92	–	–	–
AZS5	18.40	–	–	–	–	–	–	–	20.30	–	–	60.10	1.20	–	–	–
AZS6	17.84	5.25	–	–	–	–	–	–	17.73	4.31	–	53.64	1.23	–	–	–
AZS7	17.49	5.15	–	–	–	–	–	–	17.37	4.22	–	52.56	1.21	–	–	2.00 Cr_2O_3
AZS8	22.20	–	1.47	–	–	–	–	–	3.74	–	–	71.85	0.74	–	–	–
AZS9	17.91	1.47	1.61	–	–	–	–	–	17.82	4.26	0.60	55.00	1.33	–	–	–
AZS10	17.49	5.15	–	–	–	–	–	–	17.37	4.22	–	52.56	1.21	–	–	2.00 Ta_2O_5
AZS11	–	–	–	21.00	–	–	4.00	–	20.00	–	5.00	50.00	–	–	–	–
AZS12	–	–	–	31.93	–	–	3.24	–	12.66	–	5.04	47.13	–	–	–	–
AZS13	17.90	1.47	1.61	–	–	–	–	–	17.82	4.26	0.60	55.00	1.33	–	–	–
ACS1	20.70	–	–	–	–	–	–	–	–	–	2.60	43.78	–	–	–	32.92 CdO
ACS2	21.54	–	–	–	–	–	–	–	–	–	0.90	62.00	–	–	–	15.56 CdO
ACS3	25.72	–	–	–	–	–	–	–	–	–	–	38.37	–	–	–	35.91 CdO
ZBS1	–	–	–	–	–	4.75	–	–	54.30	31.73	4.37	4.85	–	–	–	–
ZBS2	11.71	–	–	–	–	–	–	–	24.50	28.64	13.04	22.11	–	–	–	–
ZBS3	–	–	–	–	–	–	–	–	41.67	21.65	10.35	26.33	–	–	–	–
ZBS4	–	2.37	–	9.12	–	–	–	–	50.46	29.48	4.04	4.53	–	–	–	–
LS1	19.43	–	1.37	–	–	–	–	–	10.38	–	–	63.55	1.22	–	4.05	–
LS2	–	–	–	–	–	–	18.51	–	–	–	5.75	34.60	–	–	41.14	–
PC1	–	40.00	–	–	–	10.00	–	–	–	–	–	–	50.00	–	–	–
PC2	–	20.00	–	–	–	30.00	–	–	–	–	–	–	50.00	–	–	–
PC3	–	–	–	–	40.30	–	5.50	–	–	–	7.40	7.80	39.1	–	–	–
E1Cu	–	2.25	26.07	–	–	–	–	–	–	4.62	–	43.90	–	–	23.16	–
E2Cu	–	–	38.84	–	–	–	–	–	–	–	–	43.81	–	–	17.35	–
E3Cu	–	16.17	4.47	–	5.96	2.92	–	–	–	12.86	4.46	53.16	–	–	–	–
E4Cu	–	9.23	1.69	–	–	–	–	–	–	2.43	–	55.54	–	–	21.21	2.94 As_2O_3 + 6.96 SnO_2
E5Cu	–	4.21	4.98	–	–	–	–	–	–	–	–	52.10	–	–	23.38	6.21 NaF + 6.21 AlF_3 + 2.90 As_2O_3
E1A1	–	12.60	–	–	–	–	0.68	0.44	–	4.41	–	55.99	–	–	21.44	4.44 V_2O_5
E2A1	9.80	23.46	–	–	–	–	–	–	–	8.13	16.31	–	22.75	–	–	19.55 NaF
E3A1	48.63	–	–	–	–	–	–	–	–	–	–	39.38	–	0.60	11.39	–
E4A1	9.90	19.60	–	–	–	–	–	–	–	–	–	54.70	–	0.50	15.30	–

2.1.1. Silicate- and borosilicate-based glasses

There are many sealing, solder and enamelling glass compositions based on the silicate and borosilicate systems (e.g. [9–15]).The most common systems include zinc borosilicates, alkali silicates, alkali borosilicates, lead silicates, lead zinc silicates, and alkali copper silicates. A wide range of thermal expansions is possible in these systems, as summarized in Table I.

2.1.2. Borate-based glasses

There are also many sealing and solder glass compositions in the alumino-borate, lead borate and zinc borate systems, some with very low softening temperatures, i.e. < 400 °C (e.g. [6, 12, 16–23]). The alumino-borate glasses have low-to-intermediate thermal expansions, i.e. $\alpha \approx 4\text{–}8 \times 10^{-6}\,°C^{-1}$, whilst a range of expansions is possible in the other systems, from $\alpha \approx 5\text{–}15 \times 10^{-6}\,°C^{-1}$. In order to lower the

viscosity and softening temperatures of borate glasses further, various halide additions have also been incorporated [12, 24–26]. Fluorine is the most useful addition, the other halides, chlorine, bromine and iodine, generally lowering the stability of the glasses to an unacceptable degree. The chemical durability of borate-based glasses, although generally superior to the phosphate systems reported in the next section, is very much lower than that of most silicate-based systems.

2.1.3. Phosphate-based glasses

Zinc, barium and lead phosphate glasses have been reported with properties suitable for sealing, enamelling or solder applications [27–37]. These glasses exhibit relatively low softening temperatures, often $< 500\,^{\circ}C$. Unfortunately, phosphate glasses are not very resistant to chemical attack by water. Although improved chemical resistance can be achieved by addition of, for example, MgO, Al_2O_3, SiO_2, B_2O_3, etc., this is usually at the expense of an increase in the softening temperature.

2.1.4. Glasses based on less-common glass-forming oxides

A number of sealing and solder glass compositions have been reported based on some of the less-common glass-forming oxides, in particular, Sb_2O_3 or As_2O_3 [38], and V_2O_5 [39–41]. Very high thermal expansions have been noted for a number of Sb_2O_3-based glasses, with values for α in excess of $20 \times 10^{-6}\,^{\circ}C^{-1}$.

2.1.5. Devitrifiable solder glasses

The glasses described in the preceding sections remain vitreous during and after sealing. A class of solder glass has been developed, however, which crystallizes either completely or partially during the sealing or soldering operation. These glasses, originally described by Claypoole [42], are referred to as *devitrifiable* solder glasses. Devitrifiable solder glasses are normally based on either the relatively high thermal expansion lead zinc borate system or the lower expansion zinc borosilicate system [17, 18, 43–47]. Crystallizable solder glasses are usually employed by application of a mixture of glass particles in a suitable binder; crystallization occurs during sealing by a surface nucleation mechanism.

More comprehensive details on glass-forming systems in general are given elsewhere (e.g. [15, 48]).

2.2. Glass-ceramics

Crystallization of conventional glasses normally occurs by the nucleation of crystals at external surfaces. This gives rise to coarse microstructures with large anisotropic crystals which grow inwards from the surfaces. Such materials are usually very weak mechanically because the large crystals can act as powerful stress concentration sites. Control over the crystallization process by the introduction into suitable glass compositions of a large number of small heterogeneities which can act as efficient bulk nucleating centres can, on the other hand, lead to the formation of isotropic microstructures consisting of small, interlocking, randomly orientated ceramic crystals, usually bonded together by some residual glassy phases. The resultant glass-ceramic materials can exhibit very good mechanical and other properties. Bulk glass-ceramics are normally prepared employing a two-stage heat-treatment schedule, as illustrated in Fig. 2. During the nucleation stage a large number of small heterogeneities are formed within the glass at a temperature which is below that at which the major crystal phases can grow at a significant rate (if the crystal growth rate is high at the temperature of nucleation, rapid crystallization will occur from a limited number of nuclei, giving rise to a coarse microstructure). High nucleation rates are achieved in practice by the use of suitable nucleating agents added to the glass batch; these include various elemental metals, certain oxides, and various metallic halides and sulphides. The most common nucleating agents for silicate systems are TiO_2, ZrO_2, P_2O_5 and MoO_3 [49, 50]. The precise manner in which a given nucleating agent acts has not been determined unambiguously for all possible glass-ceramic systems, but a number of mechanisms have been identified (e.g. [51]). These include the precipitation of small crystallites of a compound formed by reaction between the nucleating agent and constituents of the glass, e.g. reaction of P_2O_5 with Li_2O to give Li_3PO_4 nuclei, and reaction of TiO_2 with MgO to give $MgTiO_2$. After successful nucleation, the temperature is raised during the crystallization stage so that crystal growth can occur from these nuclei. The glass-ceramics are a relatively new class of material, originally discovered at Corning Glass Works in the 1950s [52–55], and subsequently defined as *polycrystalline ceramic materials prepared by the controlled bulk crystallization of suitable glasses* [49, 50, 56–64].

A major advantage offered by glass-ceramics is that a greater range of practical thermal expansion coefficients can be obtained, relative to their glassy counterparts and, in addition, complex non-linear thermal expansion characteristics can be achieved. This, in principle, enables very close thermal expansion mat-

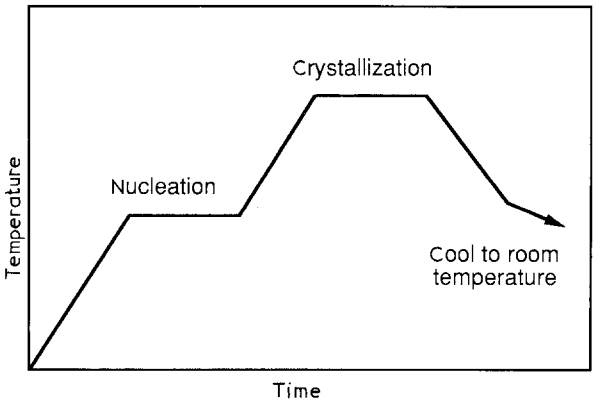

Figure 2 Heat-treatment schedule for the preparation of a bulk glass-ceramic material.

ching to a wide variety of metals and alloys, including those which exhibit non-linear behaviour due to phase transformations, etc. Data for the thermal expansions of a number of ceramic crystalline phases are summarized in Table IV. It has been shown to a first approximation [65] that the thermal expansion coefficient, α, of a glass-ceramic material is an additive function of the thermal expansions of the various phases present, and can be represented by the following relationship:

$$\alpha_{\text{glass-ceramic}} = (\alpha_1 K_1 W_1/\rho_1 + \alpha_2 K_2 W_2/\rho_2 + \cdots)/(K_1 W_1/\rho_1 + K_2 W_2/\rho_2 + \cdots) \quad (1)$$

where α_1, α_2 etc., are the thermal expansion coefficients of the various phases present in the glass-ceramic, K_1, K_2 etc., are the bulk moduli of these phases, W_1, and W_2 etc. are the weight fractions and ρ_1, ρ_2 etc., are the densities of the phases. The ability to tailor the thermal expansion characteristics of glass-ceramics is, therefore, a direct consequence of the ability to control (through selection of the starting glass composition and heat-treatment schedule) the type and proportion of crystalline phases present in the final glass-ceramic article.

Like glasses, glass-ceramics useful for sealing or coating applications can also be broadly classified according to their composition, as summarized below. Data illustrating the wide range of *practical* thermal expansions that can be achieved are summarized in Table V. Typical thermal expansion curves for a selection of glass-ceramic materials are shown in Fig. 3. Individual glass compositions are given in Table III.

TABLE IV Crystal phases and thermal expansion data

Name	Composition	Thermal expansion	
		α ($10^{-6}\,°C^{-1}$)	Range (°C)
Aluminium titanate	$Al_2O_3 \cdot TiO_2$	− 1.9	25–1000
Anorthite	$CaO \cdot AlO \cdot 2SiO_2$	4.5	100–200
Beryl	$3BeO \cdot Al_2O_3 \cdot 6SiO_2$	2.0	–
Calcium ortho-silicate	$CaO \cdot SiO_2$	10.8–14.4	–
Calcium zirconate	$CaO \cdot ZrO_2$	10.4	–
Celsian	$BaO \cdot Al_2O_3 \cdot 2SiO_2$	2.7	20–100
Chromium oxide	Cr_2O_3	7.0–9.6	–
Clinoenstatite	$MgO \cdot SiO_2$	7.8	100–200
		13.5	300–700
Cordierite	$2MgO \cdot 2Al_2O_3 \cdot 5SiO_2$	2.6	25–700
Cristobalite	SiO_2	12.5	20–100
		50.0	20–300
		27.1	20–600
Diopside	$CaO \cdot MgO \cdot 2SiO_2$	5.0	–
Enstatite	$MgO \cdot SiO_2$	9.0	20–400
		12.0	300–700
Eucryptite	$Li_2O \cdot Al_2O_3 \cdot 2SiO_2$	− 8.6	20–700
		− 6.4	20–1000
Forsterite	$2MgO \cdot SiO_2$	9.4	100–200
Geikielite (magnesium titanate)	$MgO \cdot TiO_2$	7.9	25–100
Lithium metasilicate	$Li_2O \cdot SiO_2$	13.0	20–300
Lithium disilicate	$Li_2O \cdot 2SiO_2$	11.0	20–600
Lithium zinc silicate	$Li_2O \cdot ZnO \cdot SiO_2$	9.0	20–200
Magnetite	$FeO \cdot Fe_2O_3$	7.0	–
Mullite	$3Al_2O_3 \cdot 2SiO_2$	5.3	–
Protoenstatite	$MgO \cdot SiO_2$	9.8	300–700
Quartz	SiO_2	11.2	20–100
		13.2	20–300
		23.27	20–600
Rutile	TiO_2	7.8	–
Spinel	$MgO \cdot Al_2O_3$	8.8	–
Spodumene	$Li_2O \cdot Al_2O_3 \cdot 4SiO_2$	0.9	20–1000
Stuffed keatite	$ZnO \cdot (ZnO \cdot SiO_2)$	3.0	–
Tridymite	SiO_2	17.5	20–100
		25.0	20–200
		14.4	20–600
Willemite	$2ZnO \cdot SiO_2$	3.0	–
Wollastonite	$CaO \cdot SiO_2$	9.4	100–200
Zircon	$ZrO_2 \cdot SiO_2$	4.2	–
Zirconia	ZrO_2	9.8–11.0	–
–	$ZrO_2 \cdot TiO_2 \cdot Y_2O_3$	6.5	–

2.2.1. Silicate-based glass-ceramics

2.2.1.1. Alkali and alkaline earth metal oxide silicate glass-ceramics. Glass-ceramic compositions in the alkali metal oxide silicate category are mainly based on lithium silicate, usually in combination with small

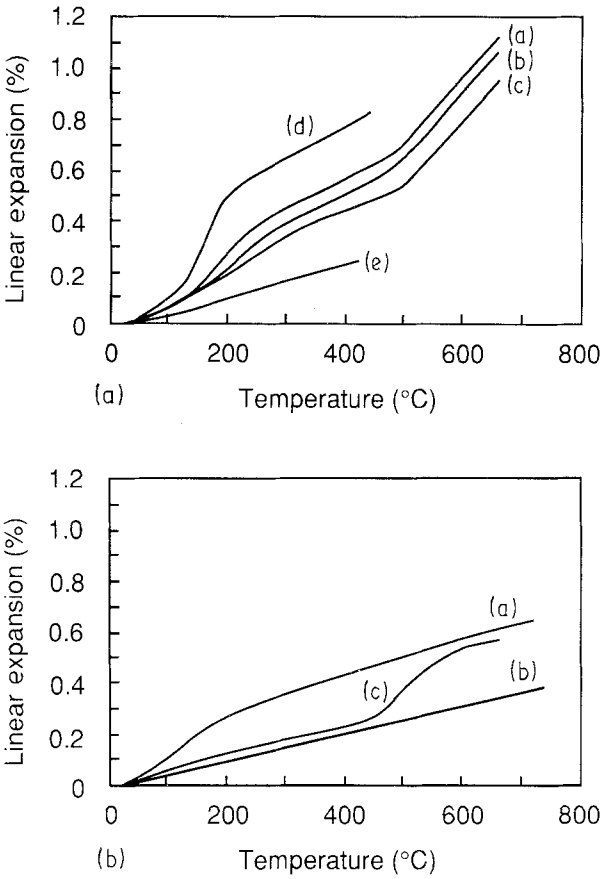

Figure 3 (a) Typical thermal expansion curves for a number of lithium zinc silicate glass-ceramic materials. (a) Composition AZS6, crystallized at 750 °C, after Donald *et al.* [98]; (b) composition AZS6, crystallized at 850 °C, after Donald *et al.* [98]; (c) composition AZS10, crystallized at 850 °C, after Donald *et al.* [98]; (d) composition AZS1, crystallized at 810 °C, after Chen and McMillan [94]; (e) composition AZS5, crystallized at 750 °C, after Chen and McMillan [94]. (b) Typical thermal expansion curves for a number of other silicate glass-ceramic materials. (a) Magnesium alumino-silicate glass (Composition AAS1) crystallized at 1150 °C, after Metcalfe and Donald [76], and Donald *et al.* [75]; (b) magnesium alumino-silicate glass (composition AAS1) crystallized at 1100 °C, after Metcalfe and Donald [76], and Donald *et al.* [75]; (c) lithium magnesium alumino-silicate glass (composition AAS5) crystallized at 900 °C, after Donald *et al.* [75].

TABLE V Glass-ceramic systems and thermal expansion data

Glass-ceramic code	Heat-treatment schedule	Thermal expansion ($10^{-6}\,°C^{-1}$)	Temperature range (°C)	Major crystalline phases	Reference
(A) Silicate glass-ceramics					
Alkali and alkaline earth metal oxide silicates					
AS1	120 min, 720 °C + 120 min, 840 °C	30.6	0–300	Cristobalite	[54, 55]
AS2	120 min, 720 °C + 480 min, 900 °C	24.4	0–300	Tridymite	[54, 55]
AS1	120 min, 720 °C + 240 min, 975 °C	23.6	0–300	Tridymite	[54, 55]
AS3	15 min, 1010 °C + 15 min, 670 °C	18.7	50–300	Lithium metasilicate + quartz	[71]
	+ 30 min, 820 °C	15.3	50–550	+ residual glass	
		13.0	50–800		
AS4	120 min, 720 °C + 480 min, 900 °C	17.7	0–300	Tridymite	[54, 55]
AS5	15 min, 1010 °C + 15 min, 670 °C	16.8	50–300	Lithium metasilicate + tridymite	[71]
	+ 30 min, 820 °C	14.0	50–550	+ lithium disilicate	
		15.0	50–800		
AS6	20 min, 1000 °C + 15 min, 650 °C	14.5	Not specified	Lithium metasilicate	[70]
	+ 20 min, 820 °C			+ lithium disilicate + cristobalite	
AS7	15 min, 1010 °C + 15 min, 670 °C	14.0	50–300	Cristobalite + lithium metasilicate	[71]
	+ 30 min, 820 °C	12.5	50–550	+ lithium disilicate + residual	
		14.1	50–800	glass	
AS8	15 min, 1010 °C + 15 min, 670 °C	13.9	50–300	Lithium metasilicate + cristobalite	[71]
	+ 30 min, 820 °C	13.2	50–550	+ quartz + residual glass	
		16.3	50–800		
AS9	60 min, 500 °C + 540 min, 700 °C	12.6	20–500	Lithium disilicate + quartz	[67]
AS9	60 min, 500 °C + 60 min, 750 °C	12.1	20–500	Lithium disilicate + quartz	[67]
AS10	Nuc. + 60 min, 850 °C	11.5	20–500	Not specified	[66]
AS11	15 min, 1010 °C + 15 min, 670 °C	10.8	50–300	Quartz + lithium metasilicate	[71]
	+ 30 min, 820 °C	9.5	50–550	+ residual glass	
		13.2	50–800		
AS12	Nuc. + 60 min, 850 °C	10.2	20–500	β-spodumene	[66]
				+ lithium disilicate	
AS13	15 min, 1010 °C + 15 min, 670 °C	10.2	50–300	Lithium metasilicate	[71]
	+ 30 min, 820 °C	10.8	50–550	+ residual glass + lithium	
		13.5	50–800	disilicate	
AS14	15 min, 1010 °C + 15 min, 670 °C	10.0	50–300	Lithium metasilicate	[71]
	+ 30 min, 820 °C	10.4	50–500	+ residual glass + quartz	
AS9	60 min, 500 °C + 60 min, 700 °C	8.1	20–500	Lithium disilicate + residual glass	[67]
Alkali and alkaline earth metal oxide alumino-silicates					
AAS1	30 min, 860 °C + 30 min, 1150 °C	9.6	20–460	$Al_6Si_2O_{13}$ + cordierite	[75, 76]
		8.5	20–700	+ magnesium phosphate	
				+ zirconium titanate	
AAS2	Nuc. + 1230 min, 1100 °C	9.2	Not specified	Dibarium trisilicate	[77]
AAS3	Nuc. + 960 min, 1200 °C	8.5	Not specified	Anorthite + cristobalite	[77]
AAS4	Nuc. + 960 min, 1300 °C	6.3	Not specified	Cordierite + cristobalite	[77]
				+ magnesium titanate	
AAS5	30 min, 860 °C + 30 min, 900 °C	5.8	20–460	$Li_2Al_2Si_3O_{10}$ + β-spodumene	[75, 76]
		8.6	20–700	+ forsterite	
AAS6	Nuc. + 60 min, 1250 °C	5.6	Not specified	Cordierite + magnesium titanate	[77]
				+ rutile + cristobalite	
AAS1	30 min, 860 °C + 30 min, 1400 °C	4.7	20–460	$Al_6Si_2O_{13}$ + cordierite + zircon	[75, 76]
		5.0	20–700	+ residual glass	
AAS7	Nuc. + 960 min, 1300 °C	4.0	Not specified	Cordierite + rutile + cristobalite	[77]
AAS8	Nuc. + 180 min, 1250 °C	3.4	Not specified	Cordierite	[77]
				+ magnesium aluminium titanate	
Zinc alumino-silicates					
ZAS1	Nuc. + 150 min, 1200 °C	19.3	Not specified	Gahnite + cristobalite + willemite	[77]
				+ rutile	
ZAS2	Nuc. + 120 min, 1250 °C	18.3	Not specified	Gahnite + cristobalite + willemite	[77]
				+ rutile	
ZAS3	Nuc. + 60 min, 1200 °C	17.2	Not specified	Gahnite + willemite + cristobalite	[77]
				+ rutile	
ZAS4	Nuc. + 2700 min, 1250 °C	16.5	Not specified	Gahnite + cristobalite + willemite	[77]
				+ rutile	
ZAS5	15 min, 925 °C	5.2	Not specified	Willemite + gahnite + $MgAl_2Si_3O_{10}$	[83]
ZAS5	120 min, 940 °C	14.0	Not specified	As above + cristobalite	[83]
ZAS6	60 min, 555 °C + 60 min, 605 °C	8.8	20–300	β-Li_2ZnSiO_4 + residual glass	[84]
	+ 60 min, 630 °C	10.0	20–450		
ZAS7	30 min, 1050 °C	4.7	20–600	Not specified	[217, 234]

TABLE V (Continued)

Glass-ceramic code	Heat-treatment schedule	Thermal expansion ($10^{-6}\,°C^{-1}$)	Temperature range (°C)	Major crystalline phases	Reference
ZAS8	60 min, 540 °C + 60 min, 710 °C + 60 min, 900 °C	4.2 4.9 5.3	20–300 20–450 20–700	β-spodumene + γ_0-Li_2ZnSiO_4	[84]
Titanium alumino-silicates					
TAS1	Nuc. + 120 min, 1250 °C	17.4	Not specified	Not specified	[77]
TAS2	Nuc. + 960 min, 1100 °C	17.0	Not specified	Not specified	[77]
TAS3	Nuc. + 960 min, 1100 °C	9.4	Not specified	Pyrophanite + tridymite + mullite + quartz	[77]
Alkali and alkaline earth metal oxide zinc silicates					
AZS1	60 min, 520 °C + 60 min, 810 °C	18.8	20–400	Cristobalite + γ_{11}-lithium zinc silicate + γ_0-lithium zinc silicate	[94]
AZS2	5 min, 950 °C + 60 min, 460 °C + 60 min, 665 °C	17.1	20–460	Cristobalite + unidentified lithium zinc silicate + residual glass	[96]
AZS3	60 min, 500 °C + 60 min, 850 °C	16.5	20–500	Not specified	[72]
AZS4	5 min, 950 °C + 60 min, 465°C + 60 min, 700 °C	16.2	20–460	Cristobalite + unidentified lithium zinc silicate + residual glass	[96]
AZS5	60 min, 520 °C + 60 min, 920 °C	15.5	20–400	Quartz + γ_{11}-lithium zinc silicate + cristobalite + γ_0-lithium zinc silicate	[94]
AZS2	5 min, 950 °C + 60 min, 465 °C + 60 min, 850 °C	15.2	20–460	Cristobalite + quartz + tridymite + unidentified lithium zinc silicate	[96]
AZS6	5 min, 950 °C + 60 min, 585 °C + 60 min, 850 °C	14.3 15.5	20–460 20–550	Cristobalite + quartz + tridymite + unidentified lithium zinc silicate	[98]
AZS6	5 min, 950 °C + 60 min, 465 °C + 60 min, 850 °C	13.9 15.6	20–460 20–550	Cristobalite + quartz + tridymite + β_1-lithium zinc silicate + γ_0-lithium zinc silicate	[98]
AZS4	5 min, 950 °C + 60 min, 465 °C + 60 min, 850 °C	13.4	20–460	Cristobalite + quartz + unidentified lithium zinc silicate	[96]
AZS7	5 min, 950 °C + 60 min, 465 °C + 60 min, 850 °C	13.4 15.3	20–460 20–550	Tridymite + zinc chromate + unidentified lithium zinc silicate	[98]
AZS8	60 min, 480 °C + 60 min, 800 °C	12.0	20–400	Not specified	[89]
AZS9	5 min, 950 °C + 60 min, 465 °C	11.6	20–460	Not specified	[96]
AZS10	5 min, 950 °C + 60 min, 465 °C + 60 min, 850 °C	10.9 11.5	20–460 20–550	Quartz + unidentified Ta-rich phase + unidentified lithium zinc silicate + residual glass	[98]
AZS11	60 min, 725 °C + 60 min, 1100 °C	10.2	20–400	Enstatite solid solution + cristobalite + willemite solid solution	[99]
AZS12	60 min, 680 °C + 60 min, 1100 °C	8.7	20–400	Enstatite solid solution + cristobalite	[99]
AZS12	60 min, 680 °C + 60 min, 1000 °C	7.3	20–400	Enstatite solid solution	[94]
AZS1	60 min, 520 °C + 60 min, 750 °C	7.0	20–400	γ_{11}-lithium zinc silicate + γ_0-lithium zinc silicate + cristobalite	[94]
AZS5	60 min, 520 °C + 60 min, 750 °C	5.5	20–400	γ_{11}-lithium zinc silicate + cristobalite + γ_0-lithium zinc silicate	[94]
AZS11	60 min, 725 °C + 60 min, 800 °C	4.5	20–400	enstatite solid solution + residual glass	[99]
AZS12	60 min, 680 °C + 60 min, 800 °C	3.5	20–400	Enstatite solid solution + residual glass	[99]
Alkali and alkaline earth metal oxide cadmium silicates					
ACS1	240 min, 600 °C	8.3	?–600	Lithium and cadmium silicates + residual glass	[232]
ACS2	240 min, 600 °C	8.1	?–600	Lithium and cadmium silicates + residual glass	[232]
Alkali and alkaline earth metal oxide zinc alumino-borosilicates					
ZBS1	120 min, 500 °C + 120 min, 700 °C	7.3	20–500	Zinc aluminate + zinc borate + quartz	[235]
ZBS2	120 min, 600 °C + 120 min, 700 °C	6.3	20–500	Zinc aluminate + zinc borate + quartz	[235]
ZBS3	120 min, 620 °C + 60 min, 900 °C	4.5	20–500	Zinc aluminate + zinc borate + quartz	[235]

TABLE V (Continued)

Glass-ceramic code	Heat-treatment schedule	Thermal expansion ($10^{-6}\,°C^{-1}$)	Temperature range (°C)	Major crystalline phases	Reference
ZBS4	120 min, 500 °C + 120 min, 700 °C	3.5	20–500	Zinc aluminate + zinc borate + quartz	[235]
Lead silicates					
LS1	120 min, 500 °C + 60 min, 725 °C	17.0	Not specified	Not specified	[189]
LS2	Nuc. + 120 min, 780 °C	4.2	Not specified	Lead titanate	[77]
(B) Phosphate glass-ceramics					
PC1	120 min, 400 °C + 120 min, 450 °C	22.5	25–250	Sodium metaphosphate or sodium trimetaphosphate + sodium barium phosphate or barium phosphate	[101]
PC2	120 min, 450 °C + 120 min, 500 °C	16.2	25–250	As above	[101]
PC3	60 min, 670 °C + 60 min, 850 °C	14.1 8.6	20–185 185–650	Aluminium phosphate + unidentified phase	[102]
PC3	60 min, 700 °C + 60 min, 850 °C	12.6 9.2	20–185 185–650	Aluminium phosphate + unidentified phase	[102]

additions (i.e. < 5 wt %) of other oxides, e.g. Na_2O, K_2O, B_2O_3, Al_2O_3, ZnO, etc., together with a suitable nucleating agent, which in the case of lithium silicate glass-ceramics is normally P_2O_5. The major crystalline phases that can be formed in this system are lithium metasilicate and lithium disilicate, together with various silica phases, e.g. cristobalite, quartz or tridymite. Depending on the proportions of phases present, moderate-to-high thermal expansion glass-ceramics can be produced, with α normally in the range $\approx 8\text{–}19 \times 10^{-6}\,°C^{-1}$ (e.g. [66–71]).

2.2.1.2. Alkali and alkaline earth metal oxide alumino-silicate glass-ceramics. Glass-ceramics in this category are mainly based on the lithium, magnesium, calcium or barium alumino-silicate systems. The nucleating agent normally employed for these compositions is TiO_2, ZrO_2 or a mixture of the two. The major crystalline phases that can be produced include β-spodumene, β-eucryptite, β-quartz solid solutions, cordierite, enstatite, wollastonite, sphene and celsian, together with silica. Depending on the precise phases, low-to-moderate thermal expansions can be achieved, ranging from zero (or even negative) to $\approx 9 \times 10^{-6}\,°C^{-1}$ (e.g. [66, 72–76]).

2.2.1.3. Zinc alumino-silicate glass-ceramics. The preparation of alkali-free glass-ceramics in the zinc alumino-silicate system was first reported by Corning Glass Works [77], using TiO_2 as the nucleating agent. The glass-ceramics so produced were of relatively low thermal expansion and contained gahnite, willemite and rutile as the major crystalline phases. Further work on this system was reported by McMillan and Partridge [78] and Partridge *et al.* [79, 80], and Vargin and Miklyukov [81], who also used TiO_2 as the nucleating agent, in addition to Strnad *et al.* [82] and Holleran and Martin [83] who employed ZrO_2. Depending on the precise glass composition and heat-treatment schedule adopted, a range of thermal expansions is possible, with values for α from $\approx 3\text{–}15 \times 10^{-6}\,°C^{-1}$. The higher expansion materials contain a significant proportion of cristobalite.

Alkali-containing zinc alumino-silicate glass-ceramics have also been reported. For example, Omar *et al.* [84] prepared glasses in the lithium zinc alumino-silicate system containing up to 13 wt% Li_2O and up to 28 wt % ZnO. These glasses, which contained TiO_2 or ZrO_2 as nucleating agent, could be crystallized to yield glass-ceramic materials with low-to-moderate thermal expansion coefficients in the range 3.6–10.0 $\times 10^{-6}\,°C^{-1}$. The predominant crystalline phases were β_{11}-Li_2ZnSiO_4, γ_0-Li_2ZnSiO_4, β-spodumene and β-eucryptite, although the higher thermal expansion materials also contained a significant proportion of residual glass.

2.2.1.4. Lithium zinc silicate glass-ceramics. Glass-ceramics based on the lithium zinc silicate system were first reported by McMillan and Partridge in 1963 [85]. These materials contained up to 59 wt% ZnO, although 30 wt% was described as an upper preferred limit. Unlike the earlier zinc alumino-silicates, the lithium zinc silicate compositions are nucleated by P_2O_5, and exhibit lower crystallization temperatures. Subsequently, further work was reported by McMillan and co-workers [86–91] on the preparation of a range of viable glass-ceramic materials from within this system. Glass-ceramics have been prepared exhibiting a wide range of thermal expansions, from $\approx 4\text{–}19 \times 10^{-6}\,°C^{-1}$.

Since the early work of McMillan and co-workers, limited additional work has been reported on this versatile glass-ceramic system [92–98]. For example, Donald and co-workers [96, 98] have examined the influence of a wide variety of transition metal oxide nucleating additives, used in conjunction with P_2O_5, on the crystallization kinetics, microstructures and thermal expansion characteristics of a lithium zinc

silicate glass. Transition metal oxide (TMO) additives investigated included TiO_2, ZrO_2, HfO_2, V_2O_5, Nb_2O_5, Ta_2O_5, Cr_2O_3, MoO_3, WO_3, NiO and CuO. It was noted that the nucleating efficiency, as measured by the activation energy for crystallization, is directly related to the ionic field strength of the additive employed, with bulk crystallization being favoured by nucleating species of high field strength, in particular molybdenum, tungsten and vanadium. It was also observed that the TMO additions have a pronounced effect on the thermal expansion characteristics of the resultant glass-ceramics. Using a standard heat-treatment schedule, it was noted that α could be varied over the range $10.9–15.8 \times 10^{-6}\,°C^{-1}$, depending on the precise TMO species involved. Variations in the thermal expansion were ascribed to differences in the concentration and ratios of the silica polymorphs cristobalite, quartz and tridymite.

2.2.1.5. Magnesium zinc silicate glass-ceramics. Only limited work has been reported on the preparation of magnesium zinc silicate glass-ceramics (see [99]). Chen and McMillan [99] noted that the glass-forming ability could be greatly expanded by incorporating small additions of Al_2O_3, together with TiO_2 as a nucleating agent. Crystallized materials contained varying proportions of enstatite solid solution, willemite and cristobalite; thermal expansions in the range $3.5–10.2 \times 10^{-6\circ}\,C^{-1}$ were obtained, depending on the crystallization temperature employed.

2.2.2. Phosphate-based glass-ceramics

Only limited attention has been devoted to the controlled crystallization of phosphate glasses to produce glass-ceramic materials. Much of this work has been aimed at the production of biomedical materials based on calcium phosphate for applications involving bone replacement and dental implants (e.g. [100]). Of particular interest for sealing work, however, Wilder *et al.* [101] examined the crystallization behaviour of a number of phosphate systems, including $Na_2O–CaO–P_2O_5$, $Na_2O–BaO–P_2O_5$, $Na_2O–Al_2O_3–P_2O_5$ and $Li_2O–BaO–P_2O_5$. The effect of a number of potential nucleating species was investigated, including TiO_2, ZrO_2, Y_2O_3, La_2O_3, Ta_2O_5, WO_3 and platinum. Of these additions, only platinum was found to be effective at promoting bulk crystallization. Relatively high thermal expansion coefficients in the range $16.2–22.5 \times 10^{-6}\,°C^{-1}$ were achieved. A more recent study by Wang and James [102] of calcium phosphate glasses containing a number of oxide and fluoride additions has shown that TiO_2 in conjunction with Al_2O_3 can be employed to promote bulk crystallization. Glass-ceramic materials with thermal expansion coefficients in the range $8.6–14.1 \times 10^{-6}\,°C^{-1}$ were successfully prepared in this study. In addition, Langlet *et al.* [103] have studied the crystallization behaviour of aluminium phosphate glasses and noted that Li_2O, $NaPO_3$ and AlF_3 can aid in the crystallization process.

3. Technology of glass- and glass-ceramic-to-metal seals and coatings

3.1. Requirements

The main requirements for the formation of a high-quality seal or coating are the ability to form a strong bond between the components and the ability either to match as closely as possible the thermal expansion characteristics of the two dissimilar materials, or, alternatively, to ensure that the expansion characteristics are such that only compressive stresses are generated in the brittle glass or glass-ceramic phase. In addition, to control the thermal expansion behaviour, the glass must meet a number of other requirements. These include an ability to wet and spread over the metal surface(s) at a realistic temperature, to bond chemically to the metal but not to promote the formation of undesirable reaction products that may alter the properties at the interface, and to possess acceptable electrical, mechanical, chemical and physical properties. The requirements for the production of strong, dense coatings are similar to those for the production of seals, although it is usual to employ systems in which the coating is in mild compression, rather than being matched in expansion. As coatings are normally initially applied to the substrate in the form of a suspension of glass particles it is, however, more critical that the glass wets and flows sufficiently to cover the substrate, and that the individual glass particles coalesce to form a dense, pore-free coating. The overall requirements may also be strongly dependent upon the specific application. For example, a *refractory* coating impervious to oxygen is required for the protection of a metal from high-temperature oxidation. In addition, *specific* requirements for seals and coatings may differ, in particular the manner in which the constituent materials are processed prior to fabrication, as described in the following sections.

3.2. Preparation of seals and coatings

3.2.1. Seals

3.2.1.1. Glass-to-metal seals. In the preparation of seals it is essential that the components are thoroughly cleaned prior to assembly and fabrication, in order to prevent the formation of gaseous reaction products during sealing which may give rise to bubbles within the seal. In the case of the metal parts this may involve vacuum annealing and/or solvent cleaning/degreasing procedures (see, for example, [104, 105]). It is also usual, although not always essential, to pre-oxidize metal parts prior to sealing. The pre-oxidation stage can be very crucial, too thick or too thin an oxide layer, or the wrong type of oxide, and the seal may be mechanically weak or not hermetic. The glass component of the seal will normally also be cleaned prior to sealing, and may also be lightly etched in an aqueous solution of hydrofluoric acid. The starting glass may be employed as a dense, solid pre-form of suitable shape which is positioned with the metal parts by the use of suitable jigging. Alternatively, the glass may be used as a powder which is packed into the components to be sealed. A further method which has been used successfully to prepare glass-to-metal seal

components is vacuum-assisted injection moulding [106–109]. In this process, molten glass is injected under pressure into the metal parts to be sealed held in a suitable mould. A vacuum is applied simultaneously to the opposite side of the mould in order to remove trapped gases and increase the flow of glass.

Seals can be classified according to a number of different criteria. For example, according to thermal expansion characteristics, e.g. matched thermal expansion seals or compression seals, or according to geometry considerations, e.g. tubular seals, bead seals, etc. Further details on the classification of seals can be found elsewhere (e.g. [104]).

3.2.1.2. Glass-ceramic-to-metal seals. In the case of a glass-ceramic seal, it is usual to employ a solid glass pre-form which is positioned relative to the metal parts by the use of suitable graphite jigging; a typical assembly is shown in Fig. 4. A heat-treatment cycle will normally include a high temperature sealing stage

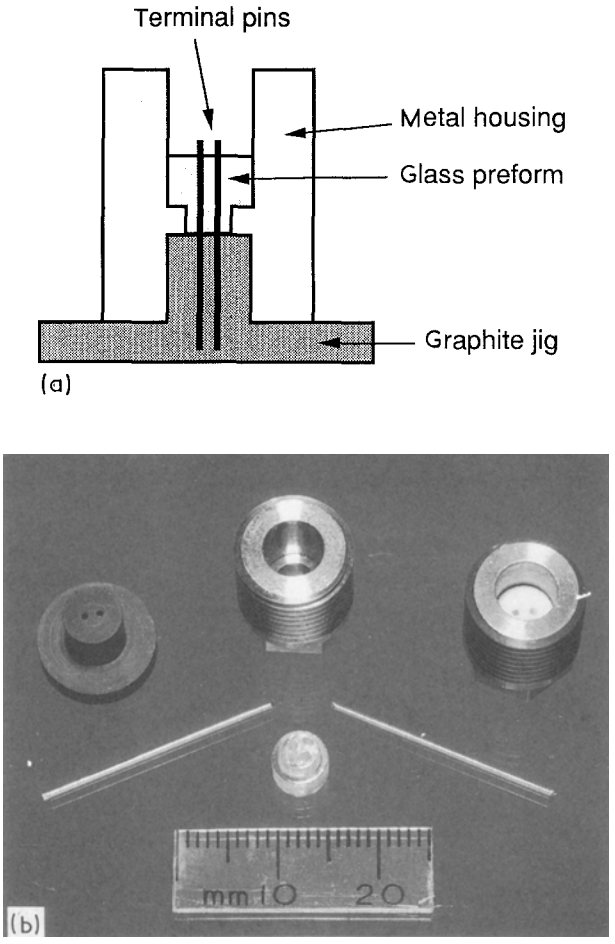

Figure 4 Example of piece-parts and fixturing employed in the preparation of an electrical feed-through seal component: (a) schematic diagram, (b) specific parts, after Metcalfe *et al.* [188]. This particular example consists of a cylindrical metal housing containing a glass-ceramic-to-metal seal into which are bonded two electrical terminal pins. During assembly of this component, a machined glass preform is inserted into the housing, with the terminal pins passing through holes drilled into the preform; the pins are held in place by a graphite jig. The assembly is subsequently taken through a controlled sealing and heat-treatment schedule, as depicted in Fig. 5, in order to bond the glass to the metal parts and to crystallize the glass to yield a glass-ceramic material with thermal expansion matched to that of the metal parts.

in order to melt the glass, followed by a lower temperature nucleation stage, and finally a higher temperature crystallization stage, as shown in Fig. 5. Hence, a modification of the standard glass-ceramic process is employed, and this must be taken into account when tailoring the thermal expansion characteristics for a specific application. Alternatively, an accurately machined glass-ceramic preform may be sealed to the metal via an intermediate solder glass bond [90]. The sealing medium can be applied in powder form to the lightly oxidized metal faces to be sealed, and the metal components heated to fuse the glass coating. The metal and glass-ceramic elements are then assembled, using jigs where necessary, and the assemblies are bonded, usually by heating under load in a reducing atmosphere. The glass is partially exuded leaving only a thin film between the components. Suitable solder glass compositions can subsequently be heat-treated to induce crystallization and produce a more refractory crystalline intermediate bond, if required. Further details on the preparation of specific glass-ceramic compositions are given in Section 2.2.

More extensive details of the technology and types of glass- and glass-ceramic-to-metal seals are given elsewhere (e.g. [104, 105, 110–115]).

3.2.2. Coatings

3.2.2.1. Glass coatings. Much of the early work in this area was concerned with the preparation of enamelled metals. An enamel, often referred to as a vitreous or porcelain enamel when applied to a metal, is a predominantly glassy coating used either to protect the metal substrate; for example, when applied to cooking ware; or, alternatively, to provide aesthetically pleasing artefacts, as in jewellery and ornaments. The first major application for glass coatings on metals was in the preparation of porcelain-enamelled iron cooking pots and baths, started around the middle of the nineteenth century [10, 116].

The composition of a porcelain enamel coating is usually quite complex, consisting of glass-forming oxides, e.g. SiO_2 or B_2O_3, fluxes, e.g. Na_2O (or B_2O_3 in a dual role), and adherence promoters, e.g. CoO or NiO,

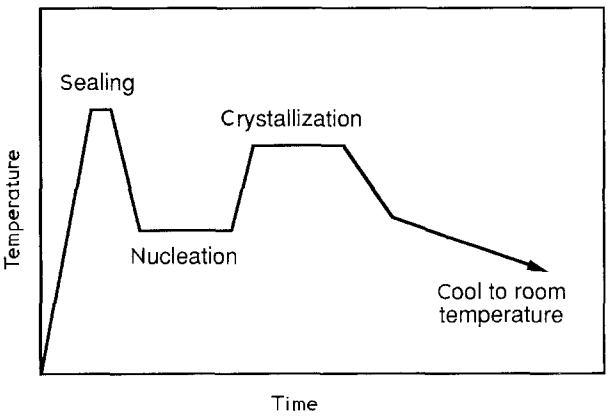

Figure 5 Modified heat-treatment schedule for the preparation of glass-ceramic-to-metal seals and coatings, consisting of a high-temperature sealing stage and lower temperature nucleation and crystallization stages.

together with colourings and opacifiers, e.g. CuO and TiO_2. Often a ground coat is applied first which possesses good bonding characteristics to the substrate. Unlike a seal, the substrate for a coating is often roughened, e.g. by grit blasting, prior to being cleaned and pre-oxidized. Subsequently, further coatings with specific properties may be laid down on top of the ground coat to provide, for example, abrasion or chemical resistance, or an aesthetically pleasing surface. Further details on the role of composition, including the use of adherence promoters, can be found elsewhere (e.g. [117, 118]).

There are many methods by which *ceramic* protective coatings may be applied to metals and alloys; for example, chemical or physical vapour deposition, sputter deposition, thermal or plasma spraying, etc. (e.g. [119, 120]). Traditionally, enamel coatings have been applied by a number of less exotic methods including dipping, painting or spraying. In these methods, the glass is added in the form of a suspension of glass particles in a liquid base, usually water, often with the addition of a suitable binder to make the suspension adhere to the substrate prior to high-temperature firing. The firing operation is carried out either in air or a controlled atmosphere at a temperature high enough to melt the glass particles and cause them to flow over and wet the substrate surface and fuse together. Firing in air leads to the formation of an oxide scale on the metal before the glass has had time to melt and flow. This oxide scale subsequently dissolves in the molten glass, and helps provide the chemical conditions necessary for strong bonding between the glass and the substrate. Alternatively, in the case of metals that are very easily oxidized, the metal substrate may be pre-oxidized prior to firing in an inert atmosphere; more control over the process is possible using the latter method. When metals are pre-oxidized prior to coating, it is essential that the conditions are chosen such that the appropriate metal oxide is formed, e.g. FeO in the case of iron (see Section 4.5), and that the oxide scale is highly adherent and non-porous. It is, therefore, necessary to have data for the oxidation behaviour of the metal or alloy in question (see, for example, [121]).

More recently, other methods have been employed to coat a metal substrate. These include electrostatic deposition in which a dry glass powder which has been given an electrostatic charge is applied to an oppositely charged substrate, electrodeposition where the component to be coated is immersed in a suitable slurry and made the anode of a galvanic cell, and screen printing in which a relatively high-viscosity suspension of glass particles is applied through a wire mesh on to the surface to be coated; this later method allows patterns to be printed on to the substrate. In addition, sol–gel methods offer potential for coating applications. Sol–gel processing [122–124] offers the advantage of being able to produce glasses at reduced temperatures, significantly below that required for preparation from the melt. This means, for example, that many refractory glasses which are very difficult to prepare by fusion techniques can now be made more readily. To date, sol–gel and ceramic coatings have mainly been applied to optical and related materials as anti-reflection coatings, and to glass articles for improving the mechanical properties [125–129]. The method does, however, offer scope for the coating of other materials, including metals.

A number of methods have also been reported for the coating of thin metal wires with an electrically insulating or protective glass layer. For example, wires may be drawn through molten glass held on a series of heated metal support loops, as reported by McMillan *et al.* [130]. Alternative methods rely on feeding wire through a heated glass tube [131], or drawing wire through a heated platinum bushing to which molten glass is metered via a platinum tube [132]. In addition, a remarkably simple and novel method for the preparation of thin metal wires coated with a glass layer in a single operation *directly* from the melt was first reported by Taylor in 1924 [133, 134]. In this method, known as the Taylor-wire or microwire process, the metal to be produced in wire form is held in a glass tube which is closed at one end. The metal is then melted and the glass softened. The end of the tube is subsequently drawn down to produce a glass-encapsulated metal filament. A micrograph of a typical microwire is shown in Fig. 6. The Taylor-wire process is illustrated schematically in Fig. 7a, and an actual production machine for the preparation of microwire [135] is shown in Fig. 7b. By suitable choice of the starting glass composition and drawing conditions it is possible to prepare wires of diameter in the range ≈ 1–$100\,\mu m$ coated with a layer of glass of thickness ≈ 2–$30\,\mu m$. Since the introduction of the Taylor-wire technique, many metals have been prepared as glass-coated filaments, including copper, silver, gold, iron, cobalt and lead, together with a number of iron-, nickel-, copper- and lead-based alloys, as reviewed recently by Donald [136].

3.2.2.2. Glass-ceramic coatings. Glass-ceramic coatings are a more recent addition to the family of coating materials. As in the case of seals, glass-ceramics offer all the advantages of glasses, in addition to the benefits of a more refractory nature and an ability to tailor the thermal expansion characteristics more closely to those of the substrate. Glass-ceramics may be applied, initially as a suspension of glass particles, employing

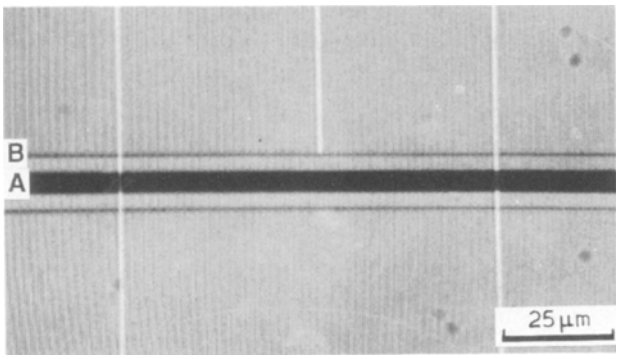

Figure 6 Copper microwire prepared using the Taylor-wire process; showing copper core, A, and glass coating, B; after Donald and Metcalfe [135].

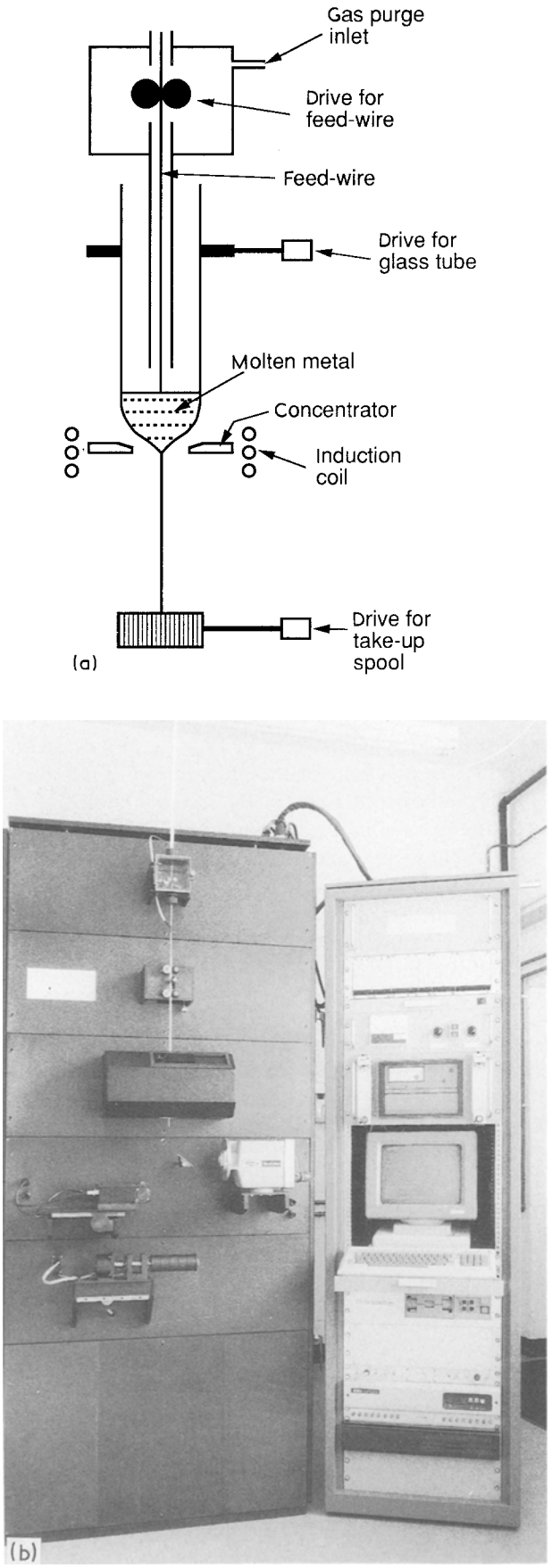

Figure 7 Taylor-wire process for the production of glass-coated metal wire: (a) schematic representation, (b) photograph of a production machine; after Donald and Metcalfe [135].

any of the standard methods. The heat-treatment schedule is normally more critical, however, and can involve separate fusing/consolidation, nucleation and crystallization stages. It is essential, during the high-temperature fusing or firing stage, that the individual glass particles do not rapidly crystallize. If crystallization does occur during this stage, it may not be possible for the individual glass particles to melt and flow adequately over the metal substrate; the production of a continuous and porosity-free coating would then not be feasible.

More extensive details of the technology of glass- and glass-ceramic-to-metal coatings are given elsewhere (e.g. [10, 116, 137–140]).

3.3. Methods used for studying seals and coatings

There are many diverse methods available for studying and characterizing seals and coatings. Only a brief summary of some of the more important techniques is given here.

Differential thermal analysis (DTA), and differential scanning calorimetry (DSC), are used extensively for the characterization of glass and glass-ceramic materials. When used in conjunction with dilatometry, which provides information on the thermal expansion behaviour of materials, the data obtained from DTA or DSC can be used in the derivation of appropriate heat-treatment schedules for selected metal/glass or metal/glass-ceramic systems. A technique related to DTA and DSC, namely dynamic mechanical thermal analysis (DMTA), has also been found useful by providing information on phase separation in glasses and in resolving the glass transition temperature, T_g, of the residual glassy phase in glass-ceramics [141, 142]. Great care must be exercised when carrying out thermal measurements using any of the above techniques, however, because the data obtained are very dependent on such parameters as sample condition, type of apparatus, use of appropriate calibration procedures, heating or cooling rates employed, etc. [143–148]. Extensive use is also made of X-ray diffraction analysis (XRD), for determining the types of crystalline phases present in glass-ceramic materials, and in scanning electron microscopy (SEM), for examination of microstructures. Use of SEM also enables (qualitative) X-ray analysis of individual microstructural features to be performed *in situ* in the SEM by means of the energy dispersive spectrometer facility (EDS), which is fitted to many modern instruments. This is particularly useful for the examination of small precipitates and other reaction products within a glass–metal interfacial region. Other useful structural and microstructural characterization techniques include transmission electron microscopy (TEM), small-angle neutron scattering (SANS), secondary ion mass spectroscopy (SIMS), and infra-red spectroscopy. Further details of these and related techniques, as applied to the materials and systems under review, are given elsewhere (e.g. [149]). The mechanical behaviour and adhesive properties of seals and coatings can be assessed using a number of techniques. For example, coating adhesion can be evaluated employing pull-off, shear or indentation methods, whilst other tests employ tribological techniques for determining resistance to abrasive, erosive and chemical media (see, for example [150, 151]).

3.4. Stresses in seals and coatings

Unless the thermal expansion characteristics of a given system are identical, stresses will be generated in a glass- or glass-ceramic-to-metal seal or coating as a result of the influence of differential contraction during cooling from the sealing or coating temperature. At temperatures close to the fabrication temperature, where the glass is in its supercooled liquid regime, rapid stress relaxation of the glass will occur so that the influence of differential contraction can normally be ignored. As the temperature is lowered, however, a point will be reached where stress relaxation of the glass becomes so slow that any differences in thermal contraction between the two materials can no longer be accommodated. A further decrease in temperature will then result in the creation, within the time-scales involved, of permanent stresses. If the contraction stresses arising within the brittle glass or glass-ceramic are tensile in nature, failure of this phase may occur either during cooling or, more seriously, at a later time when the component may be in service, due to the influence of static fatigue. It is generally accepted that residual tensile stresses should not exceed ≈ 10 MPa in order for a glass seal to remain hermetic over its service lifetime.

The point at which stress relaxation can no longer accommodate contraction stresses is often referred to as the "setting" or "set" point of the glass, T_{set}. Like the glass transition temperature, T_g, T_{set} is not, of course, a fixed temperature, but occurs over a range of temperature; and similarly, it depends on such factors as the cooling rate of the glass and its prior thermal history. The set point may be regarded as the temperature below which the glass behaves as an ideal elastic solid. It has variably been taken as equal to either the strain point of the glass (viscosity = $10^{13.5}$ Pa s) or its annealing point (viscosity = 10^{12} Pa s), or alternatively, as the strain point plus some arbitrary value, e.g. + 5 °C, or the annealing point minus an arbitrary value, e.g. − 15 °C or − 20 °C.

An estimate of the magnitude of the thermal strain due to differential contraction can be made by comparing the thermal expansion curves of the metal and the glass. The curve for the glass is then displaced, as shown in Fig. 8, so that the set point coincides with the curve for the metal. The differential contraction, δ, can then be found at any given temperature from the relative displacement of the two curves at that point. As a rough guide [152], δ should not exceed a value of $\approx 5 \times 10^{-4}$ in order to produce a satisfactory seal. From a knowledge of δ, it is possible to compute the corresponding residual stress. For example, for a thin glass coating on a metal substrate, the stress in the glass, σ_g, at a given temperature can be calculated to a first approximation using the expression [153]

$$\sigma_g = -E_g\delta/(1-\nu) \quad (2)$$

where E_g is Young's modulus of the glass, and ν is its Poisson's ratio. If the glass has a lower thermal expansion than that of the metal, the coating will be in compression on cooling; but if the compressive stresses are too high, spalling of the glass surface may occur. Conversely, if the glass has the higher expansion, the coating will be in tension, and if these stresses are of high enough magnitude cracking or crazing of the coating will occur.

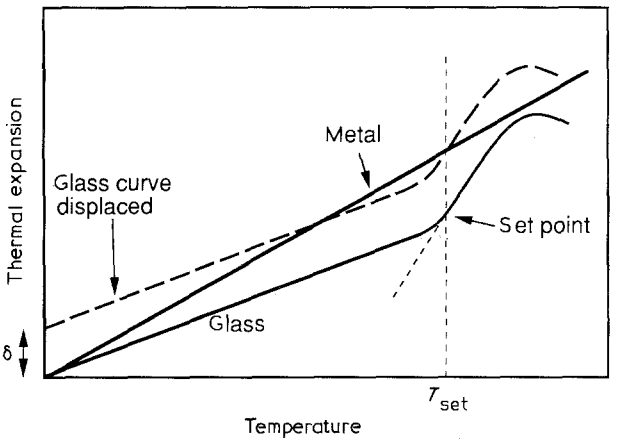

Figure 8 Thermal expansion curves of a metal and a glass illustrating one method that can be used for estimating the residual thermal stress in a seal or coating by measuring the resultant displacement of the glass curve (see text for details).

As an illustration of the effect that residual stresses can have on a more complex metal–glass system, consider the example of a seal consisting of a central metal pin sealed into a cylindrical metal housing, as depicted in Fig. 9. A number of scenarios are possible. For example, if the metal housing has a higher thermal expansion than that of the glass, the bulk glass will be in a state of radial compression on cooling, whilst the metal housing will be in a state of tension. Unless the metal is very thin this should present no serious problem for the integrity of the housing. If, however, the radial compression is sufficiently high, the glass surface near the metal may spall away under the influence of circumferential tension, as shown in Fig. 10a. In the case where the glass has a higher thermal expansion than the metal housing, on the other hand, the bulk glass will be in a state of circumferential tension, and failure may occur either at the metal–glass interface or at some distance within the glass, as illustrated in Fig. 10b. A similar case exists when the pin material has a higher expansion than that of the glass. The glass near to the pin will be in circumferential tension and either the metal–glass interface will fail, or circumferential cracks will develop in the glass near the pin. Finally, if the pin has a lower expansion than that of the glass, the glass will be in a state of radial tension, and cracks may form in the glass, as illustrated in Fig. 10c.

Approximate values for the stresses involved can be found using the following analysis, as described by Scherer [154]. This analysis assumes that plane strain conditions apply, and also assumes, to a first approximation, that the elastic moduli and Poisson's ratios of the glass and the metal components are similar in magnitude, i.e. $E_{glass} \approx E_{metal}$, and $\nu_{glass} \approx \nu_{metal}$. The stresses in the glass due to thermal expansion mismatch between the pin and the glass (neglecting any effect from the outer metal cylinder), can be given by

$$\sigma'_{z(glass)} = -(r_1^2/r_2^2)[E/(1-\nu)]\Delta\varepsilon' \quad (3)$$

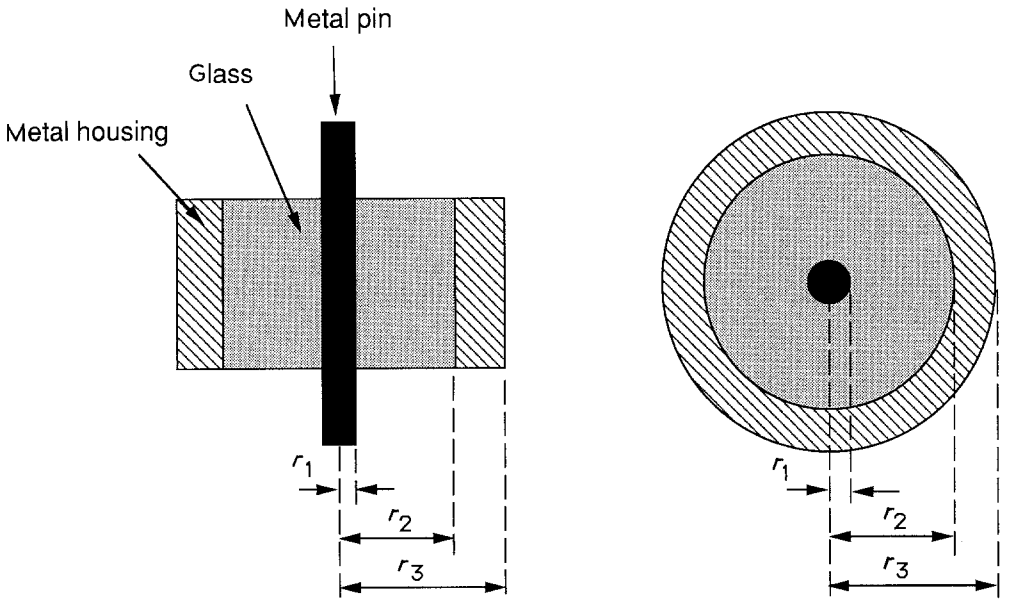

Figure 9 Schematic representation of a simple cylinder seal with a single central metal pin.

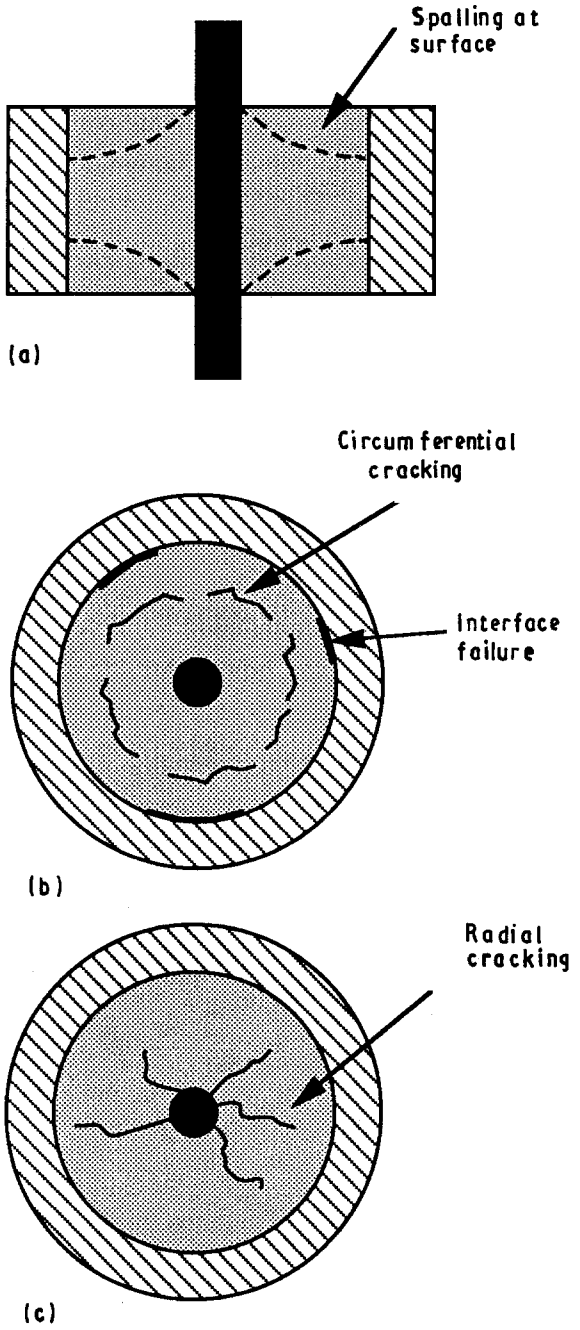

$$\sigma'_{r(glass)} = 1/2[1 - (r_2^2/r_1^2)]\,\sigma'_{z(glass)} \quad (4)$$

$$\sigma'_{\theta(glass)} = 1/2[1 + (r_2^2/r_1^2)]\sigma'_{z(glass)} \quad (5)$$

where $\sigma'_{z(glass)}$ is the axial stress, $\sigma'_{r(glass)}$ is the radial stress, $\sigma'_{\theta(glass)}$ is the circumferential (hoop) stress, and $\Delta\varepsilon' = (\alpha_{glass} - \alpha_{metal\ pin})\Delta T$, with $\Delta T = T_{set} - T_{ambient}$.

Similarly, the stress in the glass due to expansion mismatch between the glass and the outer metal cylinder (neglecting any effect from the inner metal pin), can be given by

$$\sigma''_{z(glass)} = [1 - (r_2^2/r_3^2)]\,[E/(1 - \nu)]\Delta\varepsilon'' \quad (6)$$

and

$$\sigma''_{r(glass)} = \sigma''_{\theta\,(glass)} = 1/2\,\sigma''_{z(glass)} \quad (7)$$

where $\Delta\varepsilon'' = (\alpha_{glass} - \alpha_{metal\ cylinder})\Delta T$.

Assuming superposition of stresses, the resultant stresses in the glass due to the influence of both the metal pin and the cylinder, can be given by the sums of the individual stresses

$$\sigma_{z(glass)} = \sigma'_{z(glass)} + \sigma''_{z(glass)} \quad (8)$$

$$\sigma_{r(glass)} = \sigma'_{r(glass)} + \sigma''_{r(glass)} \quad (9)$$

$$\sigma_{\theta(glass)} = \sigma'_{\theta(glass)} + \sigma''_{\theta(glass)} \quad (10)$$

Using Equations 8–10 an estimate of the stresses that are likely to occur in any given system can be made.

This description of the effect of stresses due to thermal expansion mismatch in glass–metal systems is greatly simplified, and many other factors may need to be taken into account when designing a suitable practical metal–glass component for a specific application. More comprehensive accounts of stresses in glass seals and coatings can be found elsewhere (e.g. [34, 110, 112, 154–156]).

The situation is complicated further in the case of glass-ceramic-to-metal seals and coatings due, in part,

Figure 10 Cracking in a cylinder seal due to the effect of thermal expansion mismatch stresses; (a) expansion of metal housing > expansion of glass; (b) expansion of glass > expansion of metal housing, (c) expansion of glass > expansion of metal pin.

to the more complex thermal expansion behaviour of glass-ceramic materials, coupled with the fact that the overall behaviour may be very composition and process dependent. In general, less information is available on the creation of residual stresses in metal/glass-ceramic systems. Although, in principle, it is possible to match the thermal expansion characteristics of a glass-ceramic material to those of a specific metal or alloy, in practice this can rarely be achieved over the entire temperature range of interest. High-expansion glass-ceramics (e.g. $\alpha > 14 \times 10^{-6}\,°C^{-1}$) normally rely on the presence of a significant proportion of cristobalite, α-quartz or tridymite, all of which undergo phase inversions; with the exception of tridymite, these are accompanied by relatively large volume changes, particularly in the case of cristobalite ($\approx 2\%$), as illustrated by the thermal expansion curves shown in Fig. 11. Such volume changes can lead to high residual stresses in a glass-ceramic system. The effect of these stresses can often be minimized by annealing if there is sufficient residual glassy phase present with a low enough T_g. Unfortunately, determining a value for T_g of residual glass is not usually feasible employing standard DTA or DSC techniques, unless there is a high proportion of residual glass present. It is, however, possible to determine T_g using DMTA, and this technique has been successfully employed in devising a suitable heat-treatment schedule for the preparation of glass-ceramic-to-metal seals containing quartz and tridymite [157]. The presence of cristobalite is particularly problematic because the α–β cristobalite inversion occurs at relatively low temperatures, i.e. ≈ 150–220 °C. It is, therefore, not generally practical to anneal out stresses associated with this transformation. For glass-ceramics containing cristobalite, this phase should be present as very small crystals, ideally < 1 μm in size, in order to minimize the detrimental effects of residual stresses caused by the α–β phase inversion. For glass-ceramics containing a sufficiently high proportion of residual glass, and which exhibit well-defined glass-like softening behaviour, it is possible to estimate the magnitude of residual stresses formed by sealing to a particular metal using the same method as employed for glass-to-metal seals, i.e. calculation of the thermal strain parameter, δ, from the respective thermal expansion curves, or calculation of the stresses employing Equations 8–10 (for the case of glass-ceramics it must be assumed that a set temperature can be defined, below which the material behaves elastically).

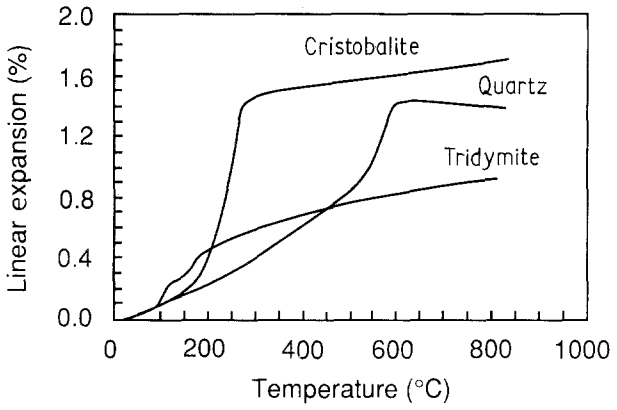

Figure 11 Thermal expansion curves for cristobalite, quartz and tridymite illustrating the large volume changes accompanying the α–β phase inversions.

An additional complication in both glass- and glass-ceramic-to-metal sealing can be caused by chemical reactions within the glass or glass-ceramic close to the metal interface which can alter the microstructure in this region, relative to the bulk material. This can have serious implications on the quality of the resulting seal or coating due to the fact that the thermal expansion characteristics of the interfacial zone may differ considerably from those of the bulk glass or glass-ceramic. Hence, an apparently thermally matched system may, in fact, exhibit high thermal expansion mismatch stresses within the interfacial zone. An assessment can be made experimentally employing strip seals, analogous to bimetallic strips, in which a thin glass or glass-ceramic layer is sealed to a thin metal strip. The curvature of the resultant composite strips can then be used to compute the magnitude of the interfacial stresses [158–160].

4. Metal–non metal bonding theories

The nature of the bond between a glass (enamel) and a metal has been the subject of considerable controversy over the years, but a clearer understanding of the factors involved has gradually emerged. A number of approaches have been applied in an attempt to elucidate the major factors responsible for attaining good bonding characteristics, as outlined below.

4.1. Thermodynamic approach

One of the first practical requirements for the formation of a viable glass-to-metal seal or coating is that the molten glass wets the surface of the metal and therefore spreads over it. When a liquid is brought into contact with a solid, a new interface is created between the liquid and the solid. This behaviour is often studied experimentally using the sessile drop method, depicted schematically in Fig. 12. As shown in this figure, the liquid may or may not spread across the solid surface. According to classical thermodynamic theory the liquid will spread only if the resultant energy of the new solid–liquid interface is less than that of the corresponding solid–vapour interface. The greater this difference, the greater will be the extent of spreading or wetting. The driving force for wetting is therefore related to the difference in energy between the solid–vapour and solid–liquid interfaces; however, because the lowest surface energy configuration for a liquid is a sphere, there is an additional force resisting this spreading. The shape of a sessile drop, as described by its contact angle, θ, is therefore a function of three energy terms, as described by Young's classical equation [161]

$$\gamma_{SV} = \gamma_{SL} + \gamma_{LV} \cos\theta \qquad [11]$$

where γ_{SV}, γ_{SL} and γ_{LV} are the interfacial energies of the solid–vapour, solid–liquid and liquid–vapour in-

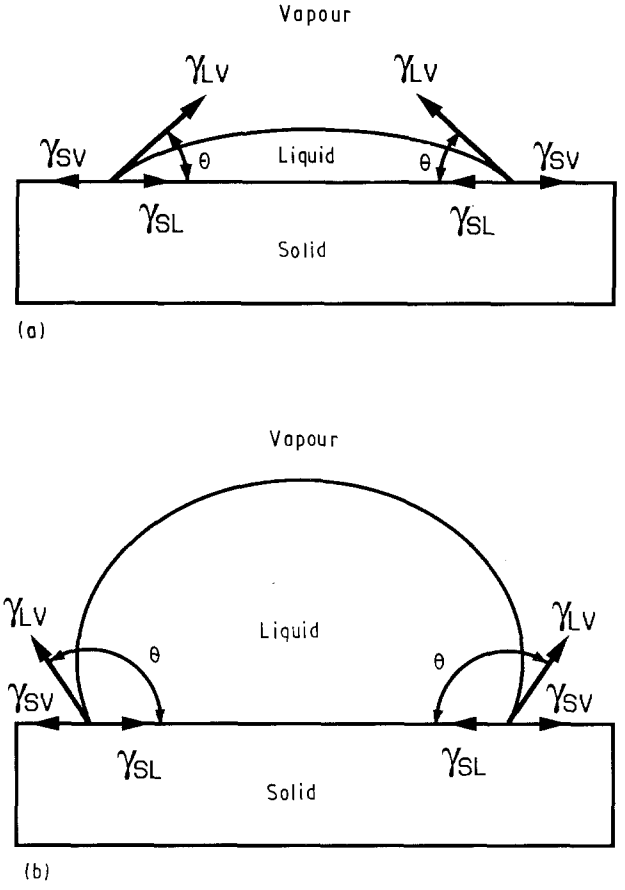

Figure 12 Sessile drop configurations: (a) wetting, (b) non-wetting (see text for details).

terfaces, respectively. A liquid will wet a solid ($\theta < 90°$) when the net energy of the system is lowered by forming a solid–liquid interface. The greater the degree of wetting, the smaller is the angle θ. Conversely, the larger this angle, the lower is the degree of wetting. It should be noted, of course, that no liquid will exhibit the maximum contact angle of 180°, even in the case of no wetting, due to the distorting influence of gravity on the liquid droplet.

The concept of the work of adhesion, W_A, was subsequently introduced by Dupré [162]. This is related to the surface energies by the equation

$$W_A = \gamma_{SV} + \gamma_{LV} - \gamma_{SL} \quad (12)$$

In order to separate the liquid and the solid, work has to be done that is equal to the lowering of the free energy through wetting. An interface is stable when W_A is positive, i.e. when forming the interface results in a decrease in the total free energy of the system. Introducing the contact angle, this equation may be written as

$$W_A = \gamma_{LV}(1 + \cos\theta) \quad (13)$$

It should, therefore, be feasible experimentally to obtain quantitative values for the bonding strength and behaviour of different glass-to-metal systems.

This simple thermodynamic approach to bonding should be treated with caution, however, and should only be employed as a preliminary guide as to whether or not bonding conditions may be favourable for a given system. One of the main conclusions that could be drawn is that if the liquid has a lower surface energy than that of the solid substrate, the system can lower its energy by spreading the liquid phase over the solid surface, i.e. by wetting the solid. This conclusion can be grossly incorrect because it suggests, for example, that a change in the solid surface that lowers its energy will also lower its wettability. For glass–metal systems this is clearly not usually the case, as the presence of an oxide layer on the metal (which reduces its surface energy) will generally enhance the wettability. Further details concerning the wetting and spreading of liquids on solids are given elsewhere (e.g. [163]).

The simple thermodynamic approach given above assumes no reaction between the liquid and the solid. If a chemical reaction occurs at the interface a new compound may be formed. Wetting and adhesion may subsequently be enhanced (as in the case of oxidation of a metal surface enhancing adhesion to a glass), and Equation 5 requires modification to take this into account [164, 165]

$$W_A = \gamma_{LV}(1 + \cos\theta) + \gamma_{Ri} - C\Delta G^\circ \quad (14)$$

where γ_{Ri} is the interfacial energy between the solid and the reacted interfacial layer, ΔG° is the Gibbs free energy of formation of the new interfacial compound, and C is a constant. A spontaneous reaction is characterized by a negative value for ΔG° which increases W_A and decreases θ. To give an idea of the most likely reactions to occur under bonding conditions, ΔG° can be calculated for different potential reactions from available thermodynamic data. Reactions with the greatest negative ΔG° values will be more favourable thermodynamically, although data so derived must again be treated with caution as a given reaction may be kinetically unfavourable. Further details in relation to chemical bonding are given in Section 4.4.

4.2. Mechanical bonding

It was originally thought that adherence between an enamel and a metal substrate occurred via mechanical keying effects. Mechanical theories of adherence originally gained acceptance due to the fact that the interface between a metal and a porcelain enamel often appeared rough, even if the substrate was originally quite smooth. Bonding was thought to occur due to the mechanical keying effect between the roughened substrate and the glass. A number of theories arose based on the mechanism by which this roughening was thought to occur. The dendrite theory, for example, favoured the precipitation within the glass of a metallic phase which provided anchor points, whilst the electrolytic theory proposed that electrolytic attack roughened the surface. In either case the result was an interlocking metal–glass structure, as described below.

4.2.1. The dendrite theory

Expounders of the dendrite theory [166–168] noted that after sealing a glass to a metal, dendrites of a metallic phase, e.g. cobalt or a Co–Fe intermetallic phase, were often found within the interfacial region. It

was suggested that these dendrites held the coating in place due to a mechanical keying effect; i.e. the dendrites acted as anchor points between the metal substrate and the glass, as illustrated in Fig. 13a. The dendrites were believed to be formed due to the reaction of a metal oxide present in the glass with a metallic element in the substrate. For a glass containing CoO bonded to an iron substrate, the following reaction was believed to occur

$$CoO_{(glass)} + Fe_{(substrate)} \rightarrow Co_{(dendrite)} + FeO_{(glass)} \quad (15)$$

4.2.2. The electrolytic theory

The electrolytic theory [169–171] proposed that roughening of the metal substrate occurred during coating due to an electrolytic or galvanic corrosion mechanism. For example, bonding of a CoO-containing glass in air to an iron substrate results in the precipitation of metallic cobalt, as proposed in the dendrite theory. It was believed, however, that those precipitates which were formed in contact with the iron substrate formed the basis of localized galvanic or electrolytic cells. The net effect was the dissolution of iron into the glass and the formation of a pitted surface into which the glass could flow, thus forming a number of mechanical keys which hold the glass on to the substrate, as illustrated in Fig. 13b. The reaction sequence proposed for this mechanism commenced as for Equation 15, which was then followed by

$$2Co_{(precipitates)} + O_{2(from\ atmosphere)} \rightarrow 2Co^{2+} + 2O^{2-} \quad (16)$$

$$Co^{2+} + 2e^{-} \rightarrow Co \quad (17)$$

$$Fe - 2e^{-} \rightarrow Fe^{2+} \quad (18)$$

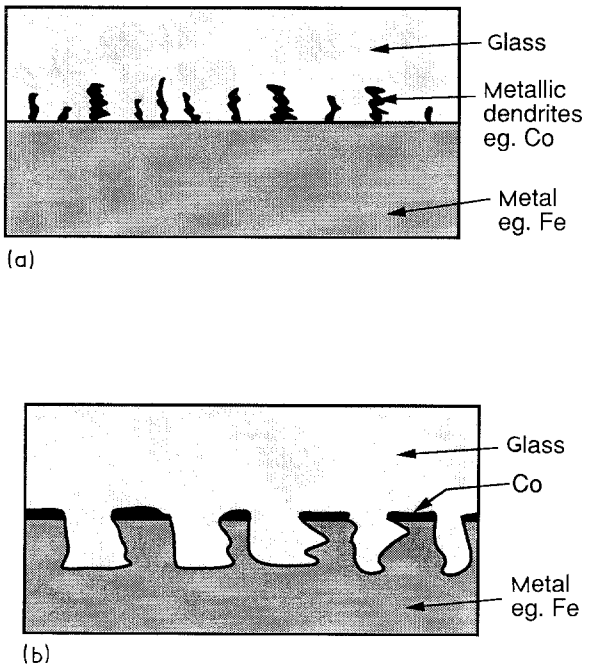

Figure 13 Schematic diagram of mechanical anchor points: (a) dendrite theory of glass-to-metal adhesion; (b) electrolytic theory of glass-to-metal adhesion.

Further work [168, 172, 173] initially tended to support the general concepts of the mechanical keying theories. It was observed by Harrison *et al.* [168], however, that there appeared to be little correlation between the ease of reduction of metal oxide additions and the strength of the resultant bond, i.e. additions which are easier to reduce than CoO and which should therefore yield a rougher substrate, did not in fact yield stronger bonding. This was one of the factors that eventually led to the mechanical keying theories falling out of favour.

4.3. Mutual solubility and intermediate compound formation

Another mechanism by which bonding between a metal substrate and a glass could be achieved is via mutual solubility between the glass and an oxide scale on the metal. For example, some of the oxide scale is dissolved by contact with the molten glass, thus forming an intermediate glassy layer which is progressively richer in the metal oxide. Alternatively, bonding could be achieved via the formation of an intermediate compound which links the glass to the metal surface or to an oxide scale. This theory is closely related to the thermodynamic and chemical approaches, and it is possible to predict compound formation.

4.4. Chemical bonding

From a chemical or molecular approach, bonding must be accomplished by a transitional zone in which the metallic bonding of the metal is gradually substituted for the ionic-covalent bonding of the glass. Strong opposition to the earlier mechanical theories of bonding came from the work by King *et al.* [2] on the bonding of glass to iron. The major conclusion of this particular work was that a strong chemical bond was formed at the glass-metal interface if the conditions were such that the glass could become saturated with an oxide of the substrate metal which when in solution in the glass would not be reduced by the metal, e.g. FeO in the case of an iron substrate. By changing the composition of the glass employed in their work, it was possible to alter the solubility of FeO. It was noted that the glass formers, e.g. SiO_2 and B_2O_3, increased the solubility of FeO in the glass, whilst the glass modifiers decreased its solubility, but as long as the glass was saturated with FeO, strong bonding occurred. A number of other metallic systems were investigated in this work, including copper, and it was confirmed that good bonding always occurred when the glass was saturated with the appropriate metal oxide. It was suggested that when the appropriate metal oxide is dissolved in the glass up to its saturation point, metal ions will remain at the surface and these will promote metal–metal bonding across the interface, as depicted in Fig. 14. At elevated temperatures when the metal ions in the glass and the atoms of the metal are relatively mobile, there will be a continuous exchange at the glass–metal interface. Metal ions from the glass will diffuse into the metal where they will gain electrons and become zero valent metal atoms,

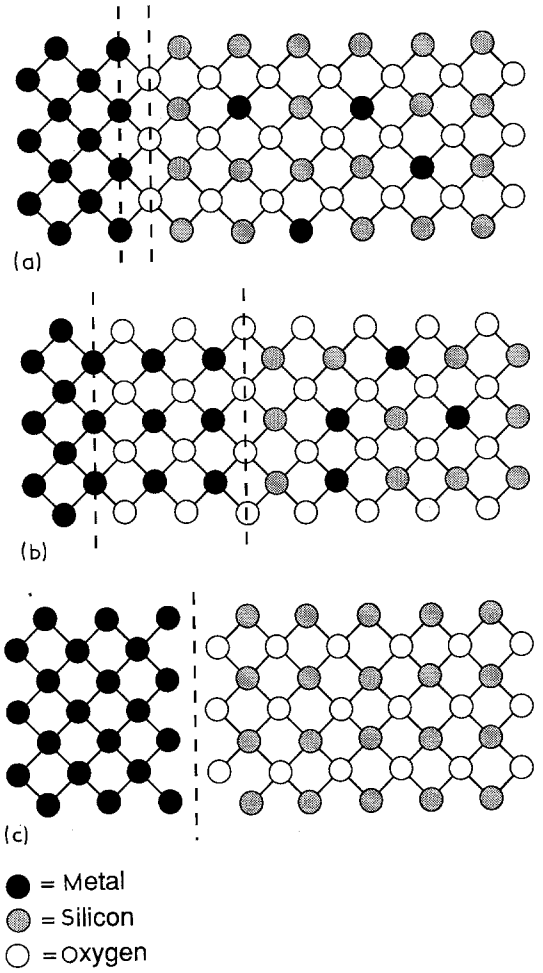

Figure 14 Simplified two-dimensional schematic representation of glass-to-metal bonding: (a) glass saturated with substrate metal oxide in the interfacial region to give strong chemical bonding via a "mono-oxide" layer; (b) as above, with chemical bonding via a "bulk" oxide layer; the strength of the resulting system is dependent on the properties of this bulk oxide layer; (c) interface is not saturated with metal oxide; only weak bonding via van der Waals forces is achieved.

whilst metal atoms will diffuse into the glass and become ionized. A state of dynamic equilibrium will therefore exist at the metal–glass interface which could not be maintained if the glass were not already saturated with the appropriate oxide. At lower temperatures when the atoms and ions will be less mobile, there may exist an exchange of electrons, and ions and atoms at the interface may alternate in properties depending on the concentration of electrons or the degree of ionization. These atoms and ions of intermediate character are therefore expected to provide a transition between the metallic and ionic states, assuming that the interface remains in a saturated state.

Traditionally, the appropriate metal oxide is provided by pre-oxidation of the metal substrate. During sealing this oxide layer will dissolve into the glass, and the interface will become saturated; favourable bonding conditions will then prevail. If, on the other hand, sealing is attempted to a "clean" metal substrate (or, alternatively, sealing conditions are maintained such that all the pre-oxidized layer is dissolved and saturation of the interface is lost) suitable redox reactions must proceed between the metal and the glass in order to achieve or maintain conditions suitable for chemical bonding. The overall reaction between a glass and a *clean* metal substrate will also normally involve two steps. In the first step, an oxide reaction product is formed on the metal at the interface by a suitable redox reaction; in the second step, this oxide dissolves into the glass. Saturation at the interface can, therefore, be achieved, even in the absence of an oxide layer formed by pre-oxidation. If, however, reactions between a glass and a metal are not favourable, i.e. values for ΔG° of potential oxide products are positive, the reaction will not proceed spontaneously under standard conditions. It may nevertheless still be possible for a reaction to proceed under certain non-standard conditions. As an example, consider the reaction between a clean iron substrate and a sodium silicate glass [114, 174–177]

$$Fe_{(substrate)} + Na_2O_{(glass)} \rightarrow FeO_{(interface)} + 2Na\uparrow \quad (19)$$

The *overall* free energy relationship for this type of reaction is

$$\Delta G = \Delta G^\circ + RT\ln\{[a(FeO)_{(interface)} \times a(Na)^2]/[a(Fe) \times a(Na_2O)_{(glass)}]\} \quad (20)$$

where a is the chemical activity of each component. Under *standard* conditions, the chemical activities are equal to unity, and $\Delta G = \Delta G^\circ$. As the value for ΔG° is positive for this particular reaction, the reaction will not proceed spontaneously. It may proceed, however, if the value for the activity quotient, $\{[a(FeO)_{(interface)} \times a(Na)^2]/[a(Fe) \times a(NaO)_{(glass)}]\}$, is sufficiently less than one. This is favoured by a low partial pressure of sodium, a low activity for FeO, and a high activity for Na_2O. Suitable conditions can be achieved in practice by control over the process parameters, e.g. sealing atmosphere and pressure, etc., as discussed in detail by Tomsia and Pask [114, 175] and Pask [174, 176, 177].

The properties of the so-called adherence promoters require special mention in relation to the chemical approach to bonding. It has been appreciated for many years since the early days of porcelain enamelling that certain oxides with easily reducible ions, e.g. CoO and NiO, will promote adhesion between an enamel and an iron substrate. During the bonding operation to a pre-oxidized substrate the oxide scale dissolves into the glass. If, during this operation, all of the oxide is dissolved, the metal surface will come into contact with the glass. The adherence-promoting oxide is then reduced by the metal substrate thus forming more substrate metal oxide so that interfacial saturation with this oxide is achieved or maintained during the enamelling operation (e.g. Equation 15 for CoO and an iron substrate). Nickel oxide will act in a similar manner. Adherence-promoting oxides can therefore play an important role by creating and maintaining interfacial saturation with the appropriate oxide of the substrate metal. Other oxides may be used, depending on the glass–metal system employed, e.g. CuO and MnO, as reported more fully in the discussion.

5. Bonding to specific metals and alloys

Work is reported on the sealing and coating of particular metals and alloys using a variety of glass and glass-ceramic compositions. Compositions of specific metallic alloys are given in Table VI, and thermal expansion data are summarized in Table VII.

5.1. Bonding to mild and low-alloy steels and iron

There has been a considerable body of work reported on the bonding of glasses to iron-based alloys, much of this being directly related to the early technological importance of porcelain enamels; in particular, the enamelling of cast irons and related materials. This early work is very adequately covered elsewhere (e.g. [10]).

More recently, a number of papers have reported on the bonding of glasses or glass-ceramics to mild and low-alloy steels [178, 179]. In the work by Sturgeon *et al.* [178], a low-alloy mild steel was coated with a lithium alumino-silicate glass-ceramic containing small additions of K_2O, ZnO and P_2O_5. The metal substrate was pre-oxidized prior to coating to yield a layer of $FeO + Fe_2O_3$ approximately 15 μm thick on the mild steel. During subsequent firing, it was observed that rapid diffusion of Fe^{2+} into the coating occurred. This resulted in the formation of a dendritic lithium iron silicate phase (possibly $Li_2Fe_{0.8}Zn_{0.2}SiO_4$) within the interfacial reaction zone which extended > 40 μm into the coating, as shown in Fig. 15.

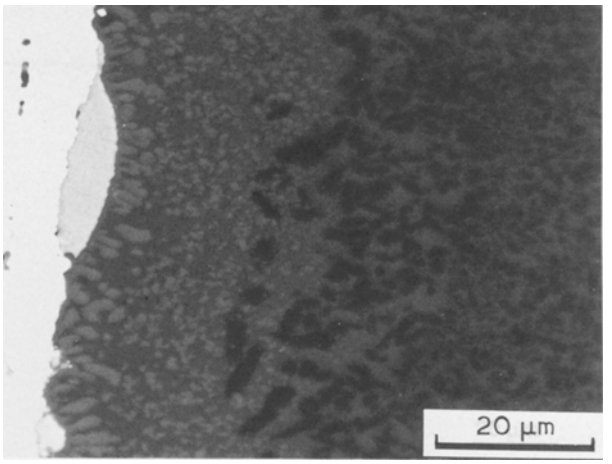

Figure 15 Coating of lithium silicate glass-ceramic on pre-oxidized mild steel showing the presence of dendritic phases within the glass-ceramic; after Sturgeon *et al.* [178]; (see text for details).

Nicholas [179] examined the interaction of sodium disilicate glass with Fecralloy (an Fe–6Cr–4Al–0.25Y alloy) in the temperature range 900–1100 °C under vacuum using the sessile drop technique. Both unoxidized and pre-oxidized samples ($\approx$ 2–6 μm thick Al_2O_3 layer) were employed. Not unexpectedly, severe de-gassing of the glass was observed during these experiments. Using unoxidized material, stable contact angles of 38°–47° were obtained, depending on the temperature, whilst with pre-oxidized samples contact angles of 2°–6° were achieved. It was noted that the predominant redox reaction when using unoxidized metal was

$$2Al_{(alloy)} + 3Na_2O_{(glass)} \rightarrow Al_2O_{3(glass)} + 6Na \uparrow \quad (21)$$

For the pre-oxidized samples, on the other hand, wetting and bonding was achieved via the Al_2O_3 oxide film.

Reasonably refractory (i.e. stable to 750–800 °C) glass-ceramic coatings have been developed recently for the protection of cast iron tubes used in the melting of aluminium alloys [180]. Two different families of glass-ceramics were investigated in this work. One, based on the K_2O–BaO–Cr_2O_3–NiO–FeO–SiO_2 system, was nucleated with MoO_3 and contained barium disilicate as the major crystalline phase. Alternative glass-ceramics were prepared in the Li_2O–Na_2O–ZnO–P_2O_5–NiO–SiO_2 system. These were also nucleated using MoO_3, but they contained cristobalite as the major crystalline phase.

5.2. Bonding to high-alloy and stainless steels

The formation of high-quality, durable seals to stainless and related high-alloy steels has proved difficult due, in part, to the relatively high thermal expan-

TABLE VI Compositional data for a number of metallic alloys

Alloy	Composition (wt %)											
	Ni	Co	Cr	Fe	Ti	Al	Nb/Ta	Mo	Cu	Si	Mn	C
Nimonic 90	Bal.	15.0–21.0	18.0–21.0	≤ 1.5	2.0–3.0	1.0–2.0	–	–	≤ 0.2	≤ 1.0	≤ 1.0	≤ 0.13
Nimonic 263	Bal.	19.0–21.0	19.0–21.0	≤ 0.7	1.9–2.4	0.3–0.6	–	5.6–6.1	≤ 0.2	≤ 0.4	≤ 0.6	≤ 0.9
Hastelloy C276	Bal.	≤ 2.5	14.5–16.5	4.0–7.0	–	–	–	14.0–17.0	–	≤ 0.08	≤ 1.0	≤ 0.01
Inconel 625	Bal.	≤ 1.0	20.0–23.0	≤ 5.0	≤ 0.4	≤ 0.4	3.15–4.15	8.0–10.0	≤ 1.0	≤ 0.5	≤ 0.5	≤ 0.1
Inconel 718	50.0–55.0	≤ 1.0	17.0–21.0	Bal.	0.65–1.15	0.2–0.8	4.75–5.5	2.8–3.3	≤ 0.3	≤ 0.35	≤ 0.35	≤ 0.08
Inconel X-750	Bal.	≤ 1.0	15.5	7.0	2.5	0.7	1.0	–	≤ 0.5	≤ 0.05	≤ 0.05	≤ 0.08
Nilo-K	29.0	17.0	–	Bal.	–	–	–	–	–	≤ 0.2	≤ 0.3	≤ 0.02
304L stainless steel	8.0–11.0	–	17.0–20.0	Bal.	–	–	–	–	–	≤ 0.4	≤ 2.0	≤ 0.03
321 stainless steel	9.0–12.0	–	17.0–19.0	Bal.	≤ 0.4	–	–	–	–	≤ 1.0	≤ 2.0	≤ 0.08

TABLE VII Thermal expansion data for some metals and alloys. Data from [236–238]

Alloy	Thermal expansion ($10^{-6}\,°C^{-1}$)	Temperature range (°C)
Nimonic 263	11.9	20–200
	13.1	20–400
	14.2	20–600
	16.2	20–800
	18.9	20–1000
Nimonic 90	13.3	20–200
	14.0	20–400
	14.8	20–600
	16.2	20–800
	18.2	20–1000
Inconel 625	13.1	20–205
	13.7	20–425
	14.8	20–650
	15.8	20–870
	16.2	20–930
Inconel 718	13.5	24–204
	14.2	24–427
	15.1	24–649
	16.0	24–760
Hastelloy C276	12.0	24–204
	13.2	24–427
	13.4	24–538
AISI 321 stainless steel	16.7	0–100
	17.1	0–315
	18.5	0–540
	19.3	0–650
	20.2	0–815
Nilo-K (kovar)	5.7	20–200
	5.3	20–300
	5.0	20–400
	6.2	20–500
Al	24.9	30–300
	31.3	300–600
Ti	8.5	25
	9.2	– 120–860
	10.5	860–960
Ni	13.0	25
	13.2	– 130–420
	17.1	420–990
Cu	16.6	25
	17.2	100
	18.5	300
	19.2	500
	20.7	700
	22.5	900
Ta	6.5	25
	7.5	– 183–1670
W	4.5	25
	5.5	– 150–2130
Mo	5.0	25
	6.6	– 190–1670

sion of many of these alloys (typically ≈ 17–$22 \times 10^{-6}\,°C^{-1}$ for conventional stainless steels). Nevertheless, a limited number of papers have reported the bonding of glasses and glass-ceramics to a variety of alloy steels, with varying degrees of success [157, 178, 181–185].

For example, Sturgeon *et al.* [178], have examined the coating behaviour of an Fe–17% Cr alloy ($\alpha \approx 12 \times 10^{-6}\,°C^{-1}$) with a lithium alumino-silicate glass-ceramic nucleated with P_2O_5. The metal substrate was pre-oxidized prior to coating to yield a layer of $Cr_2O_3 \approx 1\,\mu m$ thick. It was noted that strong bonding to the substrate was achieved via this Cr_2O_3 layer, which remained substantially unaltered during the coating process. Only limited diffusion of Cr^{3+} into the coating was observed, this extending to a depth of the order of 4 μm. The coating of an Fe–17% Cr alloy with a glass-ceramic containing a dispersion of SiC particles has also been reported by Hyde and Partridge [186]. This work indicated that mechanically stronger coatings could be obtained by using the particle-reinforcement mechanism. The thermal expansion of the glass-ceramic matrix was matched to that of the substrate, the major crystalline phases present being quartz and lithium disilicate.

Birkbeck *et al.* [181] and Cassidy and Fagin [182] have prepared glass-ceramic seals to an aluminium-containing, precipitation-hardenable stainless steel of thermal expansion coefficient $\approx 17 \times 10^{-6}\,°C^{-1}$. Both unoxidized and pre-oxidized metal samples were sealed to a lithium silicate glass-ceramic containing small additions of K_2O, Al_2O_3, B_2O_3 and P_2O_5 using a standard heat-treatment schedule. The best seals were obtained using the pre-oxidized metal, but only if a vacuum annealing stage was carried out prior to sealing. If this vacuum treatment was not carried out, a porous interface was obtained during sealing. This effect was believed to be due to the presence of water absorbed on to the Al_2O_3 layer. Sealing was also attempted between this glass-ceramic and a 304L stainless steel substrate. In this case, however, successful sealing could not be achieved, possibly due to the higher thermal expansion of this stainless steel relative to the aluminium-containing alloy. Later, Cassidy and Moddeman [185] and Moddeman *et al.* [183, 184] reported the successful bonding of a similar glass-ceramic to 304L stainless steel. In this work, significant differences in the microstructure of the interfacial zone were obtained, relative to that of the bulk glass-ceramic, depending on whether or not the alloy samples were pre-oxidized prior to sealing. In the case of unoxidized samples, a reaction zone containing iron and chromium phosphide precipitates was obtained extending $\approx 30\,\mu m$ into the glass-ceramic; a further diffusion zone containing chromium was apparent extending $\approx 200\,\mu m$ into the glass-ceramic. In the reaction zone the crystalline structure of the glass-ceramic was disrupted due to the removal of the P_2O_5 nucleating agent through reaction with iron and chromium. A high proportion of glassy phase was noted in this region. When using pre-oxidized samples, on the other hand, only a very narrow diffusion zone was apparent, and there was an absence of phosphide precipitates. In addition, the glass-ceramic retained its fine crystalline microstructure up to the interface.

Knorovsky *et al.* [187] have also prepared seals to 304L stainless steel using a similar lithium silicate glass-ceramic. The heat-treatment schedule was chosen to give a mixture of lithium metasilicate, lithium disilicate and tridymite with the desired thermal expansion characteristics. Despite the apparently favourable thermal expansion it was found, however, that seals failed during cooling. The reason for the failures was traced to excessive diffusion of chromium

from the metal immediately adjacent to the interface into the glass-ceramic. This depletion of chromium (from $\approx 12\%$ Cr within the bulk of the metal to $\approx 5\%$ at the interface) resulted in the partial transformation of the normal f c c structure of the austenitic steel into a b c c phase immediately adjacent to the interface. This particular phase transformation is accompanied by a large volume contraction of $\approx 2\%$; in addition, the bulk material possesses a lower thermal expansion coefficient. Hence, the thermal expansion of the metallic interface was no longer matched to that of the glass-ceramic, and this resulted in failure at the interface. A number of solutions to this problem were suggested, including plating the surface of the stainless steel with chromium or nickel to act as a barrier against the diffusion of chromium from the bulk metal.

Metcalfe *et al.* [157, 188] have studied the sealing of a lithium zinc silicate glass-ceramic containing a high proportion of ZnO to 321 stainless steel. A standard sealing and heat-treatment schedule of 5 min at 950 °C followed by 60 min at 465 °C and 60 min at 850 °C was employed. Sealing was carried out in argon using unoxidized metal samples. After sealing, a relatively thin interfacial reaction zone was apparent, extending ≈ 4–$5\,\mu m$ into the bulk glass-ceramic. This zone consisted of a semi-continuous precipitate of a phase which EDS revealed to contain chromium and silicon adjacent to the interface (possibly a complex mixture of CrO or Cr_2O_3 with Cr_3Si_2 or $LiCr(SiO_3)_2$), whilst acicular crystals rich in iron and phosphorous (an iron phosphide phase) were found within the glass-ceramic close to the interface. Owing to the partial removal of the P_2O_5 nucleating agent from the interfacial region, this zone contained a high proportion of glassy phase which extended ≈ 5–$6\,\mu m$ into the bulk glass-ceramic. Micrographs are shown in Fig. 16.

In the study by Metcalfe *et al.* [157, 188] the influence of a number of transition metal oxide additions on the sealing behaviour of the glass-ceramic was investigated. These oxides, which included CuO, NiO, Cr_2O_3, WO_3 and MoO_3, were added to the glass batch at the 2 mol % level. Addition of CuO resulted in the formation of a thinner reaction zone, relative to the seals which did not contain this addition, and there was a marked absence of phosphide phases in this zone. Bonding was achieved via a very thin (≈ 0.2–$0.5\,\mu m$) layer which EDS revealed to be rich in chromium. Seals made with the glass-ceramic which contained NiO also exhibited a narrow reaction zone rich in chromium, but differed in the presence of small ($\approx 1\,\mu m$) particles rich in nickel dispersed both along the interface and within the glass-ceramic close to the interface. Seals made with the WO_3-containing glass-ceramic were very similar to those containing NiO, exhibiting a very thin interfacial layer rich in chromium, and a dispersion of particles along the interface which were rich in both tungsten and silicon (possibly WSi_2 or a related phase). The seals containing MoO_3 also exhibited a thin interfacial layer but this was very rich in molybdenum, rather than chromium. Particles rich in both molybdenum and silicon (possibly $MoSi_2$) were dispersed along the interface and within the glass-ceramic close to the

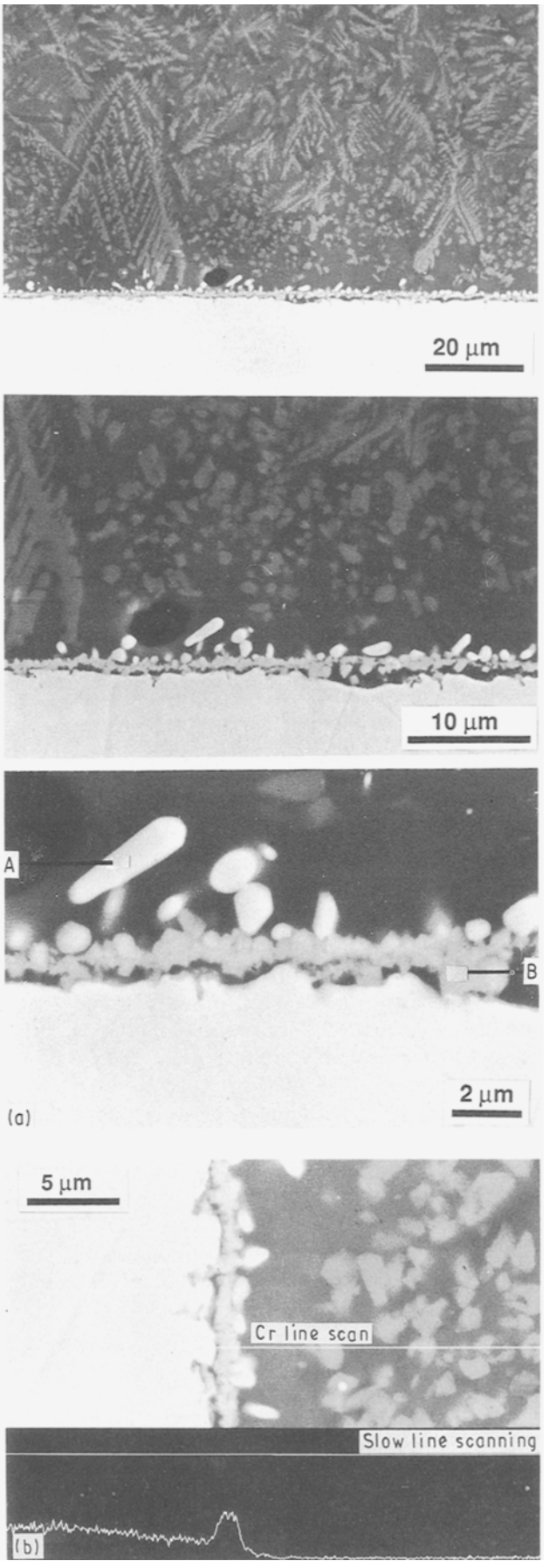

Figure 16 Lithium zinc silicate glass-ceramic seal to stainless steel showing reaction products (glass crystallized at 850 °C); after Metcalfe *et al.* [157, 188]. (a) micrographs of interfacial region showing dendritic phase in bulk glass-ceramic near to the interface, and phosphide precipitates, A, close to the granular interface, B, (b) EDS line scan for chromium, showing high concentration of chromium at the interface.

interface. The TMO additions appear to influence the diffusion of iron and chromium into the bulk glass-ceramic, and to hinder the formation of phosphide and related phases. In this respect, they are therefore beneficial in preventing the depletion of the P_2O_5 nucleating species from the immediate interfacial zone. Micrographs are shown in Fig. 17. Some of the corresponding EDS line scans are shown in Fig. 18.

Metcalfe *et al.* [157, 188] have also carried out a preliminary study aimed at examining the influence on the resultant seal quality of varying some of the process parameters, e.g. crystallization temperature. It has been noted, for example, that seals crystallized at 900 °C show marked differences to those crystallized at 850 °C. In particular, a finer interfacial microstructure was noted when using the standard LZS glass (without any TMO additions), and there was also an absence of iron phosphide precipitates in this region, as illustrated in Fig. 19a. Crystallizing at 1000 °C, on the other hand, led to severe reaction between the glass-ceramic and the metal substrate, and resulted in the formation of porous and non-hermetic seals. Addition of NiO to the seals crystallized at 900 °C resulted in the production of a thicker chromium-rich interfacial layer, relative to the seals which did not contain NiO, together with the precipitation of very well-defined nickel-rich particles close to the interface, as illustrated in Fig. 19b and c. It is clear that NiO is acting as a classical adherence promoter in this example, by reacting with chromium to yield Cr_2O_3 and nickel.

In addition to the use of silicate glass-ceramics for sealing to stainless steel, limited work has been reported [34] on the application of high-expansion phosphate glasses (based on P_2O_5 and containing additions of Na_2O, K_2O, BaO and Al_2O_3) for sealing to 304L stainless steel. This work indicated that, although the expansion of the glass could apparently be matched reasonably well to yield mildly compressive seals, failure of some seals occurred. This was explained by the generation of tensile stresses (which were not predicted using conventional elastic theory) due to viscoelastic relaxation of the glass during cooling. High thermal expansion phosphate glasses based on the K_2O–Al_2O_3–(Fe_2O_3)–P_2O_5 system which exhibit reasonable chemical durability have also been suggested as potential candidates for sealing to stainless steel [36, 37].

5.3. Bonding to other iron-based alloys

There are a number of related iron-based alloys that have been used extensively in the electrical and electronics industries for the preparation of glass-to-metal seal devices. In particular, relatively low-expansion binary Fe–Ni and ternary Fe–Ni–Co alloys have been used for many years (originally as a substitute for molybdenum and tungsten because their thermal expansion characteristics match those of a number of common "hard" borosilicate-type glasses [104, 105, 111, 189]. These alloys include the Nilo series, e.g. Nilo-K (kovar).

5.4. Bonding to platinum, copper, silver and gold

Coating (enamelling) of copper, silver and gold has been practised for many years, with particular reference to the preparation of enamelled jewellery. These enamels are usually based on relatively low softening temperature alkali oxide lead silicate compositions. Some typical enamel compositions are given in Table III. Further details of the early work can be found elsewhere [10].

Copper and platinum have also been widely utilized in the production of electrical feed-through seals, with glass normally being employed as the sealing medium [104]. In addition, seals have been produced to silver and gold for electrical applications. Less work has been reported on the bonding of these metals to glass-ceramic materials, although McMillan and Hodgson [190] showed that a lithium zinc silicate glass nucleated with P_2O_5 and exhibiting a thermal expansion coefficient of $17.4 \times 10^{-6}\,°C^{-1}$ could be employed successfully to bond to copper. More recently, Risbud *et al.* [191] have prepared copper–cordierite glass-ceramic systems. It was observed in this work that diffusion of Cu^+ into the glass-ceramic leads to the formation of small ($\approx$ 100–200 nm) metallic precipitates of copper within the interfacial zone. The bonding behaviour between copper and a crystallizable refractory lithium alumino-silicate glass has been reported by Donald [192]. In this work, the metal was sealed to the glass by fusing the metal in contact with the glass. It was noted that mutual dissolution occurred at the interface to give strong bonding. A transitionary zone $\approx 40\,\mu m$ thick was observed which contained many precipitates of copper oxide. An example is shown in Fig. 20.

5.5. Bonding to nickel-based alloys

There have been a large number of studies aimed at the preparation of glass and glass-ceramic seals and coatings to nickel-based alloys [193–208]. Some of these studies are described below.

Kelsey *et al.* [194], for example, reported the interaction of a barium silicate glass with Inconel X-750 alloy. Glass was allowed to react with the metal at 1100 °C in various partial pressures of oxygen, and the resulting interfaces were examined using scanning electron microscopy. It was observed that pre-oxidation of the metal in a partial pressure of oxygen of 10^{-14} Pa led to the formation of a $NiTiO_3$–Cr_2O_3 solid solution oxide layer which is strongly bonded to the metal substrate. It was noted that the glass employed bonded well to this oxide layer. Pre-oxidation of the metal at higher oxygen pressures, on the other hand, resulted in the formation of a poorly adherent layer containing TiO_2 and $NiCr_2O_4$ which produced non-hermetic bonds to the glass. Tomsia and Pask [201] reported the sealing of a potassium alumino-silicate glass to two 80Ni–20Cr alloys, one prepared from high-purity (99.99%) metals, the other a commercially available alloy containing 1.5% Si together with traces of aluminium, iron and manganese. The alloys were preoxidized prior to sealing. It was noted

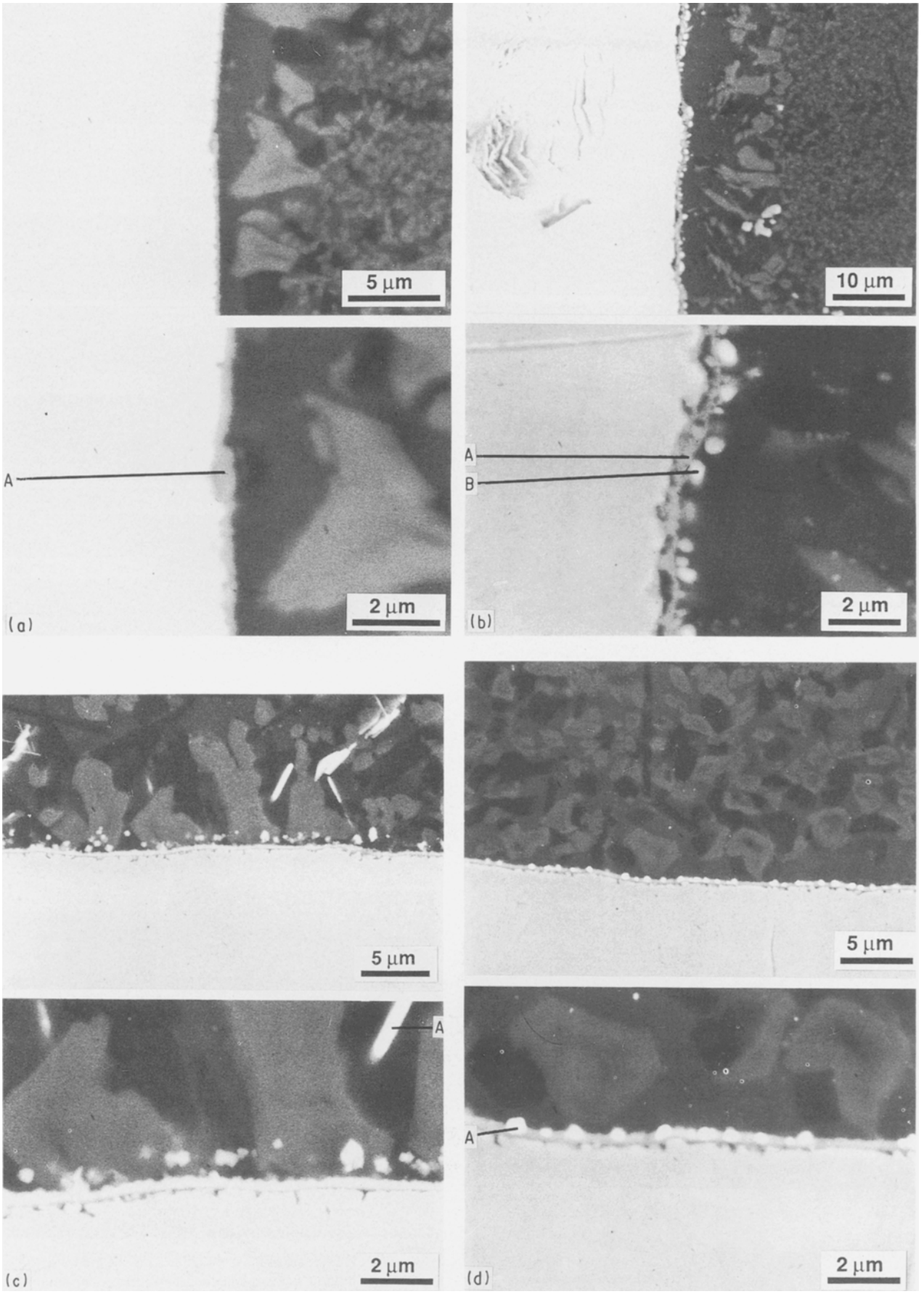

Figure 17 Lithium zinc silicate glass-ceramic seals to stainless steel showing the effect of transition metal oxide additions (TMO) to the glass on the sealing behaviour (glass crystallized at 850 °C); after Metcalfe *et al.* [157, 188]. (a) Effect of CuO addition, showing thinner interfacial zone, A, and absence of phosphide phases; (b) effect of Cr_2O_3, showing thicker interfacial reaction zone which consists of a granular region, A, rich in chromium, and a dispersion of particles, B, rich in iron and phosphorous; (c) effect of MoO_3, showing particles, A, rich in molybdenum and silicon; (d) effect of WO_3, showing particles, A, rich in tungsten and silicon.

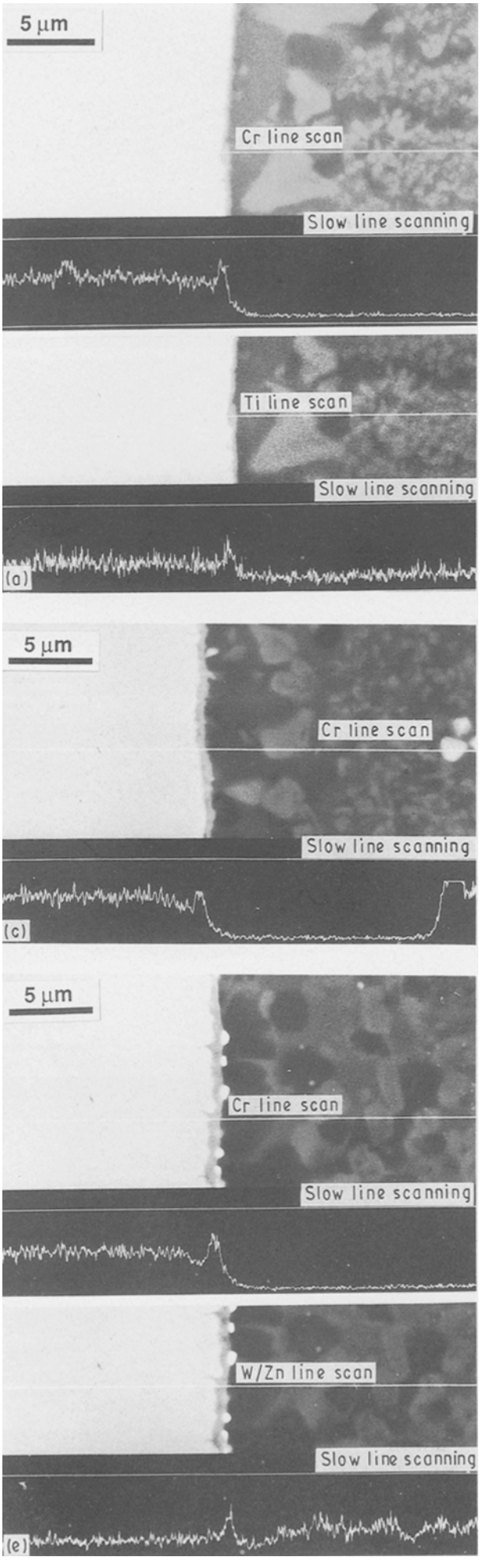

Figure 18 EDS line scans for some of the seals shown in Fig. 17: (a) with CuO addition showing high concentration of chromium and titanium at the interface; (b) with NiO addition, showing high concentration of chromium and titanium at the interface; (c) with Cr_2O_3 addition, showing high concentration of chromium (but not titanium) at the interface; (d) with MoO_3 addition, showing high concentration of molybdenum (but not chromium or titanium) at the interface; (e) with WO_3 addition, showing high concentration of chromium and tungsten at the interface.

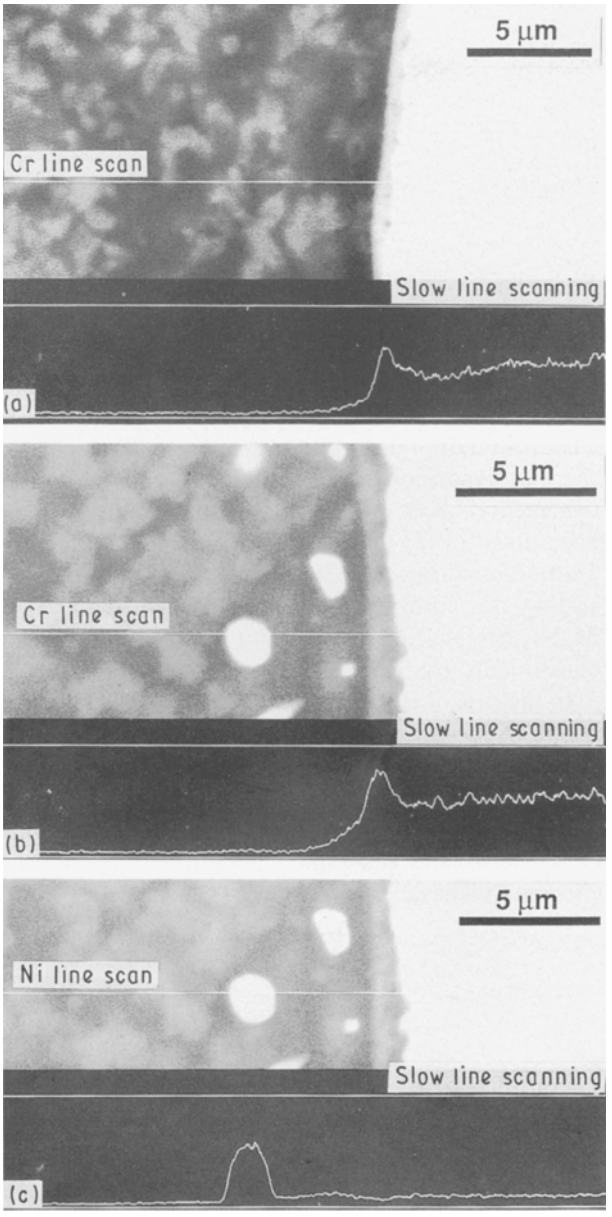

Figure 19 Lithium zinc silicate glass-ceramic seals to stainless steel (glass crystallized at 900 °C); after Metcalfe *et al.* [157, 188]. (a) Glass-ceramic without TMO additions showing high concentration of chromium at the interface; (b) glass-ceramic with NiO addition showing thicker interfacial layer with high concentration of chromium; (c) as (b) showing high concentration of nickel in interfacial precipitates.

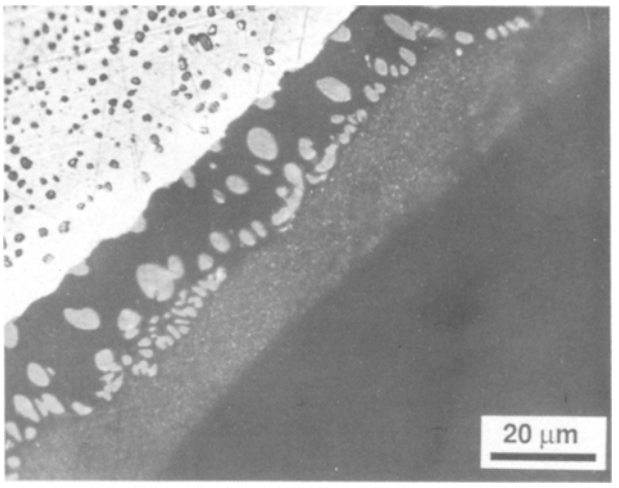

Figure 20 Glass-to-copper bonding showing copper oxide precipitates in the interfacial zone; after Donald [192].

that the high-purity alloy formed a multi-layer oxide scale, whilst the commercial alloy produced a single mixed scale with the outer portion being richer in Cr_2O_3. Subsequent sealing produced good quality coatings in each case. The seal to the pure alloy was, however, mechanically weaker with fracture occurring through the oxide layer. This difference in behaviour was explained by the presence of a high degree of porosity in the oxide layer of the commercial alloy, this allowing glass to reach the metal substrate and react directly with it. Saturation of the glass with Cr_2O_3 was maintained through dissolution of oxide from the scale.

McCollister and Reed [195] have prepared hermetic seals to nickel-based superalloys (Inconel 625 and 718, and Hastelloy C276) employing a lithium silicate glass-ceramic containing small additions of Al_2O_3, Li_2O, K_2O and B_2O_3, together with P_2O_5 nucleating agent. Sealing was carried out using a three-step heat treatment schedule using unoxidized metal samples. This consisted of a high temperature cycle at 1000 °C to melt the glass, a low temperature hold at 650 °C to initiate nucleation, and an intermediate temperature hold at 800–850 °C to crystallize the glass. In order to achieve the correct thermal expansion for sealing to the nickel-based alloys, the glass-ceramic produced using this treatment contained a high proportion of cristobalite (up to $\approx$ 30%). Further work by Headley and Loehman [209] showed that crystallization of the glass employed in these seals occurred by epitaxial growth of lithium metasilicate, lithium disilicate and cristobalite on to relatively large (0.1–1.0 μm) Li_3PO_4 nuclei which formed in the glass mainly during the high-temperature sealing stage (rather than in the classical nucleation stage). An example is shown in Fig. 21. This work therefore indicated that the use of a conventional low-temperature nucleation stage could be superfluous to the production of the microstructure required for this application.

In order to analyse the detailed interfacial chemistry of this type of glass-ceramic seal to Inconel 718 alloy, Haws *et al.* [210] studied seals that had been prepared under prolonged heating at the sealing temperature (i.e. 66 h at 1000 °C). The resultant seals were studied by scanning electron microscopy, wavelength dispersive X-ray analysis and X-ray photoelectron spectroscopy (XPS). Many particles were observed in the glass-ceramic which were identified as metal phosphides of stoichiometry close to M_2P, where M = chromium, nickel, niobium and iron. It was noted that the chromium phosphide particles extended well into the bulk glass-ceramic, whilst the other metal phosphides only occurred very close to the interface between the metal and the glass-ceramic. It was also noted that many metallic species, including nickel, niobium, titanium, chromium and iron, were dissolved in the residual glassy phase, the glass being present near to the interface due to the depletion of the P_2O_5

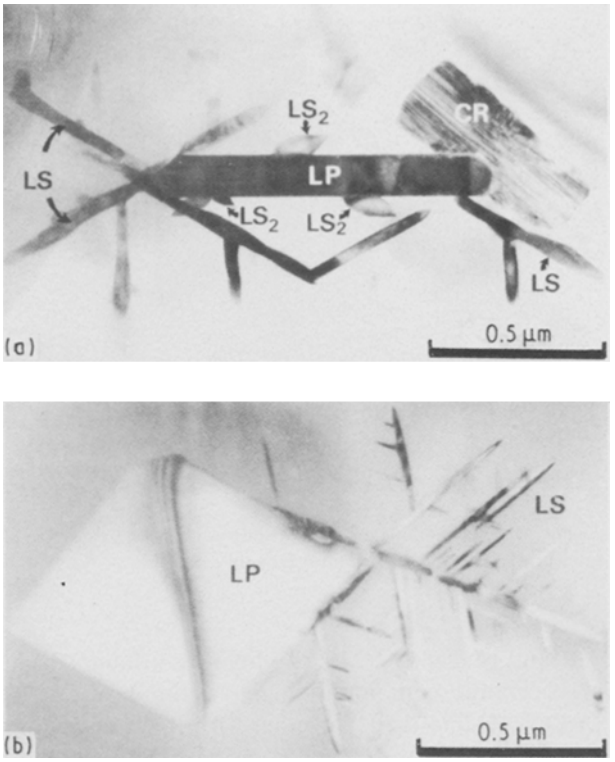

Figure 21 Epitaxial growth of crystal phases on to lithium phosphate nuclei (LP), after Headley and Loehman [209]; (a) growth of cristobalite (CR), lithium metasilicate (LS) and lithium disilicate (LS_2) on to LP; (b) growth of LS dendrite onto LP.

nucleating species. The oxidation states of these metals were determined using XPS. It was observed that niobium was present as Nb^{5+}, titanium as Ti^{4+}, iron and chromium were in mixed oxidation states, whilst nickel was apparently present in the zero-valent state. Further evidence for the presence of zero-valent metallic species in glass-ceramic seals was reported by Moddeman *et al.* [211]. In addition to the XPS data, direct evidence for the presence of zero-valent nickel has also been found using high-resolution TEM [212] where small particles, $\approx$ 100–200 nm in size, were observed in the glass-ceramic; these were identified as metallic nickel by electron diffraction.

Studies by Loehman and co-workers using the same glass-ceramic/metal system [164, 197, 198, 200, 213] indicated that during the sealing operation the glass reacts directly with the Inconel 718 by a redox mechanism, presumably after having dissolved the thin (20–200 nm) layer of oxide which is present on its surface. It was confirmed that reaction occurs in the interfacial zone between chromium, which diffuses into the glass from the metal, and the lithium phosphate nuclei, which are present in the crystallizing glass, to form chromium phosphide. The following reactions were postulated [200]

$$9Cr_{(alloy)} + 2Li_3PO_{4(glass)} \rightarrow 2Cr_2P_{(precipitate)} + 3Li_2O_{(glass)} + 5CrO_{(glass)} \quad (22)$$

or

$$22Cr_{(alloy)} + 6Li_3PO_{4(glass)} \rightarrow 6Cr_2P_{(precipitate)} + 9Li_2O_{(glass)} + 5Cr_2O_{3(glass)} \quad (23)$$

This was later revised by Loehman [213] to

$$59Cr_{(alloy)} + 14Li_3PO_{4(glass)} \rightarrow 2Cr_{12}P_{7(precipitate)} + 21Li_2O_{(glass)} + 35CrO_{(glass)} \quad (24)$$

or

$$142Cr_{(alloy)} + 42Li_3PO_{4(glass)} \rightarrow 6Cr_{12}P_{7(precipitate)} + 63Li_2O_{(glass)} + 35Cr_2O_{3(glass)} \quad (25)$$

These reactions destroy the nuclei. During subsequent crystallization of the glass this depletion of the nucleating species results in the formation of a coarse crystalline microstructure with properties, including thermal expansion characteristics, which differ markedly from that of the bulk glass-ceramic. In particular, thermal expansion is lowered [159] and this has a detrimental effect on seal quality and life. It has also been noted [197] that reaction can occur at the alloy grain boundaries in contact with the glass during sealing to form an intermetallic silicide phase, $M_6Ni_{16}Si_7$, where M may be a mixture of the alloy constituents, e.g. iron, molybdenum and niobium.

In the case of Hastelloy C276 a different set of redox reactions occur [198, 213]. This alloy contains a significant proportion of molybdenum (15–17%) which, together with chromium, diffuses into the glass during sealing. This results in the formation of precipitates of molybdenum phosphide and lithium chromium silicate according to the reaction

$$6SiO_{2(glass)} + Li_3PO_{4(glass)} + 5CrO_{(interface)} + xMo_{(alloy)} \rightarrow Mo_xP_{(interface)} + 3LiCr(SiO_3)_{2(glass)} + Cr_2O_{3(glass)} \quad (26)$$

The lithium phosphate nuclei are similarly destroyed by this mechanism, again leading to the formation of a coarse interfacial zone with different properties from that of the bulk glass-ceramic.

During the formation of glass- and glass-ceramic-to-metal seals and coatings, bubbles are often formed in the interfacial zone. The formation of bubbles has normally been attributed to reaction of the glass with the metal or with surface contaminants during sealing to give gaseous reaction products. One common mechanism involves reaction of the glass with carbides present in the metal to give CO or CO_2. This effect can be eliminated by decarburizing the metal surface prior to sealing or coating [214]. More recently, it has been observed for some of the nickel-based superalloys bonded to a lithium silicate glass-ceramic [199, 210] that reaction can also occur between metal species diffusing into the glass from the metal substrate and water present in the starting glass. In a number of cases large bubbles were observed in the glass-ceramic after sealing. It was pointed out that thermodynamic data suggest that hydrogen formation may, in fact, be responsible for bubbles in a wide range of seal systems. The metals, M, interact with this absorbed water to form hydrogen gas according to the reaction

$$xM_{(alloy)} + yH_2O_{(glass)} \rightarrow M_xO_{y(glass)} + yH_2\uparrow \quad (27)$$

Thermodynamic data for specific reactions are summarized in Table VIII. (The data are computed from

TABLE VIII Free energy change, ΔG°, for the reaction of water with metallic components of common alloys (calculated at 1300 K)

Reaction	ΔG° (kJ mol^{-1})
(a) Reaction favourable	
$Hf + 2H_2O = Hf_2O + 2H_2\uparrow$	− 524.3
$Y + 3/2H_2O = 1/2Y_2O_3 + 3/2H\uparrow$	− 500.6
$Zr + 2H_2O = ZrO_2 + 2H_2\uparrow$	− 498.8
$Al + 3/2H_2O = 1/2Al_2O_3 + 3/2H_2\uparrow$	− 366.7
$Ti + 2H_2O = TiO_2 + 2H_2\uparrow$	− 354.8
$Ta + 5/2H_2O = 1/2Ta_2O_5 + 5/2H_2\uparrow$	− 299.7
$Ti + H_2O = TiO + H_2\uparrow$	− 240.7
$Nb + 5/2H_2O = 1/2Nb_2O_5 + 5/2H_2\uparrow$	− 229.0
$Nb + 2H_2O = NbO_2 + 2H_2\uparrow$	− 211.5
$Cr + 3/2H_2O = 1/2Cr_2O_3 + 3/2H_2\uparrow$	− 129.4
$Nb + H_2O = NbO + H_2\uparrow$	− 120.7
$Mn + H_2O = MnO + H_2\uparrow$	− 113.0
$V + 5/2H_2O = 1/2V_2O_5 + 5/2H_2\uparrow$	− 77.2
$Mn + 4/3H_2O = 1/3Mn_3O_4 + 4/3H_2\uparrow$	− 76.5
$Mn + 3/2H_2O = 1/2Mn_2O_3 + 3/2H_2\uparrow$	− 46.6
$Zn + H_2O = ZnO + H_2\uparrow$	− 26.4
$Fe + H_2O = FeO + H_2\uparrow$	− 10.0
$Mo + 2H_2O = MoO_2 + 2H_2\uparrow$	− 5.7
(b) Reaction unfavourable	
$Fe + 4/3H_2O = 1/3Fe_3O_4 + H_2\uparrow$	+ 3.9
$W + 3H_2O = WO_3 + 3H_2\uparrow$	+ 16.0
$Fe + 3/2H_2O = 1/2Fe_2O_3 + H_2\uparrow$	+ 22.5
$Co + H_2O = CoO + H_2\uparrow$	+ 33.4
$Cu + 1/2H_2O = 1/2Cu_2O + 1/2H_2\uparrow$	+ 50.5
$Ni + H_2O = NiO + H_2\uparrow$	+ 51.8
$Pb + H_2O = PbO + H_2\uparrow$	+ 85.1
$Mo + 3H_2O = MoO_3 + 3H_2\uparrow$	+ 94.6
$Cu + H_2O = CuO + H_2\uparrow$	+ 134.3

the information given in the publication by Barin *et al.* [215]). This illustrates that reaction of water with, for example, iron, molybdenum, manganese, chromium, niobium, tantalum, titanium, yttrium, aluminium, etc., is thermodynamically favourable, whilst reaction with, for example, nickel, cobalt and copper is not. Reaction with chromium, which is present in high concentrations in most superalloy systems, is particularly favourable thermodynamically through the reaction

$$Cr_{(alloy)} + 3/2H_2O_{(glass)} \rightarrow 1/2Cr_2O_{3(glass)} + 3/2H_{2(glass)}\uparrow \quad (28)$$

In order to check the hypothesis that reaction with dissolved water can lead to hydrogen gas bubble formation, seals prepared to Inconel 718 using glass that had been melted under standard atmospheric conditions were compared with seals made from glass that had been prepared by bubbling dry nitrogen through the melt [210]. Glass-ceramic seals fabricated from the glass prepared under ambient conditions were found to contain a greater degree of porosity than those fabricated employing the alternatively prepared glass. In addition, it was also observed that seals prepared at increased pressure were relatively bubble free. These seals were produced by hot isostatic pressing at a pressure of 170 MPa. Presumably this overpressure is high enough to suppress the formation of pores by keeping any hydrogen formed in solution in the glass. This work showed, however, that the crystallization behaviour of the glass at increased pressure differed from the behaviour under ambient conditions; for example, sealing at ambient pressure gave a mixture of lithium metasilicate, lithium disilicate and cristobalite, whilst sealing at increased pressure gave lithium metasilicate and quartz. This study to determine the influence of water dissolved in the glass on the sealing behaviour was extended by Craven *et al.* [199] employing glasses that had been melted and cast under different atmospheric conditions. These glasses contained different proportions of dissolved water, the approximate amounts of water being determined by infra-red analysis. Seals prepared using glass that had been prepared under high relative humidity atmospheric conditions were observed to contain bubbles. The gas within these bubbles was identified as hydrogen by gas chromatographic analysis. Seals prepared employing glass that had been melted and cast under dry room conditions, on the other hand, were relatively free from bubbles. On the basis of thermodynamic data, it was proposed that as an alternative to preparing sealing glass under dry conditions (which is not always practical) it may be feasible to incorporate into the glass batch additions of suitable components that will react preferentially with chromium, so eliminating or minimizing the chromium–water reaction. Such additions include CuO (Table IX), the reaction

$$Cr + 3CuO \rightarrow 1/2Cr_2O_3 + 3/2Cu_2O_2 \quad (29)$$

having a ΔG value of $-381\,kJ\,mol^{-1}$, compared to $-129\,kJ\,mol^{-1}$ for the chromium–water reaction.

TABLE IX Free energy changes, ΔG°, for potential reactions of a number of glass and alloy components (calculated at 1300 K)

Reaction	ΔG°(kJ mol^{-1})
(a) Reaction favourable	
$Ti + 2CoO = TiO_2 + 2Co$	− 421.7
$Cr + 3CuO = 1/2Cr_2O_3 + 3/2Cu_2O$	− 380.6
$Cr + 3/2CuO = 1/2Cr_2O_3 + 3/2Cu$	− 330.8
$Al + 3/2Na_2O = 1/2Al_2O_3 + 3Na\uparrow$	− 298.2
$Cr + 3/2NiO = 1/2Cr_2O_3 + 3/2Ni$	− 207.2
$Cr + ZnO = CrO + Zn\uparrow$	− 187.4
$Cr + 1/2MoO_3 = 1/2Cr_2O_3 + 1/2Mo$	− 176.7
$Ti + 2/5B_2O_3 = 2/5TiB_2 + 3/5TiO_2$	− 146.8
$Cr + 1/2WO_3 = 1/2Cr_2O_3 + 1/2W$	− 137.4
$Cr + 3/2ZnO = 1/2Cr_2O_3 + 3/2Zn\uparrow$	− 89.8
$Cr + 3/2Na_2O = 1/2Cr_2O_3 + 3Na\uparrow$	− 61.9
$Cr + 1/2SiO_2 = CrO + 1/2Si$	− 51.2
$Fe + CoO = Co + FeO$	− 43.4
$Cr + 3/2CoO = 1/2Cr_2O_3 + 3/2Co$	− 43.0
(b) Reaction unfavourable	
$Ni + 1/3MoO_3 = NiO + 1/3Mo$	+ 20.3
$Fe + Na_2O = FeO + 2Na\uparrow$	+ 35.1
$Cr + 3/10V_2O_5 = 1/2Cr_2O_3 + 3/5V$	+ 53.5
$Mo + 3/11SiO_2 = 3/11Mo_3Si + 2/11MoO_3$	+ 80.5
$Cr + 3/4SiO_2 = 1/2Cr_2O_3 + 3/4Si$	+ 114.5
$Ni + 1/3Cr_2O_3 = NiO + 2/3Cr$	+ 138.1
$Cr + 3/2MnO = 1/2Cr_2O_3 + 3/2Mn$	+ 176.6
$Cr + 3/10Ta_2O_5 = 1/2Cr_2O_3 + 3/5Ta$	+ 187.0
$Cr + 3/2Li_2O = 1/2Cr_2O_3 + 3Li$	+ 245.1
$Cr + 1/2Al_2O_3 = 1/2Cr_2O_3 + Al$	+ 372.8
$Cr + 3/4ZrO_2 = 1/2Cr_2O_3 + 3/4Zr$	+ 381.2
$Cr + 3/4TiO_2 = 1/2Cr_2O_3 + 3/4Ti$	+ 478.0

The chromium should, therefore, react preferentially with the CuO instead of the dissolved water in the glass. This behaviour was confirmed experimentally by adding 1 wt% CuO to the glass batch prior to melting and casting under normal atmospheric conditions to yield a "wet" glass. Sealing with this glass led to the production of bubble-free, high-quality seals with Inconel 718. It was also demonstrated experimentally that doping the glass with products of Equation 27, e.g. 1 wt% Cr_2O_3 in the case of chromium-containing metals (Equation 28), could shift the equilibrium to the left and reduce hydrogen bubble formation.

Holland and co-workers [204–206] and Hong [207] have examined in some detail the coating characteristics of a lithium silicate glass-ceramic containing small additions of K_2O, ZnO and P_2O_5 to a Ni–Co–Cr alloy, Nimonic 263. The glass-ceramic was applied to both unoxidized and pre-oxidized metal surfaces in the form of a dispersion of glass particles, $\approx$ 10 μm in size, in an organic binder employing a screen-printing technique. The coatings were then fired either in nitrogen or air at various temperatures in the range 800–1100 °C. An optimum temperature of 980 °C was subsequently chosen, this providing adequate wetting of the metal substrate by the glass without the occurrence of excessive chemical reaction. Totally different reaction behaviour was observed, dependent on whether or not the substrate had been preoxidized. Examples are shown in Fig. 22.

For a substrate that had not been subjected to a pre-oxidation treatment, the following reactions were suggested. Firstly, chromium at the alloy interface reacts with ZnO in the glass to form a CrO layer at the interface; the reduced metallic zinc alloys with the substrate

$$Cr_{(substrate)} + ZnO_{(glass)} \rightarrow CrO_{(interface)} + Zn_{(substrate)} \quad (30)$$

(It should be noted that metallic zinc could be present as vapour at the coating temperature; presumably rapid alloying with the substrate occurs to minimize loss of zinc from the system.). So long as the CrO layer remains, the interface will be saturated with the substrate oxide and a strong chemical bond should exist. As firing continues, however, the rate of Reaction 30 will decrease due to a build up of reaction products; this is also coupled with a fast diffusion rate for Cr^{2+}. Under these conditions, the CrO will dissolve rapidly into the glass and the CrO layer will disappear. The glass is then again brought into direct contact with the substrate; however, further oxidation of the substrate through reduction of ZnO in the glass is now restricted due to the depletion of Zn^{2+} in the interfacial region. Under the driving force of chemical equilibrium, further redox reactions will take place between Cr^{2+} which has diffused into the glass from the substrate and the P_2O_5 nucleating agent present in the glass. The following reactions were suggested

$$59Cr_{(alloy)} + 7P_2O_{5(glass)} \rightarrow 2Cr_{12}P_{7(precipitate)} + 35CrO_{(glass)} \quad (31)$$

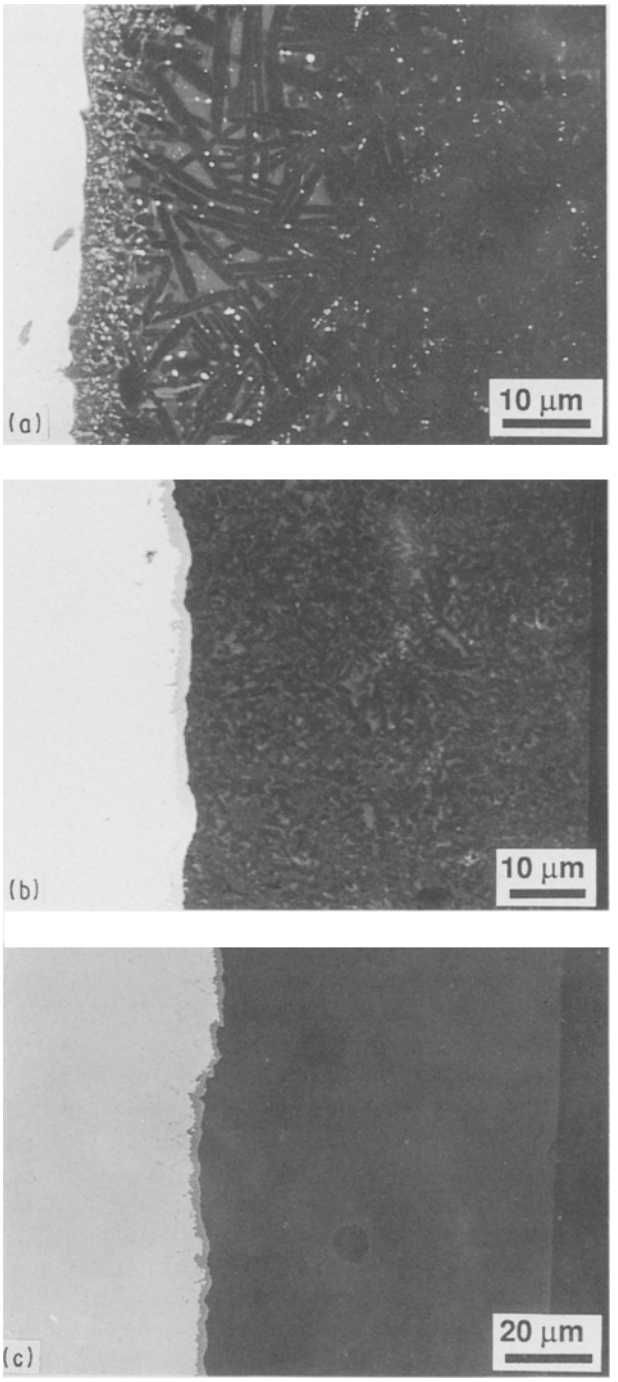

Figure 22 Glass-ceramic coatings on nickel-based superalloy illustrating the influence of the oxide layer formed by pre-oxidation of the metal substrate on the seal quality, after Hong and Holland [204]; (a) unoxidized substrate showing coarse glass-ceramic microstructure; (b, c) pre-oxidized substrates showing an adherent oxide interfacial region and a fine glass-ceramic microstructure.

or

$$152Cr_{(alloy)} + 21P_2O_{5(glass)} \rightarrow 2Cr_{12}P_{7(precipitate)} + 35Cr_2O_{3(glass)} \quad (32)$$

These reactions result in the formation of acicular precipitates within the interfacial region and they are highly undesirable because they remove the nucleating agent from the interfacial zone. During subsequent crystallization of the glass this depletion of P_2O_5 results in the formation of a coarse crystalline microstructure at the interface with properties, including

thermal expansion, that may differ markedly from that of the bulk glass-ceramic. Redox reactions also occur at the coating surface leading to the formation of $LiCr(SiO_3)_2$ crystals through the following sequence of reactions

$$2CrO_{(glass)} + ZnO_{(glass)} \rightarrow Cr_2O_3 + Zn_{(precipitates)} \quad (33)$$

$$Cr_2O_{3(glass)} + Li_2O_{(glass)} \rightarrow 2LiCr(SiO_3)_{2(precipitates)} \quad (34)$$

This effect also is undesirable, leading to physical wrinkling of the coating surface due to the relatively low thermal expansion ($\alpha \approx 5.6 \times 10^{-6}$) of $LiCr(SiO_3)_2$.

It was noted [204–207], on the other hand, that the reactions associated with the coating of a pre-oxidized substrate are very different. Suitable pre-oxidation leads to the formation of a 3–4 μm thick adherent, non-porous layer of Cr_2O_3. This layer prevents the glass from reacting directly with the metal; consequently, all the redox reactions are eliminated or significantly reduced. Saturation of Cr_2O_3 in the glass adjacent to the interface can easily be maintained (the diffusion of Cr^{3+} is slow), so creating the desired bonding conditions. Prolonged firing can, however, lead to the saturation limit of Cr_2O_3 in the glass at the interface being exceeded, and this can subsequently result in the undesirable formation of $LiCr(SiO_3)_2$ at the interface between the glass and the substrate oxide.

Donald and co-workers [188, 208] have studied in detail the bonding characteristics of a lithium zinc silicate glass-ceramic containing a high proportion of ZnO to nickel-based superalloys including Nimonic 90, Inconel 625 and Hastelloy C276. All sealing was carried out in argon using a standard heat-treatment cycle of 5 min at 950 °C followed by 60 min at 465 or 585 °C and 60 min at 850 °C, using both unoxidized and pre-oxidized metals. In the case of the unoxidized alloys, high-quality seals were obtained which were relatively free from porosity. In general, a narrow interfacial reaction zone was clearly visible, although this normally extended less than 1 μm into the glass-ceramic. In the case of sealing to Nimonic 90 the interfacial region consisted of a semi-continuous precipitate of a phase which EDS showed to be rich in chromium, titanium and silicon. It is possible that this layer is a complex mixture of CrO, Cr_2O_3 and TiO_2, together with Cr_3Si_2 or $LiCr(SiO_3)_2$. Unlike other nickel-based alloy/glass-ceramic systems, no evidence was found for the presence of transition metal phosphide phases in the interfacial zone. This suggests that the nucleating agent, P_2O_5, has not been removed by reaction with diffusing metal species for this particular system. It was noted that reduced metallic zinc had been formed at the metal interface, particularly at grain boundaries, presumably as a consequence of Reaction 30 or 33. In addition, small cubic crystals of a phase believed to be $ZnCr_2O_4$ were dispersed throughout the bulk glass-ceramic, suggesting rapid diffusion of chromium from the metal substrate into the glass-ceramic. A similar although slightly coarser interfacial reaction zone was noted when sealing to Inconel 625. In this case, however, EDS revealed the concentration of silicon to be low whilst the concentration of chromium was very high. This suggests that this zone consists mainly of CrO and/or Cr_2O_3. Again, there was no evidence for the formation of transition metal phosphide phases. Examples are shown in Fig. 23.

In the study by Donald and co-workers [188, 208] the effect of a number of transition metal oxide additions on the sealing behaviour of the glass-ceramic was investigated. These oxides, which included CuO, NiO and MoO_3, were added to the glass batch at the 2 mol % level. In the case of the CuO addition, sealing to Nimonic 90 resulted in the formation of a much coarser interfacial zone than in the case when this oxide was absent. This consisted of four or five discrete layers with a total thickness of the order of 3–4 μm. EDS analysis showed that this region was rich in nickel and chromium, with smaller additions of cobalt, titanium and silicon. It was noted that the outermost interfacial layer was richer in chromium, whilst the inner layer was richer in nickel. The microstructure of the glass-ceramic at the interface was very fine, and there was no evidence for the formation of transition metal phosphide phases. In addition, the penetration of reduced metallic zinc into the metal substrate at grain boundaries was quite severe, extending $\approx$ 4 μm into the alloy surface. Similar effects were noted for the addition of NiO. Seals to Inconel 625 were also similar in appearance. Addition of MoO_3 to an Inconel 625 seal also resulted in the formation of a layered interfacial zone, but in this case only two layers were apparent, consisting of a coarse granular inner layer and a thinner continuous outer layer. The inner zone was found to be rich in nickel, molybdenum and chromium, whilst the outer region was rich in molybdenum and chromium with some silicon. In addition, small discrete precipitates, also rich in molybdenum and chromium with some silicon (possibly a mixture of $MoSi_2$ and Cr_3Si_2), were observed within the glass-ceramic close to the interface. Examples are shown in Fig. 24.

5.6. Bonding to chromium

Little work has been reported on the sealing of glass or glass-ceramic materials to chromium, due in part to the very high chemical reactivity of this metal. Tomsia *et al.* [216] have, however, examined the bonding and associated chemical reactions between a model sodium disilicate glass and chromium, with the aim of gaining a clearer understanding of the role played by chromium in the formation of seals to chromium-containing alloys. A number of reactions were identified, depending on the partial pressure of oxygen in the sealing environment and the overall thickness of the glassy layer, including

$$Cr + Na_2O \rightarrow CrO + 2Na\uparrow \quad (35)$$

$$2CrO + Na_2O \rightarrow Cr_2O_3 + 6Na\uparrow \quad (36)$$

$$2Cr + 3Na_2O \rightarrow Cr_2O_3 + 2Na\uparrow \quad (37)$$

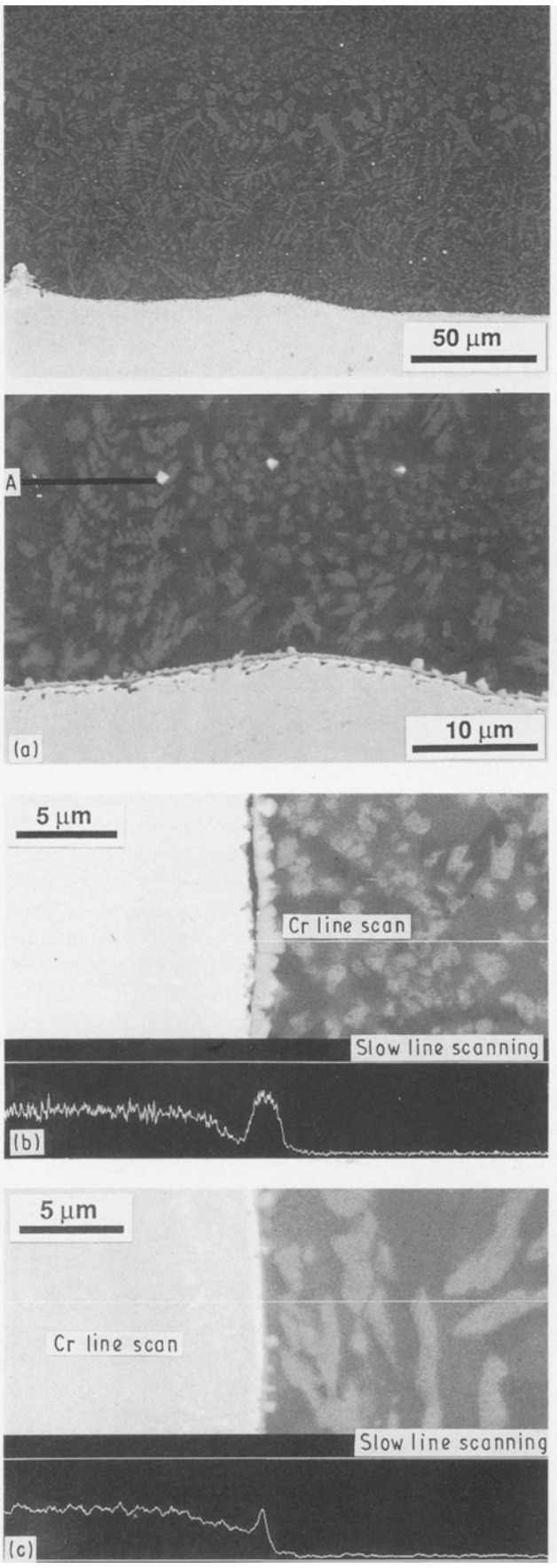

Figure 23 Lithium zinc silicate glass-ceramic seal to nickel-based alloys: (a) seal to Nimonic 90 alloy, showing dendritic phase in glass-ceramic near to the interface and presence of particles, A, believed to be $ZnCr_2O_4$, within the bulk glass-ceramic; (b) seal to Inconel 625 with EDS line scan showing high concentration of chromium at the interface; (c) seal to Hastelloy C276 with EDS line scan also showing high concentration of chromium at the interface; after Metcalfe *et al.* [188, 208].

It was noted that the formation of Cr^{2+} (CrO) may result in the formation of a mechanically weak interface, whilst formation of Cr^{3+} (Cr_2O_3) can result in the formation of a strong bond between the glass and chromium. This was related to the lower solubility of Cr_2O_3 in the glass resulting in saturation within the interfacial zone being readily achieved during sealing.

5.7. Bonding to molybdenum and tungsten

Seals have been prepared to molybdenum and tungsten in electrical applications (e.g. [104]). Limited work has also been reported on the sealing of glass-ceramics to molybdenum. In one study, Nash *et al.* [217] successfully sealed a zinc alumino-silicate glass-ceramic to unoxidized molybdenum. Sealing was initially carried out employing a conventional three-stage heat-treatment schedule. This consisted of a high-temperature stage to melt the glass, followed by a nucleation stage of 2 h at 650 °C and a crystallization stage of 2 h at 850 °C. It was subsequently noted, however, that crystal nucleation *and* growth occurred during the initial heating and cooling stages up to and down from the sealing temperature. Conventional nucleation and crystallization stages were, therefore, deemed unnecessary. The final heat-treatment consisted of a single high-temperature cycle to 1040 °C over 30 min; this was followed by a hold at this temperature before cooling down to ambient temperature. Holland *et al.* [206] have also reported the coating of molybdenum with a magnesium alumino-silicate glass-ceramic.

5.8. Bonding to titanium

The service temperature of titanium alloys is limited to around 590 °C in air due to the formation of an oxide scale with a brittle sub-surface layer which can initiate surface cracking. In addition, two allotropic forms of titanium exist, α-Ti with an h c p crystal structure and β-Ti which is b c c. The α phase exhibits greater toughness and improved fatigue performance, whilst the β phase offers superior creep behaviour. The α to β transformation occurs at 882 °C, and is accompanied by a volume change. This can hamper coating of this metal, unless a low coating temperature is employed, or a phase-stabilized titanium alloy is used. Less work has been reported on the bonding of glasses and glass-ceramics to titanium and its alloys, due in part to the problems associated with this volume change, and also in part due to the high reactivity of this metal.

In general, conventional silicate sealing glasses cannot be employed in the preparation of seals or coatings to titanium and its alloys due to the occurrence of severe interfacial reactions [218–221]. These reactions lead to porous structures and mechanically weak interfaces due to the evolution of gaseous reaction products and the formation of brittle and poorly adherent silicide phases. For example, Passerone *et al.* [220] noted that molten lithium silicate glasses react with titanium at temperatures in the range 1100–1400 °C under reducing conditions to form a number of intermediate phases, including Ti_2O_3 and

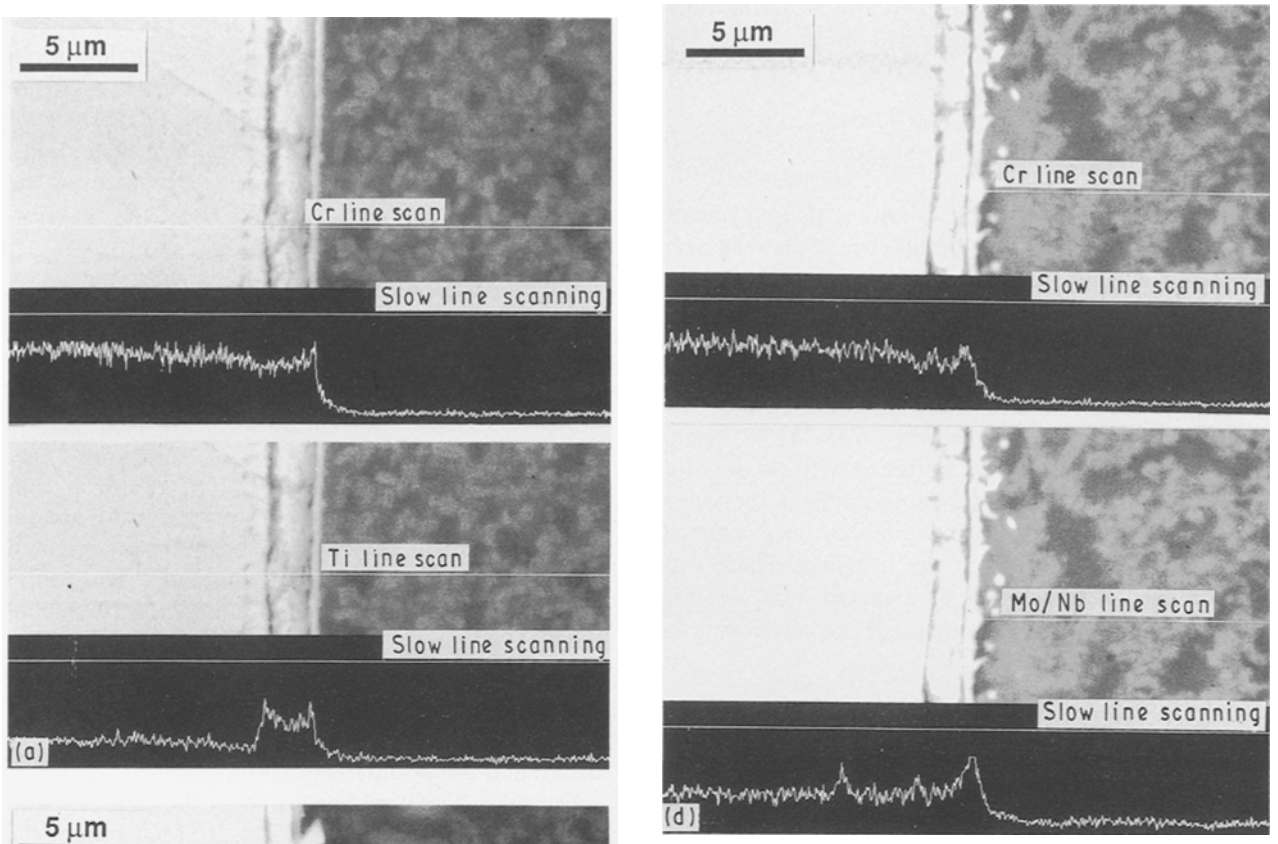

Figure 24 Lithium zinc silicate glass-ceramic seal to nickel-based alloys showing the effect of TMO additions to the glass on the sealing behaviour. (a) Seal between Nimonic 90 and glass containing CuO addition showing layered structure of the interfacial region; EDS scans show high concentration of chromium and titanium at the interface; (b) seal between Inconel 625 and glass containing NiO addition; (c) seal between Inconel 625 and glass containing Cr_2O_3 addition; note thicker layered interface structure; (d) seal between Inconel 625 and glass containing MoO_3; note high concentration of molybdenum at the interface; after Metcalfe *et al.* [188, 208].

Ti_5Si_3. In addition, silicon diffuses into the titanium substrate. At the higher temperatures, extensive solution (up to 15–20 at %) of silicon in titanium occurs, and this leads to the formation of a discrete liquid phase. Based on thermodynamic data for the free energy of reaction of titanium with various oxides, Sitnikov *et al.* [218] predicted that introduction of a number of oxides into a lithium silicate glass should reduce the corrosion of titanium by the molten glass. Their predictions were confirmed experimentally, it being observed that addition of Li_2O, BeO, CaO, SrO, BaO and CeO_2 did indeed retard the corrosion of titanium by the molten glasses. Similarly, substitution of oxides in the glass by less reactive oxides also retarded corrosion; for example, replacement of Na_2O by B_2O_3, MnO or ZnO.

Brow and Watkins [222] examined the potential of non-silicate boro-aluminate glasses for sealing to pure titanium and a β-phase-stabilized titanium alloy. The performance of these glasses was compared to that of a commercial silicate sealing glass. Bonding to the sodium silicate sealing glass at temperatures in the range 760–950 °C in argon was surprisingly found to produce good quality hermetic seals with only a thin

reaction zone $\approx$ 1 μm thick. The presence of a titanium silicide phase was confirmed in this zone, the probable reaction being

$$8Ti_{(metal)} + 3SiO_{2(glass)} \rightarrow Ti_5Si_{3(interface)} + 3TiO_{2(interface)} \quad (38)$$

The formation of reasonable quality seals to a silicate glass was believed to be a consequence of the relatively low sealing temperatures employed in this work. A number of boro-aluminate seals were also investigated, these glasses containing the alkaline earth oxides CaO (known as "CABAL" glasses), SrO ("SrBAL" glasses) or BaO ("BABAL" glasses). Sealing was carried out in the temperature range 670–745 °C. High-quality hermetic seals were obtained with no obvious interfacial reaction products being visible in sectioned seals, although the presence of titanium was detected in the glass $\approx$ 15 μm from the interface. There was some evidence from XPS of a mixed $TiB_2 + TiO_2$ interfacial region, possibly through the reaction

$$5Ti_{(metal)} + 2B_2O_{3(glass)} \rightarrow 2TiB_{2(interface)} + 3TiO_{2(interface)} \quad (39)$$

Seal strengths were monitored by measuring the load required to fracture a simple seal configuration. It was noted that the load required to fracture a seal with the boro-aluminate glass was approximately 50% greater than that required to fracture the equivalent silicate seal.

Hong and Holland [205] and Hong [207] have reported the coating of titanium with a lithium alumino-silicate glass-ceramic. Coating of unoxidized titanium in an inert atmosphere (argon) at 970 °C was observed to give a very porous coating. This was believed to be due to reaction of the glass with titanium under these sealing conditions to give Ti_5Si_3 together with gaseous oxygen

$$5Ti_{(metal)} + 3SiO_{2(glass)} \rightarrow Ti_5Si_{3(interface)} + O_2\uparrow \quad (40)$$

In addition, it was noted that a number of further reactions are possible (in particular between titanium and the P_2O_5 nucleating agent), including

$$16Ti + 6P_2O_5 \rightarrow 4Ti_4P_3 + 15O_2\uparrow \quad (41)$$

$$9Ti + 3P_2O_5 \rightarrow 2Ti_4P_3 + 7O_2\uparrow + TiO \quad (42)$$

$$17Ti + 6P_2O_5 \rightarrow 4Ti_4P_3 + 14O_2\uparrow + TiO_2 \quad (43)$$

Coating at lower temperatures, down to 900 °C, was unsuccessful because rapid crystallization of the glass powder occurred, and this prevented adequate wetting of the substrate in addition to inhibiting sintering of the powder.

It was observed that use of suitably pre-oxidized titanium can eliminate the reactions that evolve gaseous oxygen. However, owing to the fact that TiO_2 dissolves readily in the glass during coating, it was found necessary to pre-oxidize to give a relatively thick ($\approx$ 8–10 μm) oxide layer. Unfortunately, although the resultant coatings were non-porous, they were also mechanically weak due to the brittle nature of the oxide layer and its poor adhesion to the substrate. It was noted that non-porous coatings can also be formed by coating unoxidized titanium in air. In the presence of air, Reaction 40 is replaced by Reaction 38; however, it was found that the brittle behaviour of Ti_5Si_3 again led to mechanically weak coatings. In addition to pre-oxidation, the effect of nitriding the surface of titanium on the coating chemistry was also examined. A thin layer of TiN was formed by heating the metal in nitrogen at 900–980 °C. Unfortunately, on coating, a porous microstructure again resulted despite the presence of this layer. This was believed to be due to the reaction

$$5TiN_{(interface)} + 3SiO_{2(glass)} \rightarrow Ti_5Si_{3(interface)} + 3O_2\uparrow + 5/2N_2\uparrow \quad (44)$$

In addition to the lithium alumino-silicate system other alumino-silicate compositions were investigated by Hong [207] for sealing to titanium. It was found that glasses from the calcium alumino-silicate system containing 10 wt% TiO_2 gave particularly good coating results. It was suggested that for this system, Reaction 38 occurs in preference to Reaction 40. Unfortunately, the crystallization characteristics of this system are poor.

The overall coating behaviour of these silicate systems led Hong and Holland [205, 207] to examine the use of traditional adhesion promoting oxide additives on the coating behaviour of titanium. This work showed that addition of CoO, for example, can lead to the formation of a strong, non-porous interface through the reaction

$$Ti_{(metal)} + 2CoO_{(glass)} \rightarrow 2Co_{(precipitate)} + TiO_{2(glass)} \quad (45)$$

This reaction occurs because the free energy of formation of CoO has a less negative value than that of TiO_2. Reaction 45, therefore, occurs in preference to Reaction 40. Precipitates of metallic cobalt are formed in the glass-ceramic near to the interface and improve the bond strength further by mechanical keying effects. It was noted that failure of these coatings was always within the glass-ceramic, rather than at the interface, in contrast to the other coatings on titanium. Micrographs showing coatings applied to unoxidized titanium are given in Fig. 25, for glasses both with and without the addition of CoO.

Coatings have also been successfully applied to titanium by Metcalfe *et al.* [223] employing a calcium borosilicate glass. The effect on the bonding characteristics of adding a number of rare-earth metal oxide additions to the glass was also studied. Examples are shown in Fig. 26. This work is at an early stage, and further details will be reported later.

5.9. Bonding to aluminium

Coating (enamelling) of aluminium and aluminium-alloys has been practised for a number of years [10]. Owing to the relatively low melting temperature of aluminium (660 °C), coating glasses have been confined to low softening temperature lead silicate, barium borosilicate and alkali oxide phosphate compositions. Some typical compositions are given in

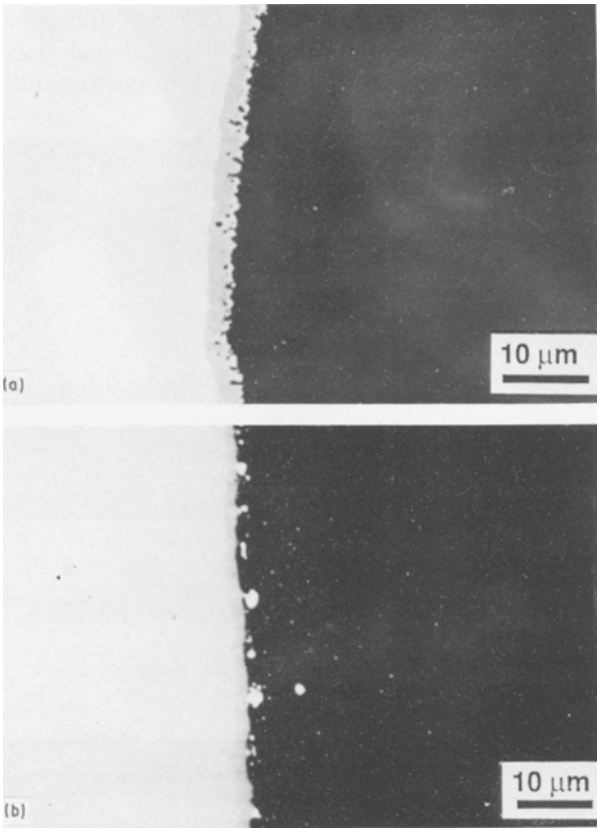

Figure 25 Glass coatings on unoxidized titanium; after Hong and Holland [205]: (a) coating without the addition of an adherence promoter; reaction has occurred to give brittle Ti_5Si_3 at the interface; (b) coating with the addition of CoO; reaction has occurred to yield TiO_2 at the interface, together with cobalt precipitates.

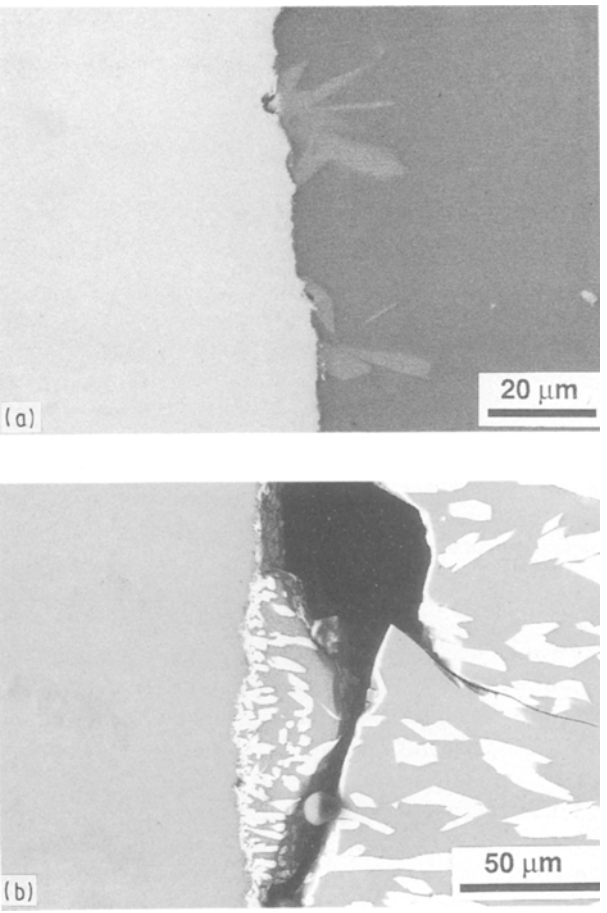

Figure 26 Glass coatings on titanium; after Metcalfe *et al.* [223]: (a) calcium borosilicate glass, showing the presence of a surface crystallized phase; (b) calcium borosilicate glass doped with Er_2O_3, showing the presence of an Erbium-rich crystalline phase both at the interface and within the bulk glass (note that the bulk glass has broken away leaving a thin layer adhering to the titanium substrate).

Table III. Further details of these systems are given by Andrews [10].

In contrast, very little work has been reported on the *sealing* of glasses or glass-ceramics to aluminium or its alloys. This is due to a combination of factors that include the relatively low melting temperature of aluminium, its high thermal expansion ($\alpha \approx 25 \times 10^{-6}\,°C^{-1}$) and its high chemical reactivity. It has been suggested [36, 37, 101] that certain low melting point phosphate-based glasses and glass-ceramics may be suitable for sealing to aluminium alloys. In addition, a lithium silicate glass has been successfully sealed to aluminium and a number of its alloys employing a novel injection-moulding technique [109]. Although the glass had a higher working temperature than the melting point of aluminium, careful control over the injection-moulding parameters was shown to lead to the formation of viable, high-quality, hermetic seals. The technique is made possible by the fact that the injection mould acts as an efficient heat sink, thereby preventing the molten glass from heating the aluminium component to beyond its melting point.

5.10. Bonding to tantalum

Little work has been reported on the coating or sealing of glasses to tantalum or its alloys. Practical bonding to tantalum is rendered particularly difficult because tantalum undergoes embrittlement at temperatures greater than about 300 °C in air. Conventional pre-oxidation treatments are therefore not feasible without seriously degrading the metal. Reasonably successful seals to tantalum have nevertheless been produced by Metcalfe *et al.* [223] employing lithium magnesium alumino-silicate and strontium titanium alumino-silicate glass-ceramics, in addition to calcium borosilicate glasses doped with Ta_2O_5. An example is shown in Fig. 27. This work is at an early stage, and further details will be reported later.

6. Applications for seals and coatings

6.1. Seals

Glass-to-metal seals are widely employed in the electrical and electronics industries in the preparation of electrically insulated feed-through connectors and related devices. Some examples include lamp envelopes, vacuum tubes, radar magnetrons and microwave connectors, TV tubes, reed and relay switches, microelectronic packaging, etc. Glass is a near ideal medium for these types of application; not only can mechanically strong, hermetic bonding be achieved to metals, but glass is also relatively impervious to gases, it is a good electrical insulator, it is reasonably refractory, and it is inexpensive. A wide variety of sealing glasses

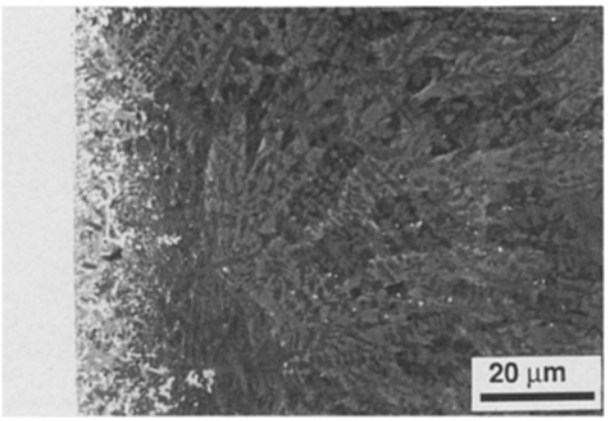

Figure 27 Glass coating on tantalum; after Metcalfe *et al.* [223]; the glass is a lithium magnesium alumino-silicate composition and has partially crystallized during sealing; note the tantalum-rich precipitates within the interfacial region.

are available commercially for bonding to a number of metals and alloys. A summary of some of these is given in Table II. Glass-to-metal seals have also been considered for use in the newer Na–S and Li–SO_2 batteries.

Glass-ceramic-to-metal seals are a more modern invention used for more arduous applications. McMillan and co-workers were the first to show that glass-ceramics could be employed to produce seals that exhibited superior properties relative to conventional glass-to-metal seals [1, 89, 90]. Some of the applications for which glass-ceramic-to-metal seals have been utilized include refractory vacuum and laser tube

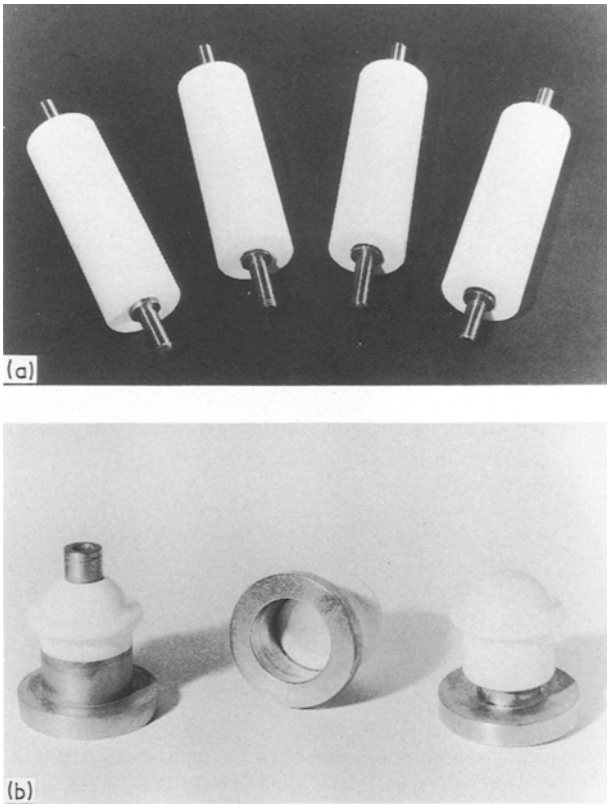

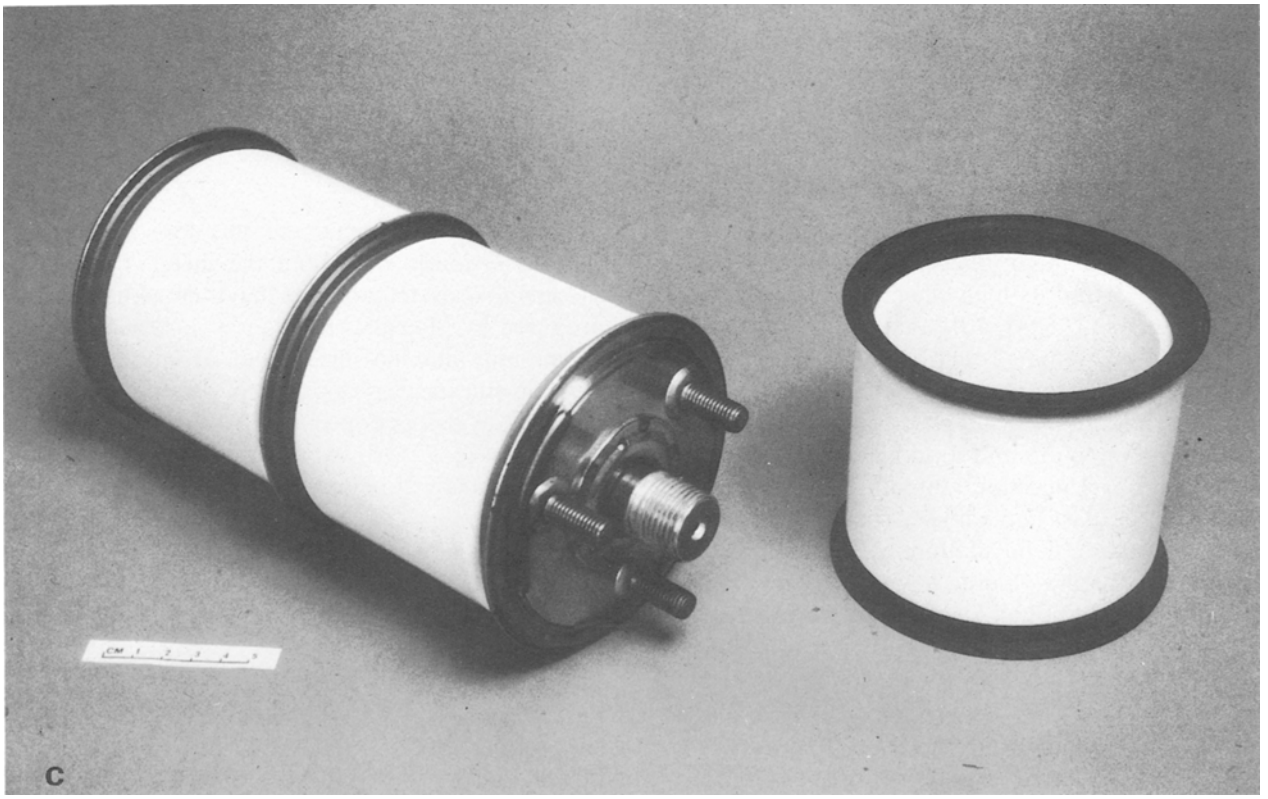

Figure 28 A selection of typical seal components: (a) glass-ceramic insulators with mild steel fixing studs sealed into the ends (courtesy of GEC Alsthom); the glass-ceramic cylinder is ≈ 102 mm long. (b) glass-ceramic-to-copper vacuum envelopes (courtesy of GEC Alsthom); the diameter of the metal rings is ≈ 30 mm. (c) Glass-ceramic/metal vacuum interrupter envelopes; these consist of a lithium alumino-silicate glass-ceramic bonded to a 17% Cr/Fe alloy (courtesy of GEC Alsthom). (d) A selection of glass-ceramic-to-metal feed-through seals and multi-pin substrates for electrical applications (courtesy of GEC Alsthom). (e) High-voltage vacuum tube envelope consisting of a zinc alumino-silicate glass-ceramic bonded to molybdenum; this figure shows sealed components together with some of the piece-parts and fixturing employed in their construction (courtesy of AWE).

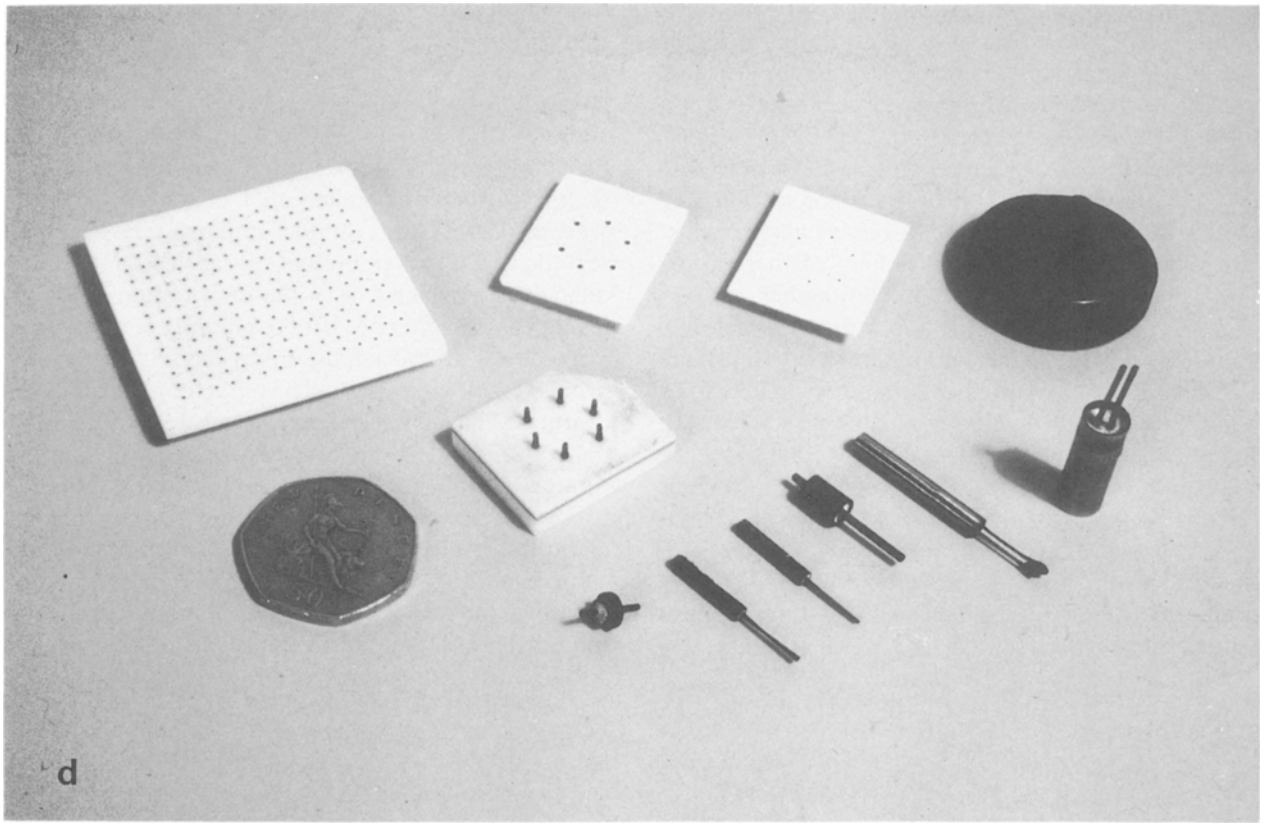

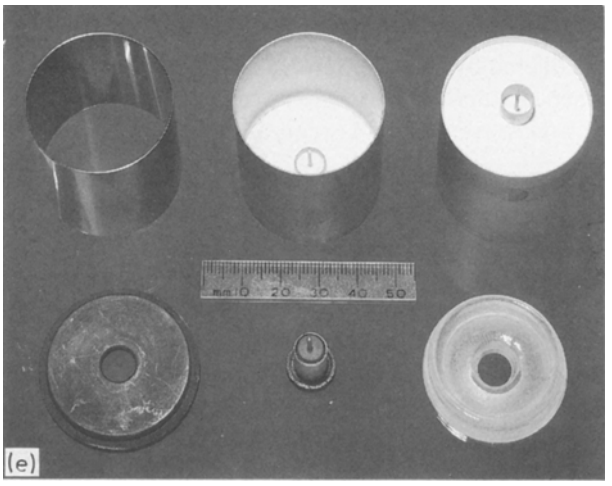

Figure 28 (Continued)

envelopes, vacuum interrupters, high temperature insulation, and high pressure pyrotechnic actuators [106, 115, 195, 217, 224, 225]. Some typical components are shown in Fig. 28.

6.2. Coatings

As described earlier, much of the early work in the area of glass-to-metal coatings was concerned with the preparation of enamelled metals. The enamelling of the metals gold, silver, bronze and copper for the production of jewellery dates back to ancient Egyptian times. Later, in the Byzantine period, the art of enamelling spread to Europe and elsewhere and was broadened to encompass the decorative enamelling of larger items, although it was still generally limited to the preparation of objects of art, rather than for the specific protection of metal surfaces. It was not until the middle of the nineteenth century that the large-scale preparation of enamelled metals was initiated, originally in Germany. This was with the industrial production of enamelled cast and wrought iron ware, including cooking utensils, baths and underground piping, the enamel being applied in order to provide a corrosion- and abrasion-resistant protective surface on the metal. More recently, vitreous-enamelled metals have been employed in a multitude of large volume/low technology applications, both in the home and industry. Examples of the use of enamelled metals in the home include their application in cookers, sink units, washers, cooking utensils, water and storage heaters, and gas fires and stoves. Industrial applications include their use in architecture, e.g. building panels and tunnel walls. Other industrial applications include enamelled vessels, pipes, valves, stirrers, etc., used in the chemical industry; for the protection of metals used in agricultural applications; and for use in heat-exchangers and related devices [10, 116, 139]. More recently, glass-ceramic coatings exhibiting superior mechanical and other properties have been applied for the protection of, for example, metal pipes and vessels in the chemical industry.

High-technology applications for glass-to-metal coatings have emerged in a number of industries over the last 20 years. For example, the use of enamelled steel or copper substrates in the electronics industry for microelectronics applications, including printed circuit boards and multi-layer electronic packaging. In these applications, circuitry is applied to the enamel coating using thin- or thick-film technology. An enamelled substrate offers a number of advantages over

more conventional alumina ceramic or organic polymer substrate materials, including lower dielectric constants (which allows higher operating frequencies), and higher thermal dissipation factors which is important in close-packed electronic systems [139, 226]. More recently, glass-ceramics have been employed to coat metal substrates for this type of application. Use of glass-ceramics provides a mechanically stronger system, provides for closer matching of thermal expansion characteristics, and allows higher temperatures to be employed in the application of thick-film circuitry; and this higher temperature capability allows the use of conventional screen printing inks to be employed [79, 80]. A number of examples are shown in Fig. 29. Enamel and glass-ceramic coatings have also been employed for the protection of metals against oxidation in the aerospace industry; for example, coating of after-burners and low-pressure turbine blades in jet engines [139]; in addition, they have also been examined as protective coatings for medical and dental prostheses [227].

7. Discussion

7.1. Advantages of glass and glass-ceramic seals and coatings

A wide range of glass and glass-ceramic materials have been investigated specifically for use in the preparation of seals and coatings to metals and alloys. The major advantages offered by these materials are their refractoriness and stability, relative to organic sealants and coatings, and their ease of application compared to other ceramic materials. The newer glass-ceramic-to-metal seals and coatings offer all the advantages associated with their glassy counterparts, i.e. ease of fabrication, good bonding characteristics, etc., and, in addition, also offer several further important benefits, including more refractory behaviour. In this respect, their performance parallels that of ceramic-to-metal seals employing, for example, alumina. Glass-ceramic seals do not, however, present the fabrication/bonding difficulties associated with the use of alumina or related ceramic materials. (In the bonding of alumina to a metal the alumina must first generally be "metallized" employing suitable refractory metal/glass coatings. This metallized layer is subsequently nickel-plated prior to using a metal braze to bond the ceramic component to the metal. The overall bonding process is therefore subject to the successful completion of a number of stages, which all add to the complexity and cost of the finished component. Alternative joining processes are available, including solid-state bonding and active metal brazing, although each method presents its own set of problems. Recent reviews on the subject of alumina- and related ceramic-to-metal joining include those by Loehman and Tomsia [228], Hey [229], Courbiere [230] and Akselsen [231].) In addition, glass-ceramics are mechanically stronger than their glassy counterparts, are more resistant to static fatigue, and can be more resistant to chemical attack. A further major advantage offered by glass-ceramics is that a greater range of practical thermal expansions can be obtained than with glasses alone. (This can also include non-linear

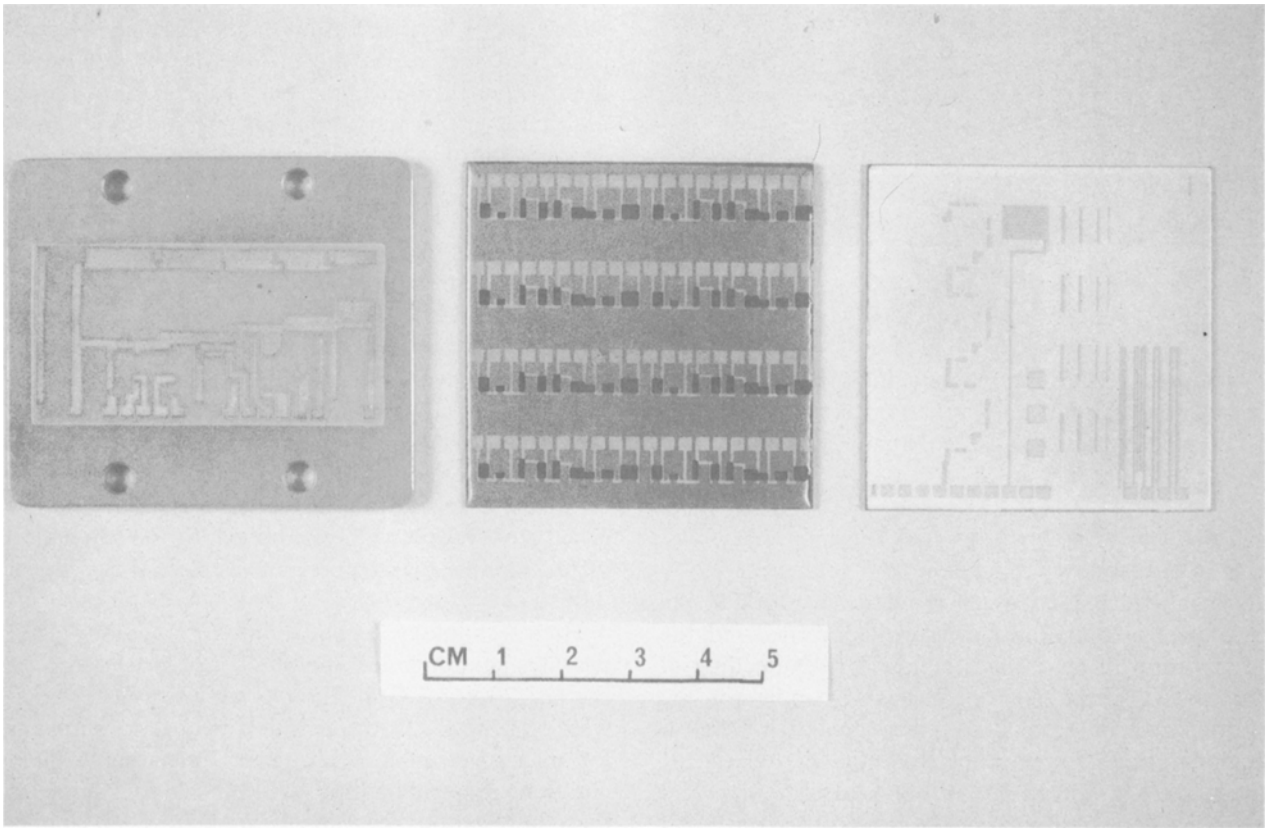

Figure 29 Some glass-ceramic-to-metal coatings: gold or copper thick-film conductor tracks screen printed onto glass-ceramic coated metal substrates; the substrates are, from left to right, copper, a copper-invar-copper sandwich, and titanium (courtesy of GEC Alsthom).

behaviour which can mimic phase transformations in metals). In principle, this enables very close thermal expansion matching to a wide variety of metals and alloys.

7.2. Thermal expansion characteristics

In the production of a high-strength glass-ceramic component with specific thermal expansion characteristics, e.g. a telescope mirror blank with zero expansion over a given temperature range, it is usual to cast the required shape in glass. This glass blank is then annealed and subjected to the heat-treatment schedule appropriate for the production of a fine grain size material containing the crystal phases necessary to impart the required thermal expansion behaviour. The heat-treatment is generally a two-stage process (Fig. 2), consisting of a nucleation stage when a large number of small crystal nuclei form within the glass, followed by a higher temperature crystallization stage when the major crystal phases grow from these nuclei to form a polycrystalline glass-ceramic material. When selecting a glass-ceramic for bonding to a particular metal or alloy it is, however, essential that a full simulated sealing/heat-treatment schedule, including the high-temperature sealing stage, is employed for determining the thermal expansion behaviour of the material (Fig. 5). This is because nucleation and growth of crystals can occur during the sealing stage, e.g. during the period required to heat the glass up to the sealing temperature or, alternatively, in the period required to cool the molten glass from the sealing temperature to the nucleation temperature. The proportion and types of major crystalline phases that subsequently form may differ considerably from those obtained when employing a standard two-stage heat-treatment schedule [96, 98, 208, 217]; hence, a glass-ceramic which exhibits the required thermal expansion characteristics in bulk form may not necessarily be suitable for sealing or coating applications unless extensive modification of the overall heat-treatment schedule is instigated. Furthermore, use of separate nucleation and crystallization stages may, in fact, sometimes be unnecessary when using glass-ceramic materials specifically for sealing or coating applications. For example, Headley and Loehman [209] showed that a separate nucleation stage is superfluous when sealing a lithium silicate glass-ceramic to nickel-based superalloys, whilst Nash *et al.* [217] have noted that a single high-temperature heat-treatment stage suffices for sealing a zinc alumino-silicate glass-ceramic to molybdenum. In addition, for coating or sealing applications, a glass-ceramic is ideally required which is relatively process parameter insensitive over as wide a range of processing conditions as possible. For example, if the required expansion behaviour can only be achieved by crystallizing within the narrow temperature range $T_X \pm 5\,^{\circ}C$, this material will be unlikely to make a good practical sealing or coating medium.

Thermal expansion data for a number of glass-ceramic materials are given in Table V, together with the corresponding heat-treatment schedules. It should be noted that many of the data relate only to a standard two-stage nucleation and crystallization heat-treatment process. Use of these materials as sealing or coating media would therefore require that the expansion behaviour be re-assessed for samples subjected to an additional high-temperature sealing stage. Examples of the influence of process variables on the resultant thermal expansion coefficient of a number of glass-ceramic materials are illustrated in Figs 30–32. Thermal expansion coefficient is plotted as a function of the crystallization temperature in Figs 30 and 31; the other heat-treatment parameters are kept constant for each composition shown in these figures. The influence of a sealing stage is illustrated in Fig. 32 which compares α of glass-ceramic samples given standard nucleation and crystallization treatments, with and without the inclusion of a high-temperature simulated sealing stage.

7.3. Bonding between a metal and a glass or glass-ceramic

It is now recognized that strong chemical bonding can be achieved between a metal and a glass if the conditions during bonding are such that the glass at the interface becomes *and remains* saturated with the appropriate substrate metal oxide. In practice this is

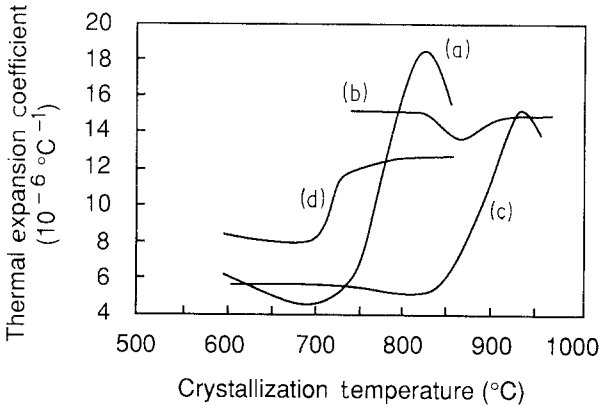

Figure 30 Thermal expansion coefficient of lithium zinc silicate glass-ceramics as a function of temperature of crystallization: (a) composition AZS-1, Table III (from [94]); (b) composition AZS-6 (from [98]); (c) composition AZS-5 (from [94]); (d) composition AS-9 (from [67]).

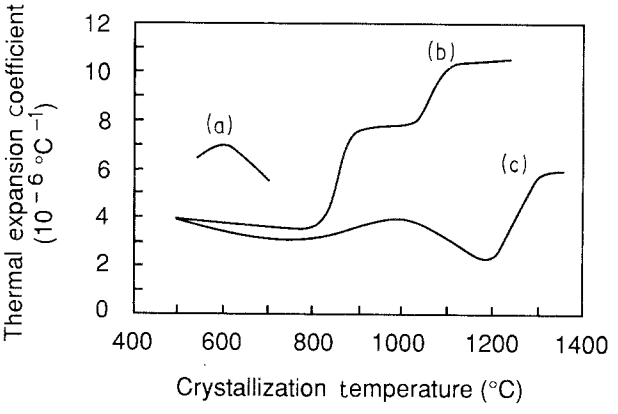

Figure 31 Thermal expansion coefficient of other glass-ceramic materials as a function of temperature of crystallization: (a) lithium cadmium silicate, composition ACS-3, (from [232]); (b) magnesium zinc silicate, composition AZS-11 (from [99]); (c) titanium alumino-silicate, composition TAS-4 (from [233]).

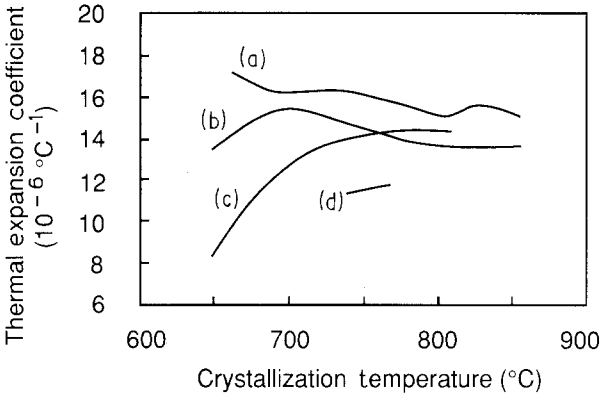

Figure 32 Comparison of thermal expansions of glass-ceramics with and without the inclusion of a high-temperature simulated sealing stage (from [96]). (a) composition AZS-2 with high-temperature sealing stage; (b) composition AZS-2 without high-temperature stage; (c) composition AZS-13 with high-temperature stage; (d) composition AZS-13 without high-temperature stage.

achieved traditionally by pre-oxidizing the metal substrate prior to sealing or coating. During bonding, the oxide layer will dissolve into the glass. Ideally, the bonding operation should be terminated at the stage when all the oxide (except for a single mono-atomic layer) has just dissolved into the glass, the interface remaining saturated with the oxide. This ideal condition is rarely met in practice. Usually, a finite thickness of oxide layer remains at the interface so that bonding is achieved, not directly between the metal and the glass, but via this discrete oxide layer. The overall properties of the seal or coating will therefore be dictated by the properties of the transitional oxide layer and its bonding characteristics both to the metal substrate and to the glass or glass-ceramic. On the other hand, if sealing conditions are maintained after total dissolution of the oxide layer has occurred, saturation at the interface will subsequently be lost due to further diffusion of the oxide into the bulk of the glass away from the interface (under the influence of a chemical gradient). The formation, or otherwise, of strong chemical bonding at the interface will then be controlled by the occurrence of suitable redox reactions between the metal substrate and the glass. For example, the reaction between chromium and ZnO (Equation [30]) to give CrO at the interface between a nickel-based superalloy and a glass-ceramic, or the reaction between titanium and SiO_2 (Equation 38) to give an interface composed of $Ti_5Si_3 + TiO_2$. Desirable reactions can also be promoted by the use of appropriate additives to the glass, e.g. the classical adherence-promoting oxides, CoO and NiO. These oxides react preferentially with the metal to promote the formation of a suitable substrate metal oxide favourable to bonding, e.g. reaction between CoO and an iron substrate (Equation 15). Depending on the metal to be coated or sealed to, various additions may be utilized to promote reactions favourable to chemical bonding. For example, the addition of a number of oxides, including CoO, NiO, CuO, MoO_3 or WO_3 to a glass to be bonded to a chromium-containing alloy could favour the formation of Cr_2O_3 at the interface. Not all redox reactions are desirable, of course, and care must be exercised to avoid reactions that create gaseous or unstable reaction products that can disrupt the bonding process, e.g. Equations 28, 40–44. For a given system, it is possible to make rule-of-thumb predictions concerning the most likely reactions using thermodynamic data. Some examples are given in Table IX. Thermodynamically favourable reactions may not necessarily proceed, however, due to kinetic considerations.

7.4. Defects in seals and coatings

There are many factors which influence the quality of a seal or coating. The occurrence of bubbles or voids at the metal/glass or metal/glass-ceramic interface is a particularly troublesome occurrence and cannot only weaken the interface mechanically, but may also prevent a seal from being hermetic. Bubbles occur for a number of reasons. In coatings, which are normally applied as a particulate suspension, very careful control over the green-coating characteristics and subsequent firing and heat-treatment schedules is required in order to prevent the entrapment of gases during the stage when the individual glass particles are melting and undergoing fusion. One of the most common causes of bubbling during sealing or coating is the formation of gaseous products due to the release of volatile contaminants, e.g. traces of cutting oils, fingerprint grease, carbon dust from jigging, etc. This can normally be avoided by the use of stringent cleaning/degreasing treatments prior to sealing, and careful assembly of components in "clean" conditions. Another common cause of bubbling during sealing is oxidation of carbon or carbides which are present near the surface of many metals and alloys (oxidation may occur either due to the presence of oxygen in the furnace atmosphere or due to redox reactions between the carbides and the glass). This can be eliminated or minimized by subjecting the metal to a de-carburization treatment prior to sealing, e.g. a high-temperature vacuum anneal. Redox reactions between the metal substrate and constituents in the glass can also result in the formation of gaseous products, e.g. liberation of gaseous sodium by reaction of Na_2O with aluminium in Fecralloy (Equation 21), or reaction of SiO_2 or P_2O_5 with titanium to release oxygen (Equations 40–43).

Another mechanism for the formation of bubbles is diffusion of gases, and in particular hydrogen which may be dissolved in the metal, into the interfacial region during cooling from the sealing temperature (the solubility of hydrogen in metals decreases with decreasing temperature, and hence hydrogen gas may be liberated during cooling of a metal seal from the sealing temperature). This effect can be particularly pronounced in the enamelling of iron, and can lead to an effect called "fishscaling" whereby the enamel surface spalls off under the influence of a build-up in hydrogen gas pressure at the interface after sealing. This effect can similarly be reduced by, for example, vacuum annealing the metal prior to sealing. The presence of water can also present a serious hazard during sealing. For example, water vapour present in the furnace atmosphere can lead to severe blistering of

an enamel [10], or to the formation of bubbles in glass-to-metal seals [189].

Perhaps less well appreciated is the influence that water *dissolved in the glass* can have on the overall sealing characteristics [199, 210]. Glasses produced by conventional techniques can contain a significant proportion of dissolved water, either in the form of molecular water or hydroxyl ions; for most glasses the water content is in the range 0.02%–0.06%, although higher concentrations of water up to $\approx$ 10% have been noted in some glasses prepared at high pressure [48]. This dissolved water can react with metallic species diffusing into the glass from the metal substrate to form hydrogen gas (Equation 27). As noted earlier, and summarized in Table VIII, thermodynamic data suggest that hydrogen gas formation may, in fact, be responsible for bubble formation in many metal/glass and metal/glass-ceramic systems; and in particular for those alloys rich in chromium, niobium, titanium or aluminium. Two different approaches have been adopted in order to minimize this effect. In the first method, the glass is produced by melting under "dry" ambient conditions (a maximum of a few parts per million of water vapour) in order to produce a glass which is virtually free from dissolved water; sealing is then carried out under similar dry conditions. In the second approach, additives to the glass can be employed which will react preferentially with constituents that would otherwise react with the dissolved water, to form non-gaseous reaction products; e.g. reaction of CuO with chromium to give Cr_2O_3 and CuO_2 (Equation 29).

In addition to the water and other reactions outlined above, many other undesirable reactions may occur during metal-to-glass or metal-to-ceramic bonding. For example, reaction of chromium with P_2O_5 nucleating agent to form chromium phosphide (Equations 22–26, 31, 32); this particular reaction is very undesirable because the nucleating agent is removed from the interfacial region resulting, upon crystallization, in the formation of a coarse microstructure which may possess thermal expansion characteristics which are very different from those of the bulk glass-ceramic. These effects can be minimized by careful control over the starting glass composition and heat-treatment schedule, or by the use of an alternative nucleating agent in the case of glass-ceramics. It is possible to use thermodynamic data in order to predict possible seal reactions. Thermodynamic data for a number of potential reactions are given in Table IX.

Acknowledgements

The author is grateful to many of his colleagues, in particular Messrs B. L. Metcalfe and D. J. Bradley, for experimental data and useful discussions. He also thanks Mr C. Ruckman and Mrs S. V. Vail, AWE, for the scanning electron microscopy. Thanks are also due to Dr D. Holland, University of Warwick, UK, for providing Figs 15, 22 and 25, Dr R. M. Charnah and Mr M. I. Budd, GEC Alsthom Engineering Research Centre, UK, for provision of Figs 28 a–d and 29, Messrs J. Gibson and M. J. Knowles, AWE, for Fig. 28e, and Dr R. E. Loehman, Sandia National Laboratories, USA, for Fig. 21. This work was carried out with the support of the Procurement Executive, Ministry of Defence.

References

1. P. W. McMILLAN and B. P. HODGSON, Engineering **196** (1963) 366.
2. B. W. KING, H. P. TRIPP and W. H. DUCKWORTH, *J. Amer. Ceram. Soc.* **42** (1959) 504.
3. J. A. PASK and R. M. FULRATH, *ibid.* **45** (1962) 592.
4. M P. BOROM and J. A. PASK, *ibid.* **49** (1966) 1.
5. J. J. BRENNAN and J. A. PASK, *ibid.* **56** (1973) 58.
6. T. TAKAMORI, in "Treatise on Materials Science and Technology", Vol. 17, edited by M. Tomozawa and R. H. Doremus (Academic Press, New York, 1979) pp. 173–255.
7. N. N. SINGHDEO and R. K. SCHUKLA, in "Glass Science and Technology", Vol. 2, "Processing", edited by D. R. Uhlmann and N. J. Kreidl, (Academic Press, Orlando, 1984) pp. 169–207.
8. E. M. RABINOVICH, *J. Mater. Sci.* **20** (1985) 4259.
9. R. H. DALTON, US Pat. 2392 314 (1946).
10. A. I ANDREWS, "Porcelain Enamels: the preparation, application, and properties of enamels" 2nd Edn. (Garrard Press, Champaign, ILL, 1961).
11. N. KATAOKA, T. KAWAMOTO and Y. MANABE, Jpn Pat. 37-4029 (1962).
12. P. W. McMILLAN, G. PARTRIDGE and F. R. WARD, Brit. Pat. 1205 652 (1970).
13. J. L. ELLIS, US Pat. 3564 587 (1971).
14. N. KATAOKA and Y. MANABE, *Osaka Kogyo Gijutsu Shikensho Kiho* **23** (1972) 204.
15. N. J. KREIDL, in "Glass-forming systems", edited by D. R. Uhlmann and N. J. Kreidl (Academic Press, New York, 1983) pp. 105–299.
16. A. E. DALE and J. E. STANWORTH *J. Soc. Glass Technol.* **33** (1949) 167.
17. P. P. PIROOZ, US Pat. 3088 833 (1963).
18. *Idem*, US Pat. 3088 834 (1963).
19. Y. SUZUKI, S. NAGAHARA and N. ICHIMURA, US Pat. 3674 520 (1972).
20. J. W. MALMENDIER, US Pat. 3883 358 (1975).
21. T. YAMANAKA and Y. TAKAGI, Jpn Pat. 50-55 612 (1975).
22. T. MORIGUCHI, K, MIWA and T. SHIBUYA, US. Pat. 3900 330 (1975).
23. Hitachi Ltd. Brit. Pat. 1563 790 (1980).
24. M. ISHIYAMA, T. MATSUDA, S. NAGAHARA and Y. SUZUKI, *Asahi Garasu Kenkyu Hokoku* **16** (1966) 77.
25. T. HIKINO and M. MIKODA, Jpn Pat. 46-3467 (1971).
26. P. W. McMILLAN and G. PARTRIDGE, Brit. Pat. 1306 727 (1973).
27. R. P. FRASER and A. L. CIANCHI, US Pat. 2660 531 (1953).
28. N. H. RAY, C. J. LEWIS, J. N. C. LAYCOCK and W. D. ROBINSON, *Glass Technol.* **14** (1973) 50.
29. N. H. RAY, J. N. C. LAYCOCK and W. D. ROBINSON, *ibid.* **14** (1973) 55.
30. Y. ASAHARA and T. IZUMITANI, US Pat. 3885 974 (1975).
31. N. H. RAY, R. J. PLAISTED and W. D. ROBINSON, *Glass Technol.* **17** (1976) 66.
32. M. A. TINDYALA and W. R. OTT, *Bull. Amer. Ceram. Soc.* **57** (1978) 432.
33. K. KOBAYASHI, *ibid*, **66** (1987) 685.
34. R. S. CHAMBERS, F. P. GERSTLE and S. L. MONROE, *J. Amer. Ceram. Soc.* **72** (1989) 929.
35. Y. ABE and H. HOSONO, in "Inorganic phosphate materials", edited by T. Kanazawa (Elsevier Science, Amsterdam, 1989) pp. 247–81.
36. Y. B. PENG and D. E. DAY, *Glass Technol.* **32** (1991) 166.
37. *Idem, ibid.* **32** (1991) 200.
38. W. R. EUBANK and W. R. BECK, US. 2863 782 (1958).
39. P. L. BAYNTON, H. RAWSON and J. E. STANWORTH, *J. Electrochem. Soc.* **104** (1957) 237.
40. H. HIRUMA and S. SHIMIZU, Jpn Pat. 48–17 848 (1973).
41. J. W. MALMENDIER and J. E. SOJKA, US Pat. 3885 975 (1975).

42. S. A. CLAYPOOLE, US Pat. 2889 952 (1959).
43. W. SACK, H. SCHEIDLER and J. PETZOLDT, *Glastech. Ber.* **41** (1968) 138.
44. Y. SUZUKI and N. ICHIMURA, *Asahi Garasu Kenkyu Hokoku* **18** (1968) 49 (in Japanese).
45. F. W. MARTIN, Jpn Pat. 45–19 982 (1970).
46. K. MINAGAWA and K. SUZUKI, Jpn Pat. 49–36 807 (1974).
47. J-S. LEE, J-C. PENG and C-W. HUANG, *Glass Technol.* **31** (1990) 77.
48. M. B. VOLF, "Chemical Approach to Glass", (Elsevier, Amsterdam, 1984).
49. P. W. McMILLAN, "Glass Ceramics" 2nd Edn (Academic Press, London, 1979).
50. Z. STRNAD, "Glass-Ceramic Materials", (Elsevier, Amsterdam, 1986).
51. I. W. DONALD, in "Encyclopedia of Materials Science and Technology", 3rd Supplement, edited by R. W. Cahn, (Pergamon Press, Oxford, 1993) pp. 1689–95.
52. S. D. STOOKEY, Brit. Pat. 752 243, (1956).
53. Anon, *Bull. Amer. Ceram. Soc.* **36** (1957) 279.
54. S. D. STOOKEY, Brit. Pat. 829 447 (1960).
55. *Idem*, US Pat. 2933 857 (1960).
56. P. W. McMILLAN and G. PARTRIDGE, *Proc. Brit. Ceram. Soc.* **3** (1965) 241.
57. M. WADA and S. KAWAMURA, *Bull. Inst. Chem. Res. Kyoto Univ.* **59** (1981) 256.
58. D. G. GROSSMAN, in "Advances in Ceramics 4, Nucleation and Crystallization in Glasses", edited by J. H. Simmons, D. R. Uhlmann and G. H. Beall (American Ceramic Society, Columbus, OH, 1982) pp. 249–60.
59. J. HLAVAC, "The Technology of Glass and Ceramics", (Elsevier, Amsterdam, 1983) pp. 228–43.
60. G. H. BEALL, in "Glass Science and Technology", Vol. 1, "Glass-Forming Systems", edited by D. R. Uhlmann and N. J. Kreidl (Academic Press, New York, 1983) pp. 403–45.
61. I. W. DONALD, "Inorganic Glasses and Glass-Ceramics: a Review", AWRE Report No. O 19/84, December 1984.
62. G. H. BEALL, *J. Non-Cryst. Solids* **73** (1985) 413.
63. G. P. SMITH, *Mater. Design* **10** (1989) 54.
64. G. H. BEALL, *Rev. Solid State Sci.* **3** (1989) 113.
65. W. D. KINGERY, "Introduction to Ceramics", (Wiley, New York, 1960).
66. P. W. McMILLAN, and G. PARTRIDGE, Brit. Pat. 924 996 (1963).
67. P. W. McMILLAN, S. V. PHILLIPS and G. PARTRIDGE, *J. Mater. Sci.* **1** (1966) 269.
68. D. P. KRAMER, R. F. SALERNO and E. E. EGLESTON, "Effect of several surface treatments on the strength of a glass ceramic-to-metal seal", Monsanto Research Corporation Report MLM-2893, February 1982.
69. W. R. HENDERSON, D. P. KRAMER and D. B. SULLENGER, "Determination of the optimum crystallization conditions of a high thermal expansion glass-ceramic", Monsanto Research Corporation Report MLM-3136, March 1984.
70. W. F. HAMMETTER and R. E. LOEHMAN, *J. Amer. Ceram. Soc.* **70** (1987) 577.
71. D. P. KRAMER, G. L. HARVILLE, D. A. BUCKNER, J. P. McCARTHY, A. B. NEASE and D. B. SULLENGER, "Physical property changes of a lithia-alumina-silica based glass as a function of composition", Monsanto Research Corporation Report MLM-3272, July 1985.
72. English Electric Co., French Pat. 1328 620 (1963).
73. P. W. McMILLAN and G. PARTRIDGE, Brit. Pat. 1028 871 (1966).
74. W. E. SMITH, US Pat. 3380 818 (1968).
75. I. W. DONALD, B. L. METCALFE and D. J. BRADLEY, in "Proceedings of the 2nd International Conference on New Materials and their Applications", University of Warwick, UK, 10-12 April 1990, Institute of Physics Conference Series no. 111, edited by D. Holland, (IOP, Bristol, 1990) pp. 207–16.
76. B. L. METCALFE and I. W. DONALD, *Silicates Industriels* **5-6** (1991) 99.
77. Corning Glass Works, Brit. Pat. 829447 (1960).
78. P. W. McMILLAN and G. PARTRIDGE, *J. Mater. Sci.* **7** (1972) 847.
79. G. PARTRIDGE, C. A. ELYARD and M. I. BUDD, "Glasses and Glass-Ceramics", edited by M. H. Lewis (Chapman and Hall, London, 1989) pp. 226–71.
80. G. PARTRIDGE, C. A. ELYARD and H. D. KEATMAN, *Glass Technol.* **30** (1989) 215.
81. V. V. VARGIN and E. M. MIKLYUKOV, *Zhurnal Prikladnoy Khimii* **11** (1968) 194.
82. Z. STRNAD, B. SPIRKOVA and J. DUSIL, *Silikaty* **20** (1976) 225.
83. L. M. HOLLERAN and W. MARTIN, US Pat. 4714 687 (1987).
84. A. A. OMAR, A. W. A. EL-SHENNAWI and A. R. EL-GHANNAM, *J. Mater. Sci.* **26** (1991) 6049.
85. P. W. McMILLAN and G. PARTRIDGE, Brit. Pat. 924 996 (1963).
86. P. W. McMILLAN and B. P. HODGSON, Brit. Pat. 944 571 (1963).
87. P. W. McMILLAN and G. PARTRIDGE, US Pat. 3170 805 (1965).
88. P. W. McMILLAN, B. P. HODGSON and G. PARTRIDGE, US Pat. 3220 815 (1965).
89. *Idem*, *Glass Technol.* **7** (1966) 121.
90. P. W. McMILLAN, G. PARTRIDGE, B. P. HODGSON and H. R. HEAP, *ibid.* 7 (1966) 128.
91. P. W. McMILLAN and B. P. HODGSON, Brit. Pat. 1063 291 (1967).
92. A. R. WEST and F. P. GLASSER, *J. Mater. Sci.* **5** (1970) 557.
93. *Idem*, *ibid.* **5** (1970), 676.
94. Z-X. CHEN and P. W. McMILLAN, *J. Amer. Ceram. Soc.* **68** (1985) 220.
95. S-B. LEE and S-M. HAN, *J. Korean Ceram. Soc.* **24** (1987) 227 (in Korean).
96. I. W. DONALD, B. L. METCALFE, D. J. WOOD and J. R. COPLEY, *J. Mater. Sci.* **24** (1989) 3892.
97. B. B. RAO, N. K. REDDY and M. A. JALEEL, *J. Mater. Sci. Lett.* **9** (1990) 1159.
98. I. W. DONALD, B. L. METCALFE and A. E. P. MORRIS, *J. Mater. Sci.* **27** (1992) 2979.
99. Z-X. CHEN and P. W. McMILLAN, *ibid.* **20** (1985) 3428.
100. W. VOGEL and W. HÖLAND, *Angew. Chem. Int. Ed. Engl.* **26** (1987) 527.
101. J. A. WILDER, J. T. HEALEY and B. C. BUNKER, in "Advances in Ceramics" Vol. 4, edited by J. H. Simmons (American Ceramic Society, Columbus OH. (1982) pp. 313–26..
102. T. H. WANG and P. F. JAMES, in "Proceedings of the 2nd International Conference on New Materials and their Applications", University of Warwick, UK, 10–12 April 1990, Institute of Physics Conference Series no. 111, edited by D. Holland (IOP, Bristol, 1990) pp. 401–10.
103. M. LANGLET, M. SALTZBERG and R. D. SHANNON, *J. Mater. Sci.* **27** (1992) 972.
104. J. H. PARTRIDGE, "Glass-to-Metal Seals" (Society Glass Technology, Sheffield, 1949).
105. J. W. PRICE, *Brit. Soc. Sci. Glass Bl. J.* **22** (1984) 34.
106. D. P. KRAMER and R. T. MASSEY, in "Advances in Ceramics", Vol. 9, "Forming of Ceramics", (American Ceramic Society, Columbus, OH, 1984) pp. 265–73.
107. *Idem*, "*In situ* Vacuum-assisted molding of glass-metal electrical components", Monsanto Research Corporation Report MLM-3267, July 1985.
108. D. P. KRAMER, R. T. MASSEY and D. L. HALCOMB, "Injection moulding sealing of glass to low melting metals", Monsanto Research Corporation Report MLM-3268, July 1985.
109. *Idem*. in "Technology of Glass, Ceramic, or Glass-Ceramic to Metal Sealing", edited by W. E. Moddeman, C. W. Merten and D. P. Kramer (American Society of Mechanical Engineers, New York, 1987) pp. 31–7.
110. R. M. RULON, in "Introduction to Glass Science", edited by L. D. Pye, H. J. Stevens and W. C. LaCourse (Plenum Press, New York, 1972) pp. 661–704.

111. R. G. BUCKLEY, *Ceram. Ind. Mag.* (1979) 20.
112. A. K. VARSHNEYA, in "Treatise of Materials Science and Technology", Vol. 22, edited by M. Tomozawa and R. H. Doremus (Academic Press, New York, 1982) pp. 241–306.
113. G. PARTRIDGE and C. A. ELYARD, *Brit. Ceram. Proc.* **34** (1984) 219.
114. A. P. TOMSIA and J. A. PASK, in "Joining of Ceramics", edited by M. G. Nicholas (The Institute of Ceramics, Chapman and Hall, London, 1990) pp. 7–30.
115. G. PARTRIDGE, *ibid.* pp. 31–55.
116. K. A. MASKALL and D. WHITE, "Vitreous Enamelling: a guide to modern enamelling practice" (Institute of Ceramics, Pergamon Press, London, 1986).
117. M A. SALAMAH and D. WHITE, in "Surfaces and interfaces in Ceramic and Ceramic–Metal Systems", edited by J. A. Pask and A. Evans (Plenum Press, New York, 1981), pp. 467–76.
118. P. KLIMONDA, O. LINGSTUYL, B. LAVELLE and F. DABOSI, *ibid.* pp. 477–86.
119. R. MEVREL, "High temperature surface interactions", AGARD Conference Proceedings, no. 461, (NATO, 1989), pp. 12-1–12-10.
120. D. S. RICKERBY and A. MATTHEWS (eds), "Advanced Surface Coatings" (Blackie, London, Glasgow, 1991).
121. F. H. STOTT, in "The Role of Active Elements in the Oxidation Behaviour of High Temperature Metals and Alloys", edited by E. Lang (Elsevier Applied Science, London, 1989) pp. 3–21.
122. S. SAKKA, in "Treatise on Materials Science and Technology", Vol. 22, "Glass III", edited by M. Tomozawa and R. H. Doremus (Academic Press, New York, 1982) pp. 129–67.
123. I. M. THOMAS, in "Sol–gel Technology for Thin Films, Fibers, Preforms, Electronics and Speciality Shapes", edited by L. C. Klein (Noyers, Park Ridge, NJ, 1982) pp. 2–15.
124. C. W. TURNER, *Bull. Amer. Ceram. Soc.* **70** (1991) 1487.
125. L. C. KLEIN, *Glass Ind.* **62** (1981) 14.
126. B. D. FABES, W. F. DOYLE, L. S. SILVERMAN, B. J. J. ZELINSKI, and D. R. UHLMANN, in "Science of Ceramic Chemical Processing", edited by L. L. Hench and D. R. Ulrich (Wiley, New York, 1986), pp. 217–23.
127. H. DISLICH, in "Sol–gel Technology for Thin Films, Fibers, Preforms, Electronics and Speciality Shapes", edited by L. C. Klein, (Noyers, Pakk Ridge, NJ, 1982) pp. 50–79.
128. P. K. BISWAS, D. KUNDU and D. GANGULI, *J. Mater. Sci. Lett.* **8** (1989) 1436.
129. H. G. FLOCH and J-J. PRIOTTON, *Bull. Amer. Ceram. Soc.* **69** (1990) 1141.
130. P. W. McMILLAN, B. P. HODGSON, D. S. CROZIER and S. T. WELLS, Brit. Pat. 1174 474 (1966).
131. W. J. MIRIAM, Brit. Pat. 1026 178 (1966).
132. A. POTTER and J. E. HENNING, "Continuous glass coating of fine metal wires", in Engineering Materials: Proceedings of Materials Process Engineering National Symposium Exhibition, Chicago, 1968 Soc. Aerosp. Mater. Process. Eng. pp. 417–430.
133. G. F. TAYLOR, *Phys. Rev.* **23** (1924) 655.
134. *Idem*, US Pat. 1793 529 (1931).
135. I. W. DONALD and B. L. METCALFE, in "Proceedings of the 7th CIMTEC World Ceramics Congress, Satellite Symposium 2", edited by P. Vincenzini, Montecatini Terme, Italy, 2–5 June 1990 (Elsevier Science, Amsterdam, 1991) pp. 479–88.
136. I. W. DONALD, *J. Mater. Sci.* **22** (1987) 2661.
137. Y. IKEDA, *Shin Nihon Denki Kiho* **3** (1968) pp. 96–106 (in Japanese).
138. R. A. EPPLER, in "Glass Science and Technology", Vol. 1, edited by D. R. Uhlmann and N. J. Kreidl (Academic Press, New York, 1983) pp. 301–38.
139. B. T. GARLAND, *Mater. Design* **7** (1986) 44.
140. B. A. CHAPMAN, H. D. DeFORD, G. P. WIRTZ and S. D. BROWN, in "Technology of Glass, Ceramic, or Glass-Ceramic to Metal Sealing", edited by W. E. Moddeman, C. W. Merten and D. P. Kramer (American Society of Mechanical Engineering, New York, 1987) pp. 77–87.
141. P. K. GILBERT. MSc thesis, Thames Polytechnic (1989).
142. R. HILL and P. K. GILBERT, *J. Amer. Ceram. Soc.* **76** (1993) in press.
143. R. C. MACKENZIE (ed.) "Differential Thermal Analysis" (Academic Press, New York, 1972).
144. T. DANIELS, "Thermal Analysis" (Kogan Page, London, 1973).
145. J. L. McNAUGHTON and C. T. MORTIMER, "Differential Scanning Calorimetry", IRS Chemistry Series no. 2 (Butterworths, London, 1975).
146. M. I. POPE and M. D. JUDD, "Differential Thermal Analysis" (Heyden, London, 1973).
147. J. SESTÁK, in "Comprehensive Analytical Chemistry", Vol. 12, "Thermal Analysis, Part D, Thermophysical Properties of Solids", edited by G. Svehla, (Elsevier, Amsterdam, 1984) pp. 303–43.
148. M. E. BROWN, "Introduction to Thermal Analysis" (Chapman and Hall, London, 1988).
149. P. R. CHALKER, in "Advanced Surface Coatings", edited by D. S. Rickerby and A. Matthews, (Blackie, London, Glasgow, 1991) pp. 278–314.
150. C. W. FAIRHURST, J. D. MACKERT, S. W. TWIGGS, R. D. RINGLE, D. T. HASHINGER and E. E. PARRY, *Ceram. Engng. Sci. Proc.* **6** (1985) 66.
151. S. J. BULL and D. S. RICKERBY, in "Advanced Surface Coatings", edited by D. S. Rickerby and A. Matthews (Blackie, London, Glasgow, 1991) pp. 315–42.
152. W. W. McLELLAN and E. B. SHAND, (eds), "Glass Engineering Handbook", 3rd Edn (McGraw-Hill New York, 1984).
153. H. RAWSON, "Properties and Applications of Glass" (Elsevier, Amsterdam, 1980).
154. G. W. SCHERER, "Relaxation in Glass and Composites" (Wiley, New York, 1986).
155. G. W. SCHERER and S. M. REKHSON, in "Treatise on Materials Science and Technology", Vol. 26, "Glass IV," edited by M. Tomozawa and R. H. Doremus (Academic Press, London, 1985) pp. 245–318.
156. C. W. LAU, A. RAHMAN and F. DELALE, in "Technology of Glass, Ceramic, or Glass-Ceramic-to-Metal Sealing", edited by W. E. Moddeman, C. W. Merten and D. P. Kramer (American Society of Mechanical Engineers, New York, 1987) pp. 89–98.
157. B. L. METCALFE, I. W. DONALD and D. J. BRADLEY, Institute of Ceramics Proceedings no. 48, edited by R. Morrell and G. Partridge (Institute of Ceramics, Shelton, Stoke-on-Trent, 1991) pp. 177–88.
158. J. H. LAUCHER, R. L. COOK and A. I. ANDREWS, *J. Amer. Ceram. Soc.* **39** (1956) 288.
159. S.C. KUNZ and R. E. LOEHMAN, *Adv. Ceram. Mater.* **2** (1987) 69.
160. F. P. GERSTLE and R. S. CHAMBERS, in "Technology of Glass, Ceramic, or Glass-Ceramic-to-Metal Sealing", edited by W. E. Moddeman, C. W. Merten and D. P. Kramer (American Society of Mechanical Engineers, New York, 1987) pp.47–59.
161. T. YOUNG, *Trans. Roy. Soc. Lond.* **95** (1805) 65.
162. A. DUPRÉ, "Theorie Mechanique de la Chaleur" (Gauthier-Villars, Paris, 1869).
163. A. W. ADAMSON, "Physical Chemistry of Surfaces", 4th Edn. (Wiley, New York, 1982).
164. R. E. LOEHMAN, *Bull. Amer. Ceram. Soc.* **68** (1989) 891.
165. *Idem*, "Joining Engineering Ceramics", Technical Report SAND-90-0966C, 1990.
166. R. M. KING, *J. Amer. Ceram. Soc.* **16** (1933) 232.
167. J. H. HEALY and A. I. ANDREWS, *ibid.* **34** (1951) 207.
168. W. N. HARRISON, J. C. RICHMOND, J. W. PITTS, and S. G. BENNER, *ibid.* **35** (1952) 113.
169. H. F. STALEY, *ibid.* **17** (1934) 163.
170. A. DIETZEL, *Ceram. Abst.* **13** (1934) 250.
171. *Idem. ibid.* **14** (1935) 107.
172. J. C. RICHMOND, D. G. MOORE, H. B. KIRKPATRICK and W. N. HARRISON, *J. Amer. Ceram. Soc.* **36** (1953) 410.
173. D. G. MOORE, J. W. PITTS, J. C. RICHMOND and W. N. HARRISON, *ibid.* **37** (1954) 1.
174. J. A. PASK, *Proc. Porcelain Enamel Inst. Tech. Forum* **33** (1971) 1.
175. J. A. PASK and A. P. TOMSIA, in "Surfaces and Interfaces in Ceramic and Ceramic–Metal Systems", edited by J. A. Pask and A. Evans (Plenum Press, New York, 1981) pp. 411–19.

176. J. A. PASK *Bull. Amer. Ceram. Soc.* **66** (1987) 1587.
177. *Idem.* in "Technology of Glass, Ceramic, or Glass-Ceramic-to-Metal Sealing", edited by W. E. Moddeman, C. W. Merten and D. P. Kramer (American Society of Mechanical Engineers, New York, 1987) pp. 1–7.
178. A. J. STURGEON, D. HOLLAND, G. PARTRIDGE and C. A. ELYARD, *Glass Technol.* **27** (1986) 102.
179. M. G. NICHOLAS, *J. Mater. Sci.* **21** (1986) 3292.
180. I. PENKOV and I. GUTZOW, *Silikattechnik* **42** (1991) 60.
181. J. C. BIRKBECK, R. T. CASSIDY, P. N. FAGIN and W. E. MODDEMAN, in "Technology of Glass, Ceramic, or Glass-ceramic-to-Metal-Sealing", edited by W. E. Moddeman, C. W. Merten and D. P. Kramer (American Society of Mechanical Engineers, New York, 1987) pp. 15–24.
182. R. T. CASSIDY and P. N. FAGIN, *ibid.*, pp. 9–14.
183. W. E. MODDEMAN, J. C. BIRKBECK, W. C. BOWLING, A. R. BURKE and R. T. CASSIDY, *Ceram. Engng Sci. Proc.* **10** (1989) 1403.
184. W. E. MODDEMAN, R. E. PENCE, R. T. MASSEY, R. T. CASSIDY and D. P. KRAMER, *ibid.***10** (1989) 1394.
185. R. T. CASSIDY and W. E. MODDEMAN, *ibid.* **10** (1989) 1387.
186. A. R. HYDE and G. PARTRIDGE, in "Advanced Engineering with Ceramics", British Ceramic Proceedings no. 46, edited by R. Morrell (Institute of Ceramics, Shelton, Stoke-on-Trent, 1990) pp. 345–50.
187. G. A. KNOROVSKY, R. K. BROW, R. D. WATKINS and R. E. LOEHMAN, "Interfacial Debonding in Stainless Steel/Glass-ceramic Seals", Technical Report SAND-89-1866C (1990).
188. B. L. METCALFE, I. W. DONALD and D. J. BRADLEY, unpublished work, AWE (1990).
189. W. B. THOMAS, *Solid State Technol.* **29** (1986) 73.
190. P. W. McMILLAN and B. P. HODGSON, Brit. Pat. 1023480 (1966).
191. S. H. RISBUD, G. D. ALLEN and J. E. POETZINGER, in "Ceramic Microstructures '86", edited by J. A. Pask and A. G. Evans (Plenum Press, New York, 1986) pp. 359–67.
192. I. W. DONALD, *J. Amer. Ceram. Soc.* **60** (1972) 89.
193. J. W. McLEAN and I. R. SCED, *Brit. Ceram. Soc. Trans.* **72** (1973) 235.
194. P. V. KELSEY, W. T. SIEGAL and D. V. MILEY, in "Surfaces and Interfaces in Ceramic and Ceramic-Metal Systems", edited by J. A. Pask and A. Evans (Plenum Press, New York, 1981) pp. 591–601.
195. H. L. McCOLLISTER and S. T. REED, US Pat. 4414 282 (1983).
196. D. P. KRAMER and R. T. MASSEY, *Ceram. Engng Sci.* **5** (1984) 739.
197. T. J. HEADLEY, R. E. LOEHMAN, R. D. WATKINS and M. C. MADDEN, in "Proceedings of the 44th Annual Meeting of the Electron Microscopy Section of America", (San Francisco Press, San Francisco, 1986) pp. 856–7.
198. R. E. LOEHMAN, S. C. KUNZ and R. D. WATKINS, *Ceram. Engng Sci. Proc.* **7** (1986) 721.
199. S. M. CRAVEN, D. P. KRAMER and W. E. MODDEMAN, "Chemistry of Glass-ceramic to Metal Bonding for Header Applications", Monsanto Research Corporation Report MLM-3403, December 1986.
200. R. D. WATKINS and R. E. LOEHMAN, *Adv. Ceram. Mater.* **1** (1986) 77.
201. A. TOMSIA and J. A. PASK, *J. Amer. Ceram. Soc.* **69** (1986) C-239.
202. R. E. LOEHMAN and T. J. HEADLEY, in "Materials Science Research", Vol. 21, "Ceramic Microstructures '86", edited by J. A. Pask and A. G. Evans (Plenum Press, New York, 1987) pp. 33–43.
203. D. P. KRAMER and W. E. MODDEMAN, "Chemistry of glass-ceramic to metal bonding for header applications", EG and G Report MLM-3556, November 1988.
204. F. HONG and D. HOLLAND, *J. Non-Cryst. Solids* **112** (1989) 357.
205. *Idem, Surf. Coatings Tech.* **39/40** (1989) 19.
206. D. HOLLAND, F. HONG, E. LOGAN and S. SUTHERLAND, in "Proceedings of the 2nd International Conference on New Materials and their Applications", University of Warwick, UK, 10–12 April, 1990, Institute of Physics Conference Series no. 111, edited by D. Holland (IOP, Bristol, 1990) pp. 459–68.
207. F. HONG, PhD dissertation, University of Warwick (1991).
208. B. L. METCALFE and I. W. DONALD, in "Proceedings of the 2nd International Conference on New Materials and their Applications", University of Warwick, UK, 10–12 April 1990, Institute of Physics Conference Series no. 111, edited by D. Holland (IOP, Bristol, 1990) pp. 469–78.
209. T. J. HEADLEY and R. E. LOEHMAN, *J. Amer. Ceram. Soc.* **67** (1984) 620.
210. L. D. HAWS, D. P. KRAMER, W. E. MODDEMAN and G. W. WOOTEN, "High Strength Glass-Ceramic-to-Metal Seals", Monsanto Research Corporation Report MLM-3288(OP), December 1985.
211. W. E. MODDEMAN, S. M. CRAVEN and D. P. KRAMER, *J. Amer. Ceram. Soc.* **68** (1985) C-298.
212. L. D. HAWS, private communication (1991).
213. R. E. LOEHMAN, in "Technology of Glass, Ceramic, or Glass-Ceramic-to-Metal Sealing", edited by W. E. Moddeman, C. W. Merten and D. P. Kramer (American Society of Mechanical Engineers, New York, 1987) pp. 39–45.
214. M. R. NOTIS, *J. Amer. Ceram. Soc.* **45** (1962) 412.
215. I. BARIN, O. KNACKE and O. KUBASCHEWSKI, "Thermochemical Properties of Inorganic Substances", (Springer Berlin, 1973).
216. A. P. TOMSIA, Z. FEIPENG and J. A. PASK, *J. Amer. Ceram. Soc.* **68** (1985) 20.
217. T. R. NASH, E. M. PASHBY and R. L. COLLETT, *Glass Technol.* **24** (1983) 298.
218. A. Ya. SITNIKOVA, A. A. APPEN, I. S. ANITOV, V. N. FEDOROV, A. M. KALININA and M. M. PIRYUTKO, *J. Appl. Chem. USSR* **47** (1974) 1981.
219. I. J. McCOLM and C. DIMBYLOW, *J. Mater. Sci.* **9** (1974) 1320.
220. A. PASSERONE, G. VALBUSA and E. BIAGINI, *ibid.* **12** (1977) 2465.
221. Z. FEIPENG, A. P. TOMSIA and J. A. PASK, in "Proceedings of the 33rd Pacific Coast Regional Meeting of the American Ceramic Society", San Francisco, 1980, pp. 76–78.
222. R. K. BROW and R. D. WATKINS, in "Technology of Glass, Ceramic, or Glass-Ceramic-to-Metal Sealing", edited by W. E. Moddeman, C. W. Merten and D. P. Kramer (American Society of Mechanical Engineers, New York, 1987), pp. 25–30.
223. B. L. METCALFE, I. W. DONALD and D. J. BRADLEY, unpublished work, AWE (1992).
224. G. PARTRIDGE, Institute of Physics Conference Series no. 89, (IOP, Bristol, 1987) pp. 161–70.
225. R. E. LOEHMAN, *J. Metals* **38** (1986) 42.
226. ANON, *Bull. Amer. Ceram. Soc.* **70** (1991) 1454.
227. A. KRAJEWSKI, A. RAVAGLIOLI, G. DE PORTU and R. VISANI, *Bull. Amer. Ceram. Soc.* **64** (1985) 679.
228. R. E. LOEHMAN and A. P. PASK, *ibid.* **67** (1988) 375.
229. A. W. HEY, in "Joining of Ceramics", edited by M. G. Nicholas (The Institute of Ceramics, Chapman and Hall, London, 1990) pp. 56–72.
230. M. COURBIERE, in "Interfaces in New Materials", edited by P. Grange and B. Delmon (Elsevier Applied Science, London, New York, 1991) pp. 29–41.
231. O. M. AKSELSEN, *J. Mater. Sci.* **27** (1992) 1989.
232. J. M. RINCÓN, J. M. GONZÁLEZ-PEÑA and V. A. BOSCH, *Bull. Amer. Ceram. Soc.* **66** (1987) 1124.
233. M. KAJIWARA, *Glass Technol.* **29** (1988) 188.
234. L. F. TASWELL and M. W. JONES, *ibid.* **31** (1990) 44.
235. P. W. McMILLAN and G. PARTRIDGE, Brit. Pat. 1151860 (1969).
236. H. WIGGIN and Co. Ltd, Hereford, UK, and Haynes Int., Kokomo, USA. Alloy data sheets (1976–78) and (1987).
237. R. C. WEAST, "Handbook of Chemistry and Physics", 55th Edn (CRC Press, Cleveland, 1974).
238. G. V. SAMSONOV, "Handbook of Physicochemical Properties of the Elements" (Oldbourne Book Co, London, 1968).

Received 30 June
and accepted 15 July 1992